



**AN ANALYTICAL STUDY OF T-38 DRAG REDUCTION IN TIGHT
FORMATION FLIGHT**

THESIS

Eugene H. Wagner, Jr.
Major, USAF

AFIT/GAE/ENY/02-2

DEPARTMENT OF THE AIR FORCE
AIR UNIVERSITY
AIR FORCE INSTITUTE OF TECHNOLOGY

Wright-Patterson Air Force Base, Ohio

APPROVED FOR PUBLIC RELEASE; DISTRIBUTION UNLIMITED.

The views expressed in this thesis are those of the author and do not reflect the official policy or position of the United States Air Force, Department of Defense, or the U.S. Government.

**AN ANALYTICAL STUDY OF T-38 DRAG REDUCTION IN TIGHT
FORMATION FLIGHT**

THESIS

Presented to the faculty

Department of Aeronautics and Astronautics

Graduate School of Engineering and Management

Air Force Institute of Technology

Air University

Air Education and Training Command

In Partial Fulfillment of the Requirements for the Degree for the
Degree of Master of Science in Aeronautical Engineering

Eugene H. Wagner, Jr., B.S.

Major, USAF

March, 2002

APPROVED FOR PUBLIC RELEASE; DISTRIBUTION UNLIMITED.

**AN ANALYTICAL STUDY OF T-38 DRAG REDUCTION IN TIGHT
FORMATION FLIGHT**

Eugene H. Wagner, Jr., B.S.
Major, USAF

Approved:

David Jacques, PhD
Thesis Advisor

Date

J. Michael Phillips, PhD
Committee Member

Date

Meir Pachter, PhD
Committee Member

Date

Acknowledgements

A thesis of this nature requires the support of numerous people and is a culmination of many hours of work, both at AFIT and the USAF Test Pilot School. The author received help from numerous individuals during this project. The initial idea for the project came from my AFIT advisors, Lt Col Dave Jacques and Dr. Meir Pachter. Lt Col Jacques was instrumental in getting the thesis published at two separate AIAA conferences to bring this work to the attention of the aviation community. The initial direction and inputs of these two gentlemen was crucial to the project's success.

The help and direction I received from Mr. Bill Blake at AFRL/VA was invaluable. Without his guidance and expertise, this effort would have been very narrow in scope as the author would have spent an inordinate amount of time learning FORTRAN instead of applying it and getting tangible results. It was a pleasure working with Mr. Blake and I can't emphasize his contributions enough.

The author was also lucky enough to have an outstanding flight test team to work with at TPS. The team included Majors Jeff Wharton and Wim Libby, Captains Aaron Reed and Mike Stepaniak of the US Air Force, Captain Harry Van Hulten of the Royal Netherlands Air Force, and the T-38C Modernization Program at Edwards AFB.

Of course, a huge thank you goes out to my family for the support in pursuing my goals. My wife and two children were wonderful during the 2½ years of moving our household twice and giving me the inspiration I needed when things weren't going as planned. I owe a lot to their support!

Table of Contents

	Page
Acknowledgements	iv
Table of Contents	v
List of Figures	vii
List of Tables	viii
List of Abbreviations, Symbols, and Acronyms	ix
Abstract	xi
I. Introduction	1-1
Background	1-1
Objectives	1-7
Research Focus and Limitations	1-9
Payoff of Research	1-11
II. HASC95 Analysis	2-1
Transforming the T-38 into a HASC95 Model	2-2
Validation of the Model Against Actual T-38 Data	2-5
Two-Dimensional Versus Three-Dimensional Model	2-7
Optimal Position Determination: Two-Ship, No-Trim Losses	2-9
Drag Savings for a Three-Ship with No Trim Loss	2-14
Two-Ship Analysis with Trim Losses Included	2-16
Three-Ship Analysis with Trim Losses Included	2-19
Total Drag Savings	2-22
Implementation Considerations	2-22
III. Flight Test Setup	3-1
Overview	3-1
Test Procedures	3-4
IV. Flight Test Results	4-1
Overview	4-1
Two-Ship Data	4-2
Three-ship Data	4-4
Pilot Comments	4-8
Positions C and D	4-11
Position B	4-11

	Page
Position A	4-12
Operational Feasibility of Vortex Position B	4-13
V. Conclusions and Recommendations	5-1
Appendix A	A-1
Appendix B	B-1
Appendix C	C-1
Appendix D	D-1
Bibliography	BIB-1

List of Figures

	Page
Figure 1-1. Rotation of Lift and Drag due to Upwash	1-2
Figure 1-2. Effect of Streamwise Spacing on Lead/Wing Benefit	1-4
Figure 1-3. Hummel's Theoretical Multi-Ship Formation Savings	1-6
Figure 2-1. 2-D Model of T-38 for HASC95 Input	2-4
Figure 2-2. The 3-D Model in Formation with Spacing = 1	2-4
Figure 2-3. Comparison of the 2-D versus 3-D Model: Rolling Moment	2-8
Figure 2-4. Drag Savings for the Two-Ship, No-Trim Case	2-12
Figure 2-5. Rolling Moment for Two-Ship Case	2-13
Figure 2-6. Three-Ship, No-Trim Case	2-15
Figure 2-7. Two-Ship, Trimmed Case	2-17
Figure 2-8. Three-Ship Case with Optimally Placed #2	2-19
Figure 2-9. Blow-Up of Figure 2-8	2-20
Figure 2-10. Rolling Moment of #3 Wingman	2-21
Figure 2-11. Fuel Savings without Rotation	2-25
Figure 2-12. Fuel Savings with Rotation	2-25
Figure 3-1. Lateral Separation Definitions	3-3
Figure 4-1. Two Method Comparisons Between Lateral Positions	4-3
Figure 4-2. Average Fuel Flow Comparison Between Lateral Position	4-4
Figure 4-3. Comparison Between Formation Positions – Fuel Flow Method	4-7
Figure 4-4. Comparison Between Formation Positions – Airspeed Method	4-7
Figure 4-5. Average Fuel Flow Comparison Between Formation Positions	4-8
Figure 4-6. Workload in Fingertip Formation – Cruise	4-10
Figure 4-7. Workload in Fingertip Formation – Powered Approach	4-10
Figure 4-8. Workload in Test Position B	4-12
Figure 4-9. Operational Feasibility	4-14
Figure D-1. Fuel Flow Model Correction for Gross Weight and Ambient Ambient Air Temperature	D-5
Figure D-2. Standardized Fuel Flow versus Calibrated Airspeed	D-6

List of Tables

		Page
Table 2-1.	Comparison of Simulator Data to HASC Model	2-5
Table 2-2.	Effect of Rotating Formation Positions	2-23
Table 3-1.	Lateral Positions	3-2
Table 4-1.	Two-Ship Results for Each Lateral Position	4-4
Table 4-2.	Three-Ship Results for Varying Wingman Position	4-8
Table D-1.	Data Summary Table – Test Position A	D-10
Table D-2.	Two-Ship Sortie Analysis of Variance Table	D-12
Table D-3.	Data Summary Table – Test Position A, Two-Ship Sortie	D-15
Table D-4.	Data Summary Table – Test Position B, Two-Ship Sortie	D-15
Table D-5.	Data Summary Table – Test Position C, Two-Ship Sortie	D-16
Table D-6.	Data Summary Table – Test Position D, Two-Ship Sortie	D-16
Table D-7.	Data Summary Table – Test Position B, Three-Ship Sortie, First Wingman	D-17
Table D-8.	Data Summary Table – Test Position B, Three-Ship Sortie, Second Wingman	D-17
Table D-9.	Two-Ship Sortie ANOVA (Fuel Flow)	D-18
Table D-10.	Two-Ship Sortie ANOVA (Airspeed)	D-19
Table D-11.	Two-Ship Sortie ANOVA (Average)	D-20
Table D-12.	Three-Ship Sortie ANOVA (Fuel Flow)	D-21
Table D-13.	Three-Ship Sortie ANOVA (Airspeed)	D-22
Table D-14.	Three-Ship Sortie ANOVA (Average)	D-23

List of Abbreviations, Symbols, and Acronyms

<u>Abbreviation/Symbol</u>	<u>Definition</u>
α	Angle of Attack
ξ	Downstream Spacing
#1	First Wingman, or Second Aircraft
#2	Second Wingman, or Third Aircraft
2-D	Two-Dimensional
3-D	Three-Dimensional
AOA	Angle of Attack
AEF	Air Expeditionary Force
AFB	Air Force Base
AFFTC	Air Force Flight Test Center
AFIT	Air Force Institute of Technology
AFRL	Air Force Research Laboratory
ANOVA	Analysis of Variance
AR	Aspect Ratio
b	Wingspan
b'	Horseshoe Wingspan
C_D	Drag Coefficient
C_L	Lift Coefficient
CR	Cruise Configuration
D	Drag Vector
DAS	Data Acquisition System
DS	Drag Savings
E	Efficiency Factor
FTT	Flight Test Technique
HASC	High Angle of Attack Stability and Control

Abbreviation/SymbolDefinition

HVM	Horseshoe Vortex Model
KIAS	Indicated Airspeed in Knots
K_{xx}	Induced Drag Correction Factor
L	Lift Vector
NACA	National Advisory Committee for Aeronautics
NASA	National Aeronautics and Space Administration
PA	Powered Approach Configuration
SPC	Leading Edge Suction Multiplier
TPS	Test Pilot School
UAV	Unmanned Aerial Vehicle
UCAV	Unmanned Combat Air Vehicle
UHF	Ultra-high Frequency
UPT	Undergraduate Pilot Training
USAF	United States Air Force
V	Velocity Vector
V_{cruise}	Cruise Velocity in Free-Stream Air
V_{vortex}	Vortex Velocity
W	Upwash Vector

Abstract

This thesis explores the benefits of flying in a tight formation, mimicking the natural behavior of migratory birds such as geese. The first phase of the research was to determine an optimal position for the wingman of a tight formation flight of T-38 *Talon* aircraft using the HASC95 vortex lattice code. A second wingman was then added to determine the benefit derived by increasing formation size. The second wingman was predicted to derive an even greater induced drag benefit than the first wingman for T-38s operating at Mach 0.54 at a 10,000-foot altitude. The predicted values were 17.5% savings for the second wingman versus 15% for the first wingman.

The flight test phase flew two and three-ship formations to validate the computational work. The results of the two-ship flight tests showed with 80% confidence that the wingman saved fuel in the predicted optimal position (86% wingspan lateral spacing). This position yielded actual fuel savings of $8.8\% \pm 5.0\%$ versus the predicted 15%. The other lateral positions did not show a statistically significant fuel savings. The flight test team felt that the three-ship formation data was inconclusive due to the difficulty of trying to fly a stable position as the third aircraft in the formation without station-keeping ability.

The analytical study was accomplished at the Air Force Institute of Technology, Wright-Patterson AFB. The flight test was conducted at the USAF TPS, Edwards AFB, California. The flight test was performed in three USAF T-38 *Talon* aircraft modified to give accurate fuel flow readings as a gauge of drag savings.

AN ANALYTICAL STUDY OF T-38 DRAG REDUCTION IN TIGHT FORMATION FLIGHT

I. Introduction

Background

For centuries, humans have observed and tried to interpret the behavior of migratory birds such as geese, especially the natural tendency of the birds to fly in a tight formation. It stands to reason that birds have learned to work with the laws of nature, so the cooperative behavior of formation flight must be mutually beneficial to the flock as a whole. Indeed, this benefit is due to the effect of the vortex wake coming from the lead bird on the birds in trail. In the military, the formation concept has been used for its defensive value to the entire flight, not for fuel savings. The basic rationale for formation flight is to position the aircraft in such a way that they can enhance mutual survival in a hostile environment. This formation geometry became known as the *fighting wing*, or *welded wing*, concept (12:196-197). It has a strategic advantage, but offers no drag benefit. In today's environment of rising fuel costs and increasing demands on aircraft range, it is time to look back at the behavior of birds and apply nature's solution for drag reduction in aircraft formations. The results of this research will be extremely beneficial for manned flight with automatic station-keeping controllers to alleviate pilot workload, or to UAV or UCAV formations.

The basic premise behind reducing induced drag in tight formations is to use the vortex of the lead aircraft to give a slight upwash vector (W) to the wingman's wing,

provided the wingman is properly positioned in the formation. The geometry of drag reduction is shown in Figure 1-1.

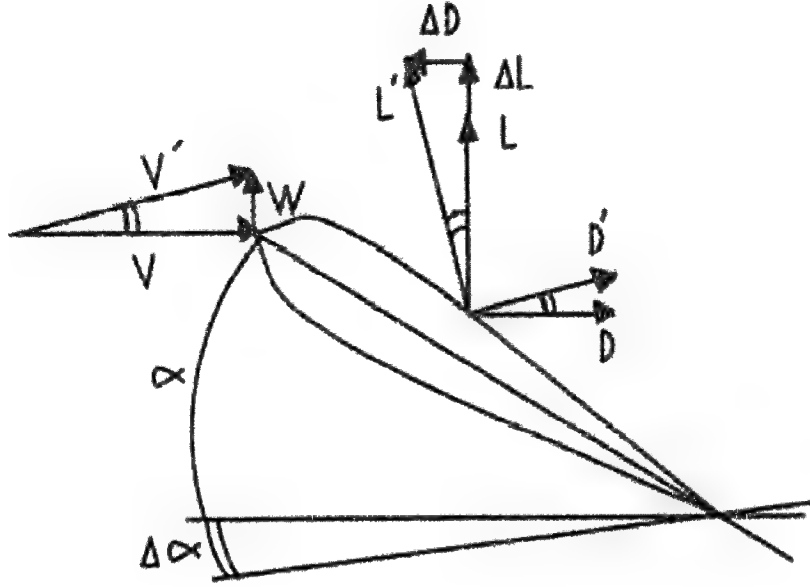


Figure 1-1. Rotation of Lift and Drag due to Upwash (11:1235)

Using small angle approximations, where L and D are the original lift and drag components and L' and D' are the lift and drag with upwash, W :

$$L_{Total} = L' \cos(\Delta\alpha) + D' \sin(\Delta\alpha) \approx L' + D' \Delta\alpha \approx L' \quad (1-1)$$

$$D_{Total} = D' \cos(\Delta\alpha) - L' \sin(\Delta\alpha) \approx D' - L' \Delta\alpha \quad (1-2)$$

A small angle approximation gives the relation:

$$\Delta\alpha = \tan^{-1}\left(\frac{W}{V}\right) \approx \frac{W}{V} \quad (1-3)$$

Hence the drag reduction becomes:

$$\Delta D \approx \frac{L' W}{V} \quad (1-4)$$

A finite wing produces a vortex trailing each wingtip. There are various degrees of fidelity in modeling the vortex flow behind the lead aircraft. The vortex generates a tangential velocity downward (relative to the aircraft) on the inboard side and upward on the outboard side. The simplest model is the Horseshoe Vortex Model (HVM) described by Hummel (6:3-4) among others. This model assumes a simple horseshoe shaped vortex with a span of reduced width, b' (b is the original wingspan). The derivation shows the value of b' to be:

$$b' = \frac{\pi}{4} b, \text{ or roughly } \frac{3}{4} \text{ span.} \quad (1-5)$$

This model has been widely used, both for tight formation controller design (11) and in numerous papers on bird migratory behavior simulation (Hummel (5) and Lissaman and Schollenberger (8)). The Horseshoe Model predicts the position described by Equation (1-5) to provide the greatest drag savings for the wingman.

In an attempt to increase the fidelity of the basic HVM, NASA developed a Vortex Lattice Code called HASC95 (2). Essentially, it breaks down the surface of the aircraft into a user-determined number of horseshoe vortices and predicts the overall vortex effect. Blake and Multhopp (3) did an extensive formation flight study comparing the HASC95 and HVM results. Their results for a rectangular wing predicted a vortex core approximately in line with the wingtip of the generating aircraft. The results for the given wing predicted the maximum drag reduction would occur at 5% wingspan overlap. This compared with the 22% overlap predicted by the HVM. The HASC95 method moved the wingman's optimal position towards the wingtip-to-wingtip, or "welded wing," line as opposed to the overlapping wingtips of the HVM. In both cases however,

this optimal position was found without due regard to the trim losses incurred by the wingman. As the wingman moves from directly behind the leader (assuming wing on left side of lead), the rolling moment will go from positive to negative, with the point of reversal occurring at about the $\frac{3}{4}$ wingspan point. The HASC95 code prediction for optimal position put the wingman very near the point of maximum negative rolling moment. However, as the aircraft is trimmed in roll to negate this moment, trim drag will increase due to the required aileron deflections. This thesis will examine the effect of these deflections.

An important consideration in the dynamics of the formation is the effect of the wingman on the lead aircraft in subsonic flow; if the wingman is close enough he will have an upstream effect on the leader. Blake and Multhopp also discussed this effect, represented by Figure 1-2.

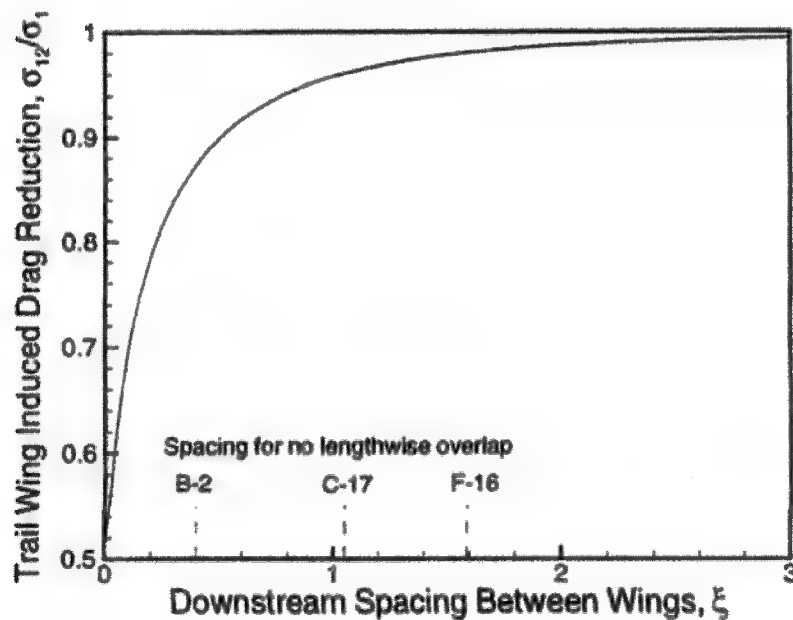


Figure 1-2. Effect of Streamwise Spacing on Lead/Wing Benefit (3:477)

Figure 1-2 shows the spacing required for the wingman to incur most of the benefit of the drag reduction. The term, σ_{12}/σ_1 , is the percentage of the total drag reduction obtained by the wingman. The downstream spacing, ξ , is given in wingspans. At $\sigma_{12}/\sigma_1 = 0.5$, the two aircraft are side-by-side, i.e. the downstream spacing is zero. As the wingman moves back in the formation, he will enjoy more of the benefit in relation to the leader. The figure also gives a safety consideration reference for no lengthwise overlap of the fuselages for specific aircraft. For the T-38 *Talon*, the no-overlap point is at about 1.8 wingspans. The flight test portion of this research used a spacing of $2 \frac{1}{2}$ wingspans to give the wingman essentially all of the benefit. This spacing still provided good visual cues to the wingman, allowing the wing aircraft to stay in the optimal position with respect to the leader. This facilitated the measurement of the achieved reduction in drag since the wingman was the primary instrumented aircraft. For the formation to reap the benefits of range increases, the lead position would have to be rotated. This rotation will be discussed later in Chapter 2. Blake and Multhopp (3:480-481) provide an excellent discussion of various procedures to accomplish this rotation, preferring the echelon formation.

Hummel published flight test results for a two-ship of Do-28 aircraft in a formation (6:8-12). He found a decrease in power required of about 15%. This deteriorated rapidly as the lateral spacing moved away from his optimal position of wingtip-on-wingtip separation. Longitudinal separation did not degrade his results appreciably until the wingman was four wingspans behind the leader. He did not present any data with less than wingtip-to-wingtip lateral clearance.

As for the effect of multiple wingmen, Hummel's paper hypothesized the formation benefits increase with more wingmen up to a limiting value for an infinite formation. Hummel predicted, using HVM, a 10% total power reduction for the two-ship formation, versus about 13-14% for a three-ship formation. The infinite number of aircraft formation asymptotically yields about 26% savings in power. His results are reproduced in Figure 1-3.

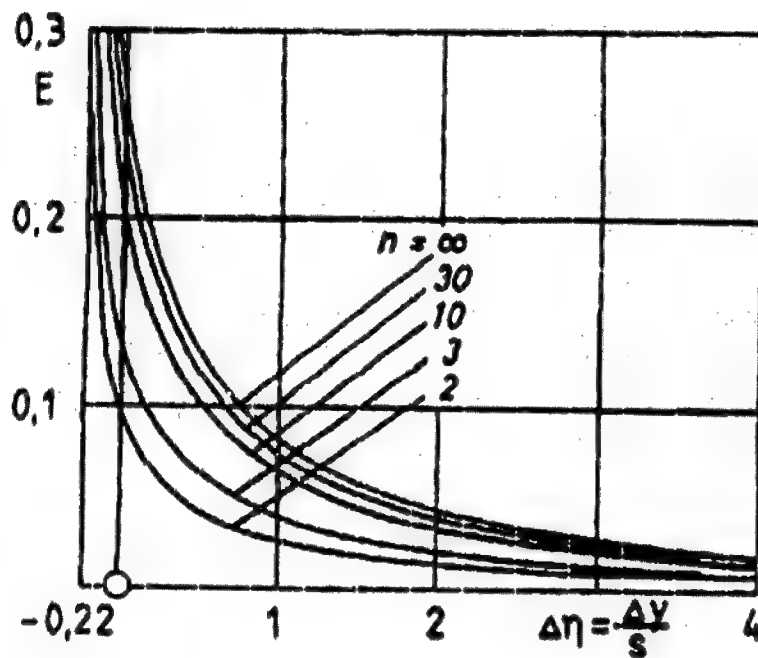


Figure 1-3. Hummel's Theoretical Multi-Ship Formation Savings (6:4)

In Figure 1-3, the vertical axis, E , is the efficiency factor, which is the improvement in range for the n -ship formation. The big, open circle on the horizontal axis represents the $\pi/4$ position, although Hummel did not flight test anything inside of his zero wingspan position. This is a different notation from this thesis in that one span

in this thesis corresponds to Hummel's zero wingspan. Hummel's -0.22 is therefore the $\pi/4$ position. The figure shows the efficiency increasing asymptotically as it approaches Hummel's optimal position. This figure was based on a plane vortex sheet as opposed to a rolled-up vortex sheet with a core. The rolled-up sheet would exhibit behavior that would peak at the optimal point, then show a decrease in the efficiency as one would expect. This is discussed in Hummel's work as well.

Objectives

The objective of this thesis was to examine the induced drag reduction in tight, multi-aircraft formation. The intent was to validate the predictive power of two current vortex models (one simple, one complex) by comparing the results to flight test data. In an analysis where trim effects were ignored, the models gave two different optimal positions. The HVM predicted an approximately $\frac{3}{4}$ wingspan optimal lateral spacing, while the HASC95 model predicted an optimal position closer to one wingspan. The analysis was restricted to an in-plane vertically (co-altitude), $2\frac{1}{2}$ wingspan longitudinal separation. Therefore, the only variable spacing was in the y-direction, or the lateral spacing. All spacings were non-dimensionalized to the wingspan, so that a spacing of one was when the wingtips would just touch each other if the longitudinal separation were zero (essentially a physically joined, or "welded wing"). To hold this position, the wingman had to trim the aircraft to relieve the associated control pressures, thus creating increased drag from the deflected ailerons. As the aircraft moved from the center of the trailing vortex to this optimal position, it would go from a very strong positive rolling moment to a strong negative moment (assuming the wingman was to the left of lead). As

it moved through the vortex, it would encounter a position of zero rolling moment. The drag reduction at this point is theoretically less than that achieved at the optimal position, but the optimal position calculation doesn't include the drag effects introduced by the deflected control surfaces to account for lateral retrim. This thesis investigated the optimal position of the wingman when the trim losses were taken into account. The flight test evaluated four positions to determine which was the best to fly for the wingman. The flight test showed that the HASC95 code with the trim drag effects included predicted the best of the four evaluated test points.

The second part of the thesis extends the work to three airplanes (two wingmen) using the vortex lattice code HASC95 provided by AFRL at Wright-Patterson AFB. The code had not been run in a three-ship configuration, so this required modifications of existing code available at AFRL for a third airplane. These results give a theoretical prediction of the induced drag reduction benefit achieved by the third aircraft. The code predicts what effect the combination of the leader's and the first wingman's vortices has on the second wingman (third airplane).

The final step was the flight test of the three-ship formation using the optimal position found in the two-ship flight test and comparing data with the code to determine its value as a multi-ship predictor of induced drag effects. Even if the #2 wingman sees the exact same benefit as the #1 wingman, the entire formation's range would be extended more than a single wingman's by simply rotating the lead aircraft at specified times. However, it was shown theoretically that the #2 wingman sees an even greater drag reduction benefit than the #1 wingman. Unfortunately, the three-ship flight test proved inconclusive for reasons discussed in Chapter 4.

The flight test portion was accomplished on specially instrumented T-38 *Talon* aircraft with the ability to accurately measure fuel flow as an indicator of induced drag reduction. The formation was a similar aircraft formation, meaning lead and both wingmen were T-38 *Talons*. The flight was manually flown without the benefit of an automatic controller, although a chase aircraft was utilized initially to provide position awareness to the formation.

Research Focus and Limitations

The focus of this effort was on incorporating a model of the T-38 into the HASC95 code and using it as a predictor of the effects of the vortex wake on a tight formation flight of two and three-ship formations of T-38 aircraft. The constraints of the HASC95 program affected the model, as the dimensions had to be altered slightly to produce a workable solution. This had a minimal effect on the results and was not determined to be a limiting factor in the project. This limitation is discussed in further detail in Chapter 2.

The main focus in the two-ship phase of this research was to incorporate control surface deflections into the code and to determine the induced drag savings of the wingman flying a trimmed aircraft in the optimal position. This optimal position was then compared to the HVM and HASC95 models for use in predicting the most fuel-efficient lateral formation spacing.

The focus of the three-ship formation research was to determine how well the HASC95 code predicted the induced drag reduction benefit when applied to multiple wingmen. Using the results of the two-ship flight test of the first phase, the three-ship

flight test focused on the position deemed optimal for the wingmen. One of the limitations in the three-ship case was the ability of the code to run a full-up 3-D model of all three airplanes due to internal constraints of the HASC95 program. The program only allowed a finite number of elements to complete an analysis of the formation. This limitation is discussed in detail in Chapter 2.

Another limitation in the three-ship case was the current code's lack of ability to change the relative angles-of-attack on the three airplanes. They must all be trimmed at the same angle-of-attack for the code to run, resulting in different lift coefficients for each aircraft. Obviously, the formation dynamics dictate that all three airplanes must be operating at the same lift coefficient to maintain position, so a correction factor based on biplane theory is used to account for this problem.

Perhaps the biggest limitation of HASC95 was the additive nature of the code, meaning the vortices produced from each element on the aircraft wing were directly added to any produced upstream. Because of this, the #2 wingman sees the vortex effects of the leader directly, without any of that vortex being altered by the #1 wingman. In reality, it is highly unlikely the flow would go unaltered as the code predicted. The flight test was unable to shed light on how much the vortex is altered from the simple, superposition-based, method.

A final set of limitations came into play during the actual flight test. The first was the lack of an automatic station-keeping controller aboard the T-38s. The pilot had to manually hold the position using visual references and explore the envelope to feel for the maximum rolling moment or no-rolling moment positions. Unfortunately, without the benefit of an automatic controller, the pilot was limited in the amount of time spent

holding this spot due to the workload required. An automatic controller would have required the availability of an onboard sensor, which was beyond the scope of this project. Another limitation was the ability during the flight to accurately measure the position of one aircraft relative to another. The pilots did this by using visual cues briefed and tested on the ground, as well as a chase aircraft providing audio cues over the radio as needed.

Payoff of Research

With the availability of a formation-hold autopilot and a rotating lead aircraft, a formation's range can be extended in a very cost effective way compared to other modifications (power plant, airfoil, etc). This gain is solely based on using the laws of nature in a more efficient manner. The next chapter will show that HASC95 estimates the #1 wingman can achieve a 15% fuel savings and the #2 wingman can expect 17.5% fuel savings. If these optimally spaced wingmen were to achieve this reduction in fuel flow, the entire formation could extend its cruise range by 11.5%! This is totally free -- nothing is added structurally, no wonderfully efficient engine has been designed, the payload remains the same, etc. The only cost would be a station-keeping system to relieve the pilot workload of staying in the optimal position. The fuel savings derived from tight formation flight are potentially groundbreaking in terms of economizing long-range flights of multiple aircraft such as Air Expeditionary Force (AEF) deployments or Unmanned Aerial Vehicle (UAV) formations. The payoff of this research is high.

II. HASC95 Analysis

This chapter deals primarily with the vortex computer code portion of the project. The first step was to incorporate the T-38 aircraft geometry into a FORTRAN model that could be used by the vortex code. The second step involved comparing this model to actual aircraft data to see if the two were similar enough to consider the results credible. The third step was determining if a 2-D model would suffice instead of a 3-D model in the two-ship run. The 2-D model was more attractive in some aspects as will be discussed in the appropriate section. The next step was to run a sweep of the wingman through the leader's vortex to find the two-ship, no-trim loss, optimal position, in order to validate the model against past research. The fifth step of the project was the three-ship, no-trim loss run, to determine the additional benefits derived by the #2 wingman (or third ship). Next, the code was modified again to put aileron deflections in, and a two-ship, trimmed case was run to examine the effects of trimmed aileron deflections on the optimal position. Finally, the code was run again with the second aircraft trimmed, allowing the #3 wingman to sweep across an optimally placed #2 wingman. The last two steps were the main thrust of this thesis, as neither had been done before in past research with a vortex code.

It is important to note the wingman terminology as far as numbering goes. This thesis will refer to the first aircraft as Lead, or the lead aircraft. The first wingman is the #1 wingman, while the second wingman is the #2 wingman. This may seem insignificant, however it is important to note that the number is NOT the position of the aircraft in the formation. The numbers refer only to the sequential number of wingmen.

Transforming the T-38 into a HASC95 Model

The initial step of the project was choosing an aircraft. The T-38 was a logical choice due to its availability and operating cost (especially since three were needed to form the formation and one to chase). This also turned out to be a fortuitous choice due to its very simple geometry. It has no incidence on the wings and a simple planform shape that fit quite nicely into the file to be called by the FORTRAN code.

As was pointed out in the Limitations section of Chapter 1, the geometry had to be modified slightly to make the lattice elements line up correctly. The trailing vortices from each lattice element are aligned with the element edges, while the control points are centered within the element. In order to obtain a good solution, no vortices can overlap a control point on an element downstream. For a single aircraft, this can easily be accomplished by defining suitable panel break points. For example, to model a wing and tail, the wing can be broken into two spanwise panels, with the panel edge corresponding to the tip of the tail. If an equal number of spanwise elements are used on the panel where the wing and tail overlap, there will be no vortex/control point problem. Additional panel breaks can be inserted for fuselage, inlet, and flap segments. To do a formation flight analysis, each panel of the entire aircraft must be broken into elements of equal width. If the trail aircraft is moved laterally with respect to the lead aircraft in integer multiples of this width, the vortices and control points will never overlap. To accomplish this, slight adjustments to the actual aircraft geometry were made. For this case, an element spacing of 8.5 inches worked out nicely. This gave 36 total spanwise elements, which corresponds to a wingspan of 306 inches as opposed to the actual wingspan of 303 inches. All other dimensions were much closer than the three-inch

deviation on the wingspan. This difference in dimension was negligible to the results. The actual geometry of the T-38 is shown in Appendix C and can be compared to the model dimensions in Appendix A.

Another limitation to work with was the number of panels allowed by the program, the limit being 20 panels. The addition of flight controls put the model right at 20. Due to symmetry, this allowed 10 panels for each side. The panels can be seen in the model (Appendix A) and include: the 1) tailpipe, 2) elevator, 3) aft-fuselage, 4) outer wing, 5) aileron, 6), mid-wing, 7) inner wing, 8) mid-fuselage, 9) engine, and 10) forward fuselage. The code used a Leading Edge Suction Multiplier (or SPC) for the boundary condition on the panel (2). An SPC of zero implies that the leading edge of the panel does not see the flow, whereas a value of one implies that the leading edge of the panel sees 100% of the flow. This necessitated dividing the wing into four panels. The inner, mid, and outer wings get an SPC of one, along with the forward fuselage, and engine. The tail would have been logical to separate into two panels so it could get an SPC of one outboard of the fuselage line and a zero inboard of the line. The panel limit of 20 didn't allow this, so the tail is set with a boundary condition, or SPC, of .45, which is the area of that panel that sees the flow.

The *wing* file for the aircraft build-up is shown in Appendix A along with the rest of the code. The *mt38a.f* file reads the wing file before the *hasc* (the vortex code) subroutine is called. The *prisrf.f* file is the code that breaks out the *hasc* data into the wing and lead aircraft and calculates the data of interest, i.e. lift and drag coefficients. The actual aircraft model in 2-D is shown in Figure 2-1. The 3-D model in formation is shown in Figure 2-2. The 2-D versus 3-D issue will be discussed later in this chapter.

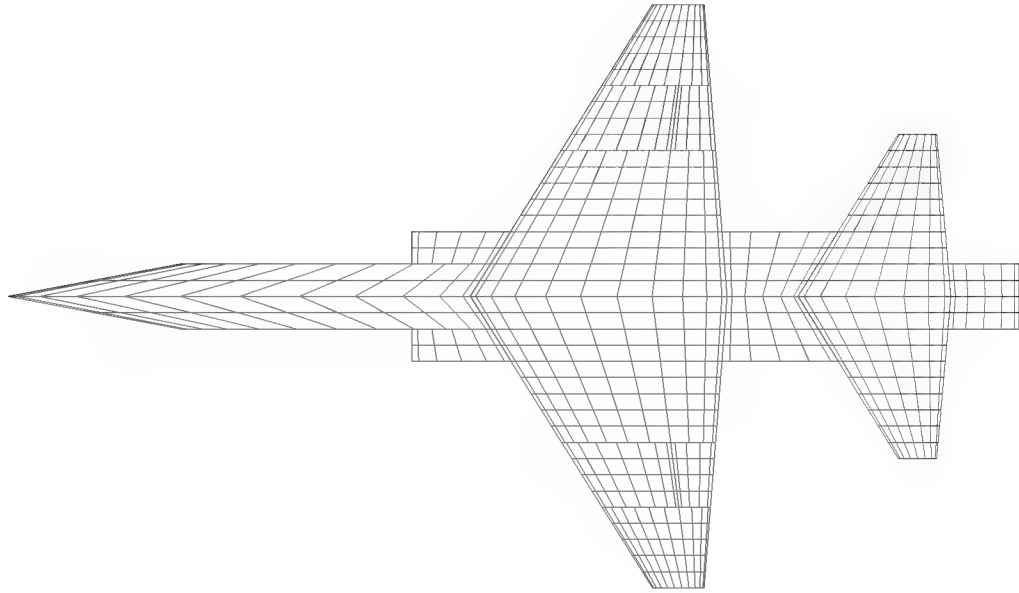


Figure 2-1. 2-D Model of T-38 for HASC95 Input

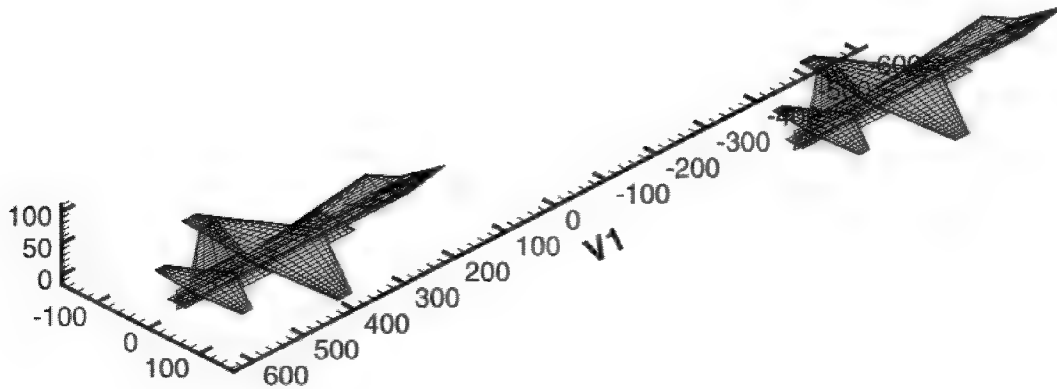


Figure 2-2. The 3-D Model in Formation with Spacing = 1

Validation of the Model Against Actual T-38 Data

The next step in the process was to compare model predictions to actual T-38 data. This was done to confirm the theoretical data acquired from the code had some credibility when compared to the actual flight test. The best way to accomplish this task was to simply run the model as a single ship at a given condition. From the author's experience flying formation in the T-38, an altitude and airspeed of 10,000 feet and 300 KIAS was chosen. This was a reasonable envelope to fly the formation due to the safety concerns of vortex ingestion into the T-38 engine at higher altitudes. This condition roughly translates to an angle-of-attack of three degrees and a Mach number of 0.54, which were the values used for the HASC95 analysis. The Special Program Office at Kelly AFB provided the T-38 Simulator Manual (7), which contained look-up tables for the Undergraduate Pilot Training simulators. Using these numbers, the lift and drag of the model were compared to the actual aircraft at the same conditions. The results were very close:

Table 2-1. Comparison of Simulator Data to HASC Model

<u>SIM DATA</u>	<u>HASC MODEL</u>	<u>% DIFF</u>
$C_L = 0.2342$	$C_L = 0.2344$	0.09 %
$C_{Di} = 0.0059$	$C_{Di} = 0.0053$	10.1 %

As can be seen from the data, the lift coefficient, C_L , is almost perfect. The drag coefficient, C_D , is further off, so the numbers were examined a different way to see if they make sense. Numerous textbooks such as McCormick (9:185-195) give the well-

known equation for induced drag from basic wing theory:

$$C_{Di} = \frac{(1 + \sigma)C_L^2}{\pi AR} \quad (2-1)$$

AR is the aspect ratio, which is 3.75 for the T-38, while σ is an efficiency factor for non-elliptical wings. Using this formula with the HASC95 data, the elliptical wing at the same C_L would give $C_D = 0.0047$, so the efficiency factor is about 0.13, which is a realistic number for the airplane. The higher number for the simulator data could be a factor of a non-parabolic drag polar curve. In the absence of actual T-38 data, data for the F-5B was obtained from the Air Force Research Lab (1). The F-5B, aerodynamically, is virtually the same aircraft with slight modifications. According to the data, there is a C_L breakpoint around 0.5 Mach, resulting in a steeper C_D curve at this point and beyond. Since this divergence occurs before the Mach = 0.54 point where the data was being run, it was most likely a factor in the accuracy of the absolute drag value. This may be why the simulator numbers don't agree better with the HASC95 numbers. The code did not account for this factor, but the results should be valid as long as they are used to predict relative savings, not exact drag numbers.

The rest of the coefficients (side force, pitch moment, etc), while important, are very difficult to compare since a 2-D representation of the aircraft was used. For instance, without a vertical tail, the side force prediction was meaningless as a data point. The basic idea of comparing the data to the model was to get a reasonable idea of the predictive capability of the code as far as lift and drag were concerned. Overall, the computer model of the T-38 provided accurate results in approximating relative data like drag reduction, while it may not have done as well predicting absolute values like actual

induced drag. Since this research was only interested in the relative savings, the model was sufficient for the theoretical formation runs.

Two-Dimensional Versus Three-Dimensional Model

The third step in the theory build up pertained to the fidelity of the model in two dimensions versus the three-dimensional model. The three-dimensional model was actually a horizontal plane and a vertical plane, so in reality, it was not a true 3-D depiction of the aircraft. While it lacked roundness, the 3-D model did allow for a vertical tail and the ability to calculate side forces resulting from the tail. It also allowed for the analysis of the formation in a fully trimmed case, i.e. rudder, elevator, and ailerons. From this discussion, it seems the three-dimensional model should have been the model of choice. There was a very good reason it was not, however.

Looking back at Figure 2-1, one can see the individual little squares in the grid. While the HASC95 program calls them panels, the nomenclature used here refers to panels as the 20 bigger surfaces, so they were termed elements. There were 664 elements on the 2-D model. The basic premise behind the HASC95 program was that it calculated a horseshoe vortex for each one of the elements depending on the geometry and boundary conditions. The program was not set up to run any system with more than 2000 elements. If the number of elements were reduced, the fidelity of the model suffered, especially if they were taken out of the wings. The 2-D, three-ship model used 1992 elements, or horseshoe vortices, for the calculation. Obviously, if the vertical plane were added to make the model 3-D, it would have far exceeded the 2000 element limit.

One solution to this problem was to run the two-ship phase of the program with

the three-dimensional model and the three-ship phase with the two-dimensional model. This was not done since the optimal position results of the two-ship case were used to run the three-ship case. To see if this was reasonable, the 2-D and the 3-D cases were compared.

The results of running the two cases showed almost no distinguishable difference between the two models as far as the drag savings went (drag calculations are discussed in later sections). Figure 2-3 shows the difference in rolling moment between the two cases. Again, there is almost no difference between the two models.

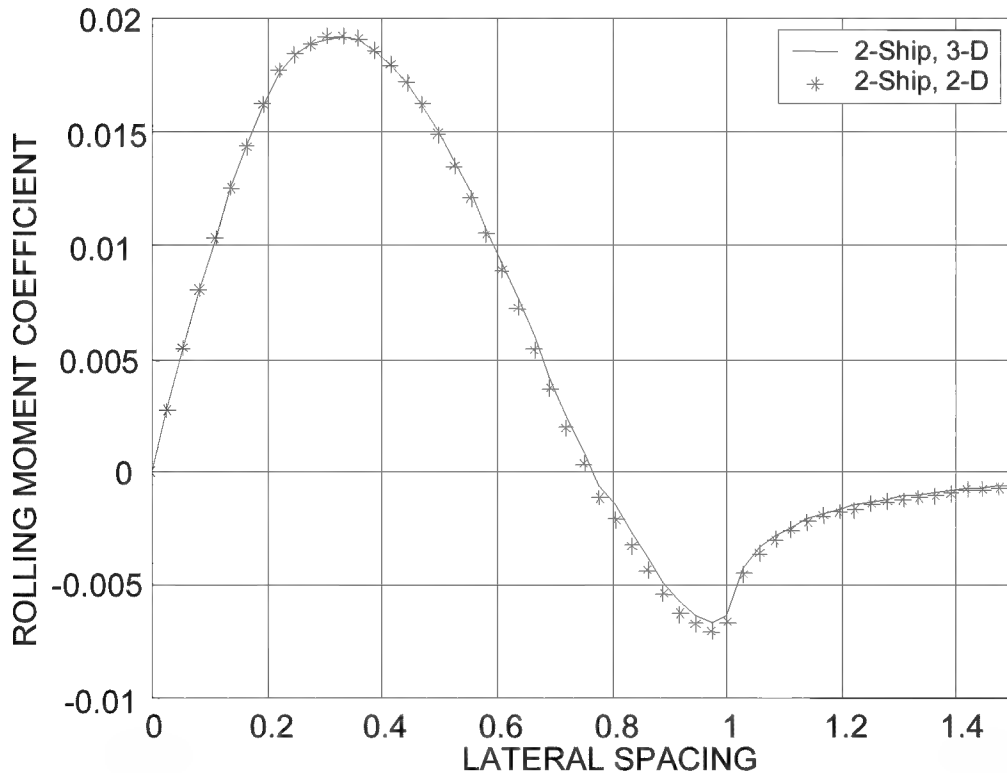


Figure 2-3. Comparison of the 2-D versus 3-D Model: Rolling Moment

Based on the results of comparing the two cases side-by-side, it can be seen that little was lost by going to the two-dimensional model for the rest of the project. Later research may want to investigate side forces, yaw coefficients, etc. and would require an enhanced model at the expense of running only two aircraft or a less accurate model. Another option would be to modify the HASC95 code. The last option was beyond the scope of this project.

An important consideration in looking at Figure 2-3 was the roll stability of the wingman in the formation. The wingman (positioned to the left of Lead) will have positive stability when $dC_l/dy > 0$, where C_l is the rolling moment coefficient. From the figure, this means the wingman would be stable in roll from zero wingspan (i.e. as in air refueling) up to about 1/3 wingspan spacing, and again at one wingspan and greater spacing. A disturbance in lateral spacing outside of these points would introduce a rolling moment away from the direction that would return the wingman to the desired position. Therefore, the wingman was unstable in roll between these two points, making it challenging for the pilot to stay in the position. As pointed out previously, an automatic controller would immensely help the pilot in a tight formation geometry.

Optimal Position Determination: Two-Ship, No-Trim Losses

The next step entailed taking the model of the T-38 *Talon* and putting it into a two-ship formation to evaluate the optimal position, while neglecting the effects of retrimming the aircraft. The rolling moments were also evaluated and compared with past data such as Blake's rectangular wing formation model (3).

The basic idea of running the sweep was to move the wingman in increments of 8.5 inches from directly behind the lead aircraft out to 1.5 wingspans, or 459 inches (38.25 feet). The aircraft were kept in the same plane and at the same streamwise distance of 2 ½ wingspans (or 63.75 feet) from wingtip-to-wingtip. A FORTRAN code was written with a call to the HASC95 vortex code embedded in the lateral sweep loop. For each spacing position, the aerodynamic coefficients were written to a separate file to be plotted after completing the run of the wingman through the entire sweep.

The biggest challenge in this phase was evaluating the numbers for the lift and drag results. The problem was that the two aircraft came out with differing lift coefficients, C_L (see Appendix B for data points). This obviously can't be the case in a real formation, as each aircraft must be operating at the same C_L (assuming the same weight). If the lift coefficients are not the same, the formation dynamics (i.e. spacing and altitude between aircraft) could not be maintained. This issue of differing lift coefficients is nothing new. Biplane researchers were looking at this phenomenon as early as the 1920s. Munk's stagger theorem, summarized in Prandtl's NACA paper (11), resolved this problem. From Munk's work, the induced drag for a wing in a system of aircraft is:

$$C_{D,j} = C_{D,j_o} + \sum_{i \neq j} K_{ij} C_{L,i} C_{L,j} \quad (2-2)$$

The subscript, o , indicates the aircraft in single-ship flight. The summation is the effect of the other aircraft in the formation on the wingman. A quick glance at the equation shows that a negative value for K_{ij} is desirable for reducing the induced drag of the wingman. The equation obviously allows for the differing lift coefficients of each aircraft. All of the following equations go against the wingman numbering system used

in this report to avoid using the letter L for Lead and Lift at the same time. Therefore, in the equations, the number is the actual aircraft position (Lead is 1, #1 wingman is 2, #2 wingman is 3).

Using Munk's equation, the induced drag for the wingman becomes:

$$C_{D,2} = C_{D,2o} + K_{12}C_{L,1}C_{L,2} = K_o C_{L,2}^2 + K_{12}C_{L,1}C_{L,2} \quad (2-3)$$

K_o is the correction factor from the wing theory induced drag equation for a single-ship aircraft. For the 2-D T-38 model, HASC95 gave $K_o = .09646$. K_{12} is the correction factor for the effect of the #1 aircraft on the #2 aircraft. The drag reduction is simply the ratio of K_{12} to K_o , or percent savings = K_{12}/K_o . Solving for K_{12} gives:

$$K_{12} = \frac{C_{D,2} - K_o C_{L,2}^2}{C_{L,1}C_{L,2}} \quad (2-4)$$

All of the data in the above equation can be pulled out of the code output, divided by K_o , and plotted to evaluate the drag savings.

It was useful to look at the case where the lift coefficients are the same to make sure the ratio does indeed give the drag savings. The term K_o is independent of the lift coefficients as it is the result of the drag polar curve for the single-ship aircraft. The drag ratio of the wingman to the leader is:

$$\frac{C_{D,2}}{C_{D,1}} = \frac{K_o C_{L,2}^2 + K_{12}C_{L,1}C_{L,2}}{K_o C_{L,1}^2} \quad (2-5)$$

If $C_{L,1} = C_{L,2}$, equation (2-5) reduces to:

$$\frac{C_{D,2}}{C_{D,1}} = \frac{K_o + K_{12}}{K_o} = 1 + \frac{K_{12}}{K_o} \quad (2-6)$$

From examining equation (2-6), the drag saving was easy to see as the aforementioned ratio:

$$\text{Induced Drag Saving} = K_{I2} / K_o. \quad (2-7)$$

In order to see an actual drag saving, the K_{I2} correction factor must be negative. A positive K_{I2} implied that the wingman was in the leader's downwash and was experiencing an adverse effect of flying in the formation. If the K_{I2}/K_o ratio was -0.6 for instance, the drag saving would be 60%. The ratio of the induced drag was indeed $C_{D,2}/C_{D,1} = 0.4$, or 40%, which agreed with the 60% savings.

Figure 2-4 and Figure 2-5 show the results of running the two-ship, no-trim loss model.

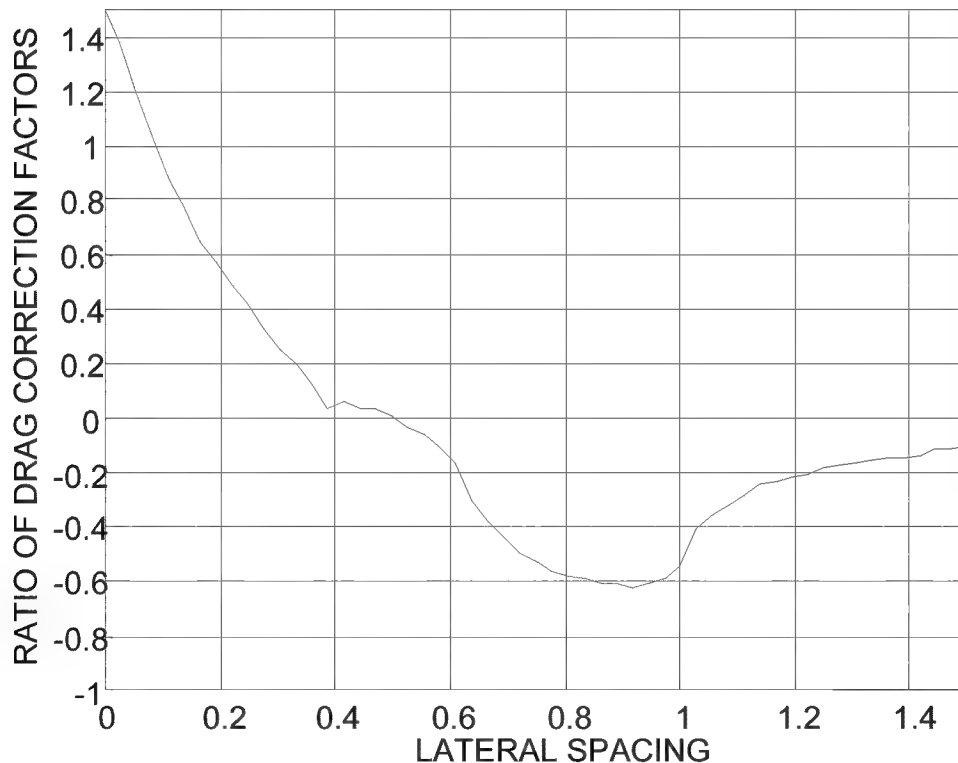


Figure 2-4. Drag Savings for Two-Ship, No-Trim Case

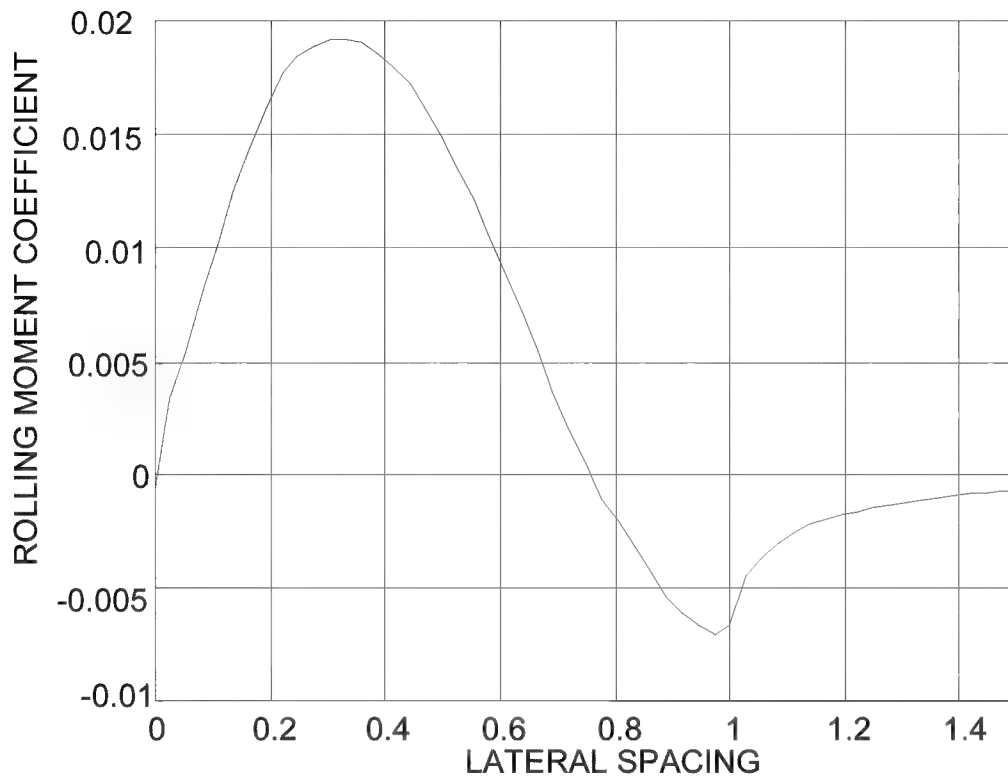


Figure 2-5. Rolling Moment for Two-Ship Case

From the figures above, it was evident that the results paralleled past results with different wings, i.e. Blake (3:478,483). The optimal, no-trim loss position was approximately 0.9 wingspan separation, although there was not a big difference between 0.8 and about 0.95 spacing. However, this was also the range where the rolling moment increased to its maximum negative value (rolling away from lead). The rolling moment was zero at about the $\frac{3}{4}$ wingspan point, which translated to a saving of about 55% as opposed to the saving of 62% at the best no-trim loss point. It was important to note this was a decrease in induced drag only, not in total drag (parasite, pressure, etc.). This was where previous research had stopped. The next two steps were to incorporate another

wingman, and to include the effect of aileron deflections for retrimming the wingman's aircraft.

Drag Savings for a Three-Ship with No Trim Loss

The next step in the process was to build up the code to take a third airplane. As was discussed earlier, there was a limit on the number of elements the code could handle. For this analysis, the wingmen were again swept across the vortex using a single formation spacing between Lead and the #1 wingman and the #1 and #2 wingmen. The lift coefficients for the three aircraft again came out all different, so they had to be corrected as in the two-ship case. The resulting equation, derived from equation (2-2), for the induced drag on the #2 wingman is:

$$C_{D,3} = C_{D,3o} + K_{13}C_{L,1}C_{L,3} + K_{23}C_{L,2}C_{L,3} \quad (2-8)$$

Substituting for $C_{D,3o}$:

$$C_{D,3} = K_o C_{L,3}^2 + K_{13}C_{L,1}C_{L,3} + K_{23}C_{L,2}C_{L,3} \quad (2-9)$$

The coefficient K_o remains the same in the three-ship case as it was in the two-ship case since single-ship dynamics were the same. The effect of the #1 wingman on the #2 wingman in isolation was the same as the effect of Lead on the #1 wingman in the two-ship case since they were in the same relative position, therefore $K_{12} = K_{23}$. Solving for K_{13} , the effect of lead on the #2 wingman, gives:

$$K_{13} = \frac{C_{D,3} - K_o C_{L,3}^2 - K_{23}C_{L,2}C_{L,3}}{C_{L,1}C_{L,3}} \quad (2-10)$$

Now the effect of the lead aircraft on the #2 wingman is simply K_{13}/K_o and the cumulative effect of both aircraft on the #2 wingman is:

$$\text{Drag Savings for \#2 wingman} = \frac{(K_{13} + K_{23})}{K_o} = \frac{(K_{13} + K_{12})}{K_o} \quad (2-11)$$

Figure 2-6 gives the results of the three-ship, no-trim loss analysis.

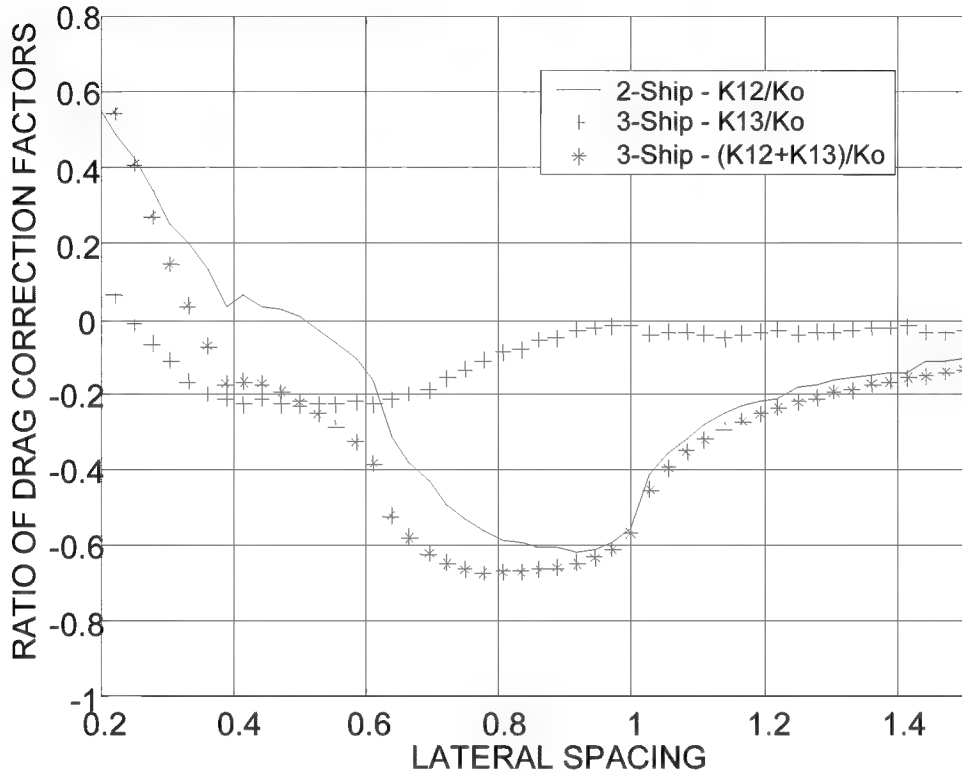


Figure 2-6. Three-Ship, No-Trim Case

The most important result of the three-ship case was that the #2 wingman received an additional benefit over the #1 wingman when the spacing was close enough for the #2 wingman to reap some benefits of the leader's vortex. The leader's effect on the #2 wingman started to disappear at a spacing of one wingspan, which meant the #2 wingman was two wingspans away from the leader. Any spacing larger than that and the #2 wingman's savings approached the savings of the #1 wingman since lead's vortex was essentially not affecting the #2 wingman anymore. The results of the simulation showed

that the #2 wingman had a large, flat area of the curve from about 0.75 to 0.95 wingspans in which the #2 wingman derived about the same benefit. From Figure 2-6, the benefit was about 67% at a spacing of 0.8 wingspan. The #1 wingman had a savings of about 58% at the same spot. At 0.9 wingspan, the #2 wingman saw a 65% savings, versus a 62% savings for the #1 wingman. At about 0.97 wingspan, both of the wingmen experienced a 60% saving.

It was interesting to see the bottom of the drag reduction curve slip to the left for the additional wingman. It begs the question as to whether or not the curve will continue to the left as more aircraft are added. This case was not run due to the limit on the number of finite elements, but it should not change significantly for a fourth aircraft. This is because the #3 wingman would see the vortex from #1 and #2 as seen in Figure 2-6, but the effect of the lead aircraft would not be a factor as the last wingman would be spaced too far laterally spaced to derive any benefit from lead's vortex.

One of the limitations of the program was that it would not account for the leader's vortex being altered by the #1 wingman before reaching the #2 wingman. For this reason, these results were additive in nature, as was discussed earlier. Again, flight test proved inconclusive on this issue as discussed in Chapter 4. Another factor not accounted for was the rolling moment imparted to the wingman from the vortex and the trim losses to counteract it, which is the subject of the next section.

Two-Ship Analysis with Trim Losses Included

The next step was to include the trim drag caused by the aileron deflections required of the wingman to fly in a laterally trimmed condition in the leader's vortex.

Modifying the *wing* subroutine for the deflections was easy enough as the code could accept an angle of incidence for a panel. The hard part of this analysis was the time-consuming task of deflecting the aileron, running the sweep over a limited range, then interpolating between points to find the zero moment position. The T-38 aileron deflections are limited to 14° . In actuality, the greatest deflection (around 0.3 wingspan) was only 9° . The greatest deflection for the negative moment was 2° . Linear interpolation was used to find the zero moment case using 0.25° aileron deflection increments. The results shifted the curve around the zero moment point near the $\frac{3}{4}$ wingspan lateral separation point, as expected. The results are shown in Figure 2-7.

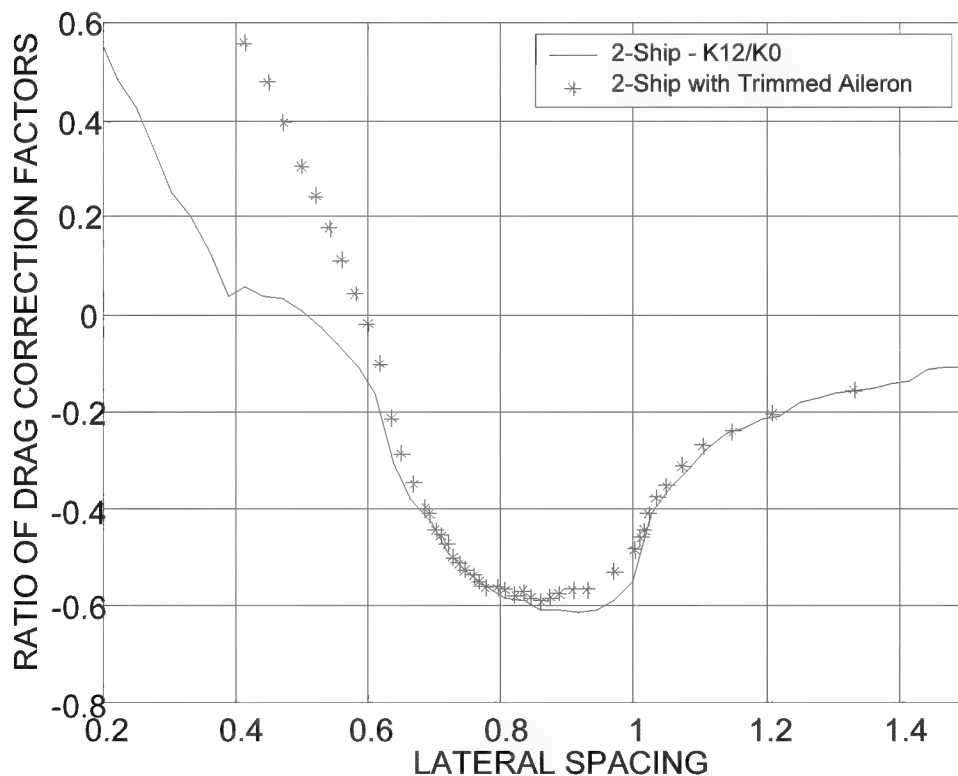


Figure 2-7. Two-Ship, Trimmed Case

The results show the new optimal position for the T-38 model to be at 0.86 wingspan separation where the induced drag reduction is 59%. This result was important because in previous work the two optimal positions were assumed to be $\pi/4$ wingspan by Pacher (10) and Hummel (6) or nearly one wingspan as found by Blake and Multhopp (3). The results showed the best point was somewhere between the two previous points for the T-38 wing geometry. Another interesting point to look at was how much the curve shifted up as the lateral separation was reduced. The breakeven point shifted from 0.5 wingspan to 0.6 wingspan separation due to the large aileron deflections required to trim this rolling moment. It resulted in a tighter envelope for the wingman to stay in to optimize drag reduction.

An important factor to remember was that this analysis included only trimmed ailerons. The real aircraft would also need to be trimmed with the rudder for yaw moments and the elevator for pitch moments. A pitch trim calculation at the zero rolling moment point was accomplished and found to yield nearly the same drag savings. It was not investigated further since the pitch moment does not change much in the region of interest from 0.7 to 1.0 wingspans. The flight test bore this out as very little pitch trim relative to lateral trim was needed as the wingman moved into the vortex. The yaw moment could not be analyzed using a two-dimensional airplane model, so the effects of a trimmed rudder were not considered. Again, flight test showed little tendency for the aircraft to be out of trim directionally when stable in the vortex positions. Both pitch and yaw moments may be something to investigate in a future project with a 3-D model.

Three-Ship Analysis with Trim Losses Included

The last HASC95 run was set up with the #1 wingman in the optimal 0.86 wingspan separation position, allowing the #2 wingman to sweep from directly behind Lead, to positions between Lead and #1, then to the outboard of the formation. The following plots show the results of these runs. There were numerical problems directly behind the #1 wingman, thus the gap in the data. Figure 2-8 shows the entire sweep, while Figure 2-9 shows only the outboard portion of the sweep.

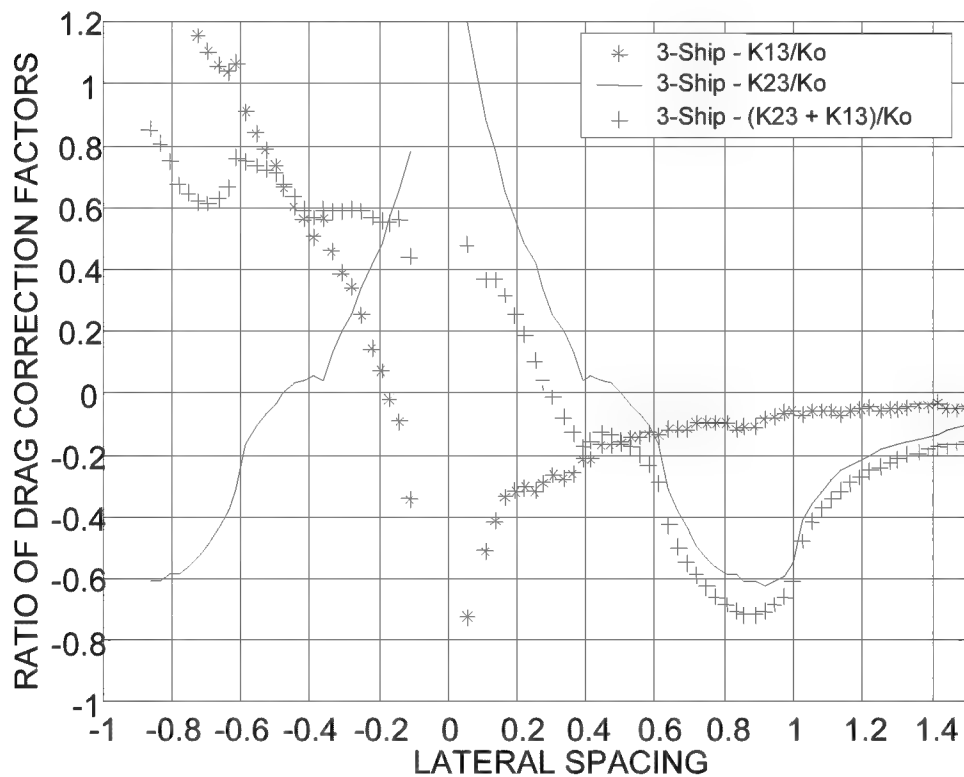


Figure 2-8. Three-Ship Case with Optimally Placed #2

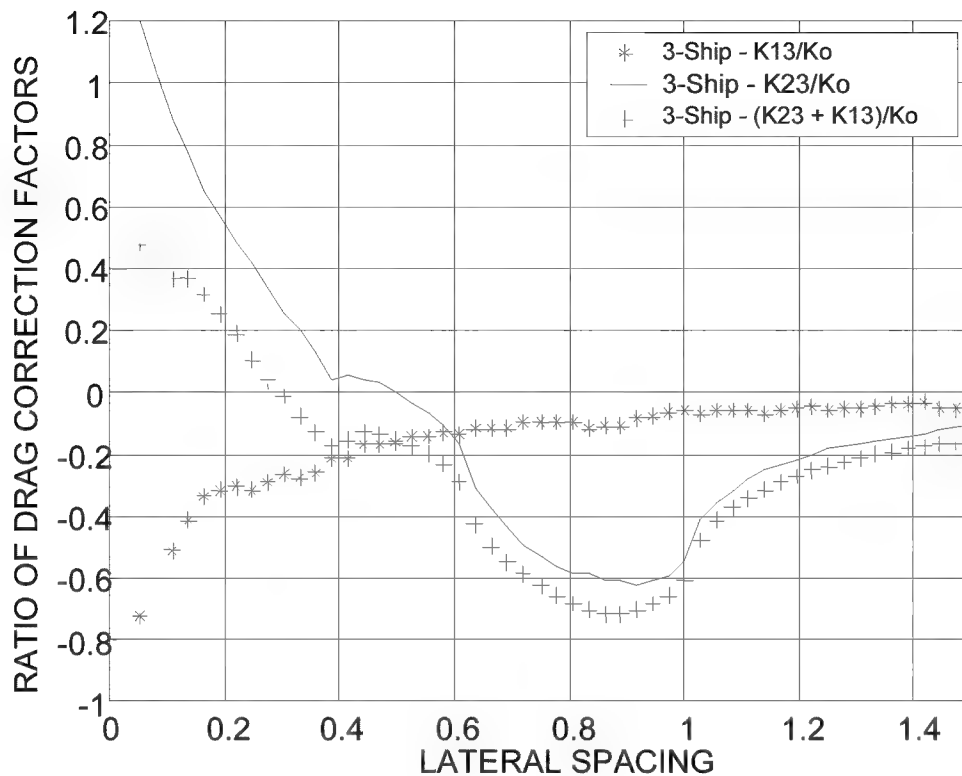


Figure 2-9. Blow-Up of Figure 2.8

The overall drag savings ratio became negative (i.e. beneficial) at 0.3 wingspan separation due to the larger influence of the Lead aircraft on the #2 wingman. There was no spot between Lead and the #1 wingman where the #2 wingman derived any benefit. The best spot for the #2 wingman relative to Lead was at zero (with respect to the #1 wingman), which was actually where the #2 wingman was at the 0.86 wingspan separation point from Lead, as expected. It is very important to remember that this analysis optimized the position of each aircraft for its own drag reduction - it was not meant to represent the optimal overall formation benefit. The ability to optimize the aircraft in a formation with unequal spacings would require a code that was capable of

accurately predicting the alteration of the vortex by the #1 wingman. Since the HASC95 code couldn't do this, each aircraft was optimized separately as to what was the best position for its own drag saving. It was then assumed that this was the best geometry for the overall formation.

The #2 wingman derived a benefit of approximately 70% according to Figure 2-9. This was without the trim penalty however, so in reality the drag savings would be about 2-3% less, as discussed in a previous section. This was due to the rolling moment that is shown in Figure 2-10. By trimming the #2 wingman, it can be expected that drag savings would decrease to about 67%, which was the number used for the following section.

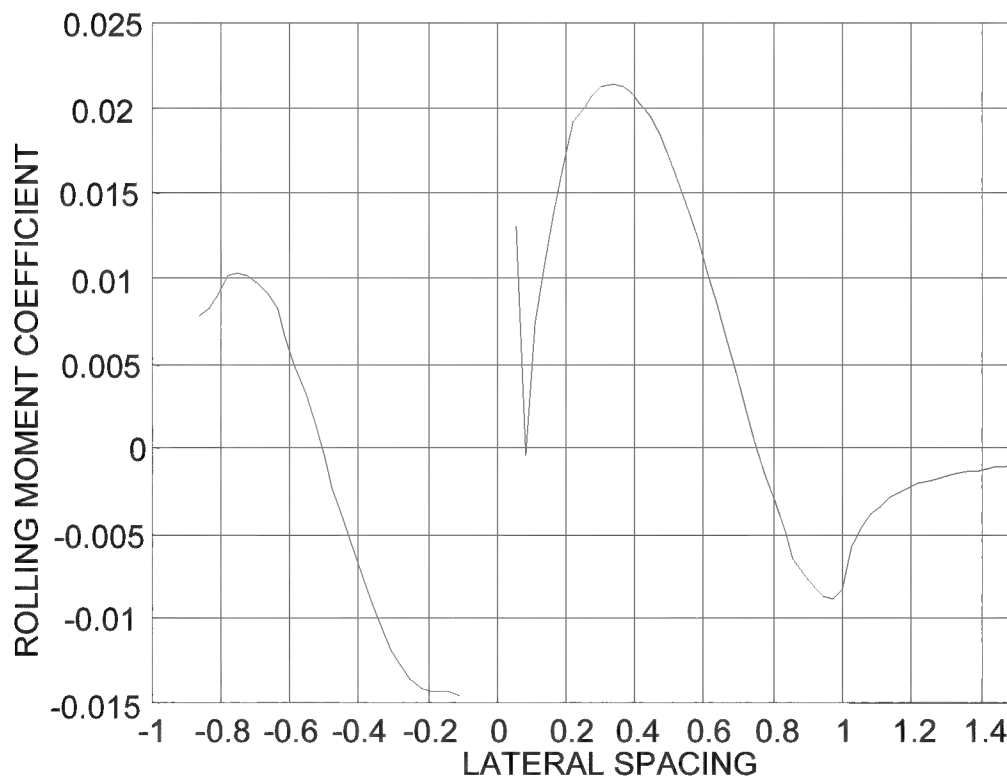


Figure 2-10. Rolling Moment of #3 Wingman

Total Drag Savings

As pointed out previously, the drag saving was only with respect to induced drag, not total drag. The total drag includes friction drag and pressure drag. For instance, in the two-ship case, the 59% saving in induced drag had to be incorporated with friction and pressure drag to get a meaningful total drag reduction result. Using the simulator look-up tables (7), the friction and pressure drag were estimated at $C_{Do} = 0.015$. The total saving then becomes:

$$\frac{C_{D_{tot},2}}{C_{D_{tot},1}} = \frac{C_{Do} + (1 - DS) \times C_{Di,ss}}{C_{Do} + C_{Di,ss}} \quad (2-12)$$

DS is the Drag Saving for the second ship and $C_{Di,ss}$ is the single-ship induced drag coefficient (.0053 for the T-38 HASC95 case). With the second airplane seeing a 59% saving, the total drag relative to a single airplane becomes:

$$\frac{C_{D_{tot},2}}{C_{D_{tot},1}} = \frac{.015 + .41 \times .0053}{.015 + .0053} = .85 \quad (2-13)$$

Thus, the total drag saving for the second ship in a formation is about 15%, a substantial savings. A similar application of Equation (2-12) shows the #2 wingman reaping a benefit of 17.5%.

Implementation Considerations

The fuel savings don't mean much for range if the formation is not rotated as the fuel burns off. If there were no rotation, the wingmen will simply be limited to the range of the leader, although the wingmen will land with more fuel. The total drag savings are simply the two values above (15% for #1, 17.5% for #2). The T-38 fuel savings associated with these drag savings are essentially one-to-one, therefore the fuel savings

are also 15% and 17.5% for this analysis. The real range benefit, and thus fuel benefit, comes if the lead ship is rotated to the back of an echelon formation after an incremental time. Table 2-2 shows how the fuel savings of the wingmen affects the cruise range of the formation. Each aircraft started at cruise with a non-dimensional fuel quantity of 10 units and burned one unit of fuel in one unit of time in a single-ship case. The leader was rotated after burning one unit of fuel in the rotation case. The number in parenthesis is the ship number, not the wingman number (#1 is lead, then #2 and #3) and is provided for bookkeeping purposes. If the leader was not rotated, the final cruise time will be 10 units of non-dimensional time. The Time column shows a prefix of End1, meaning the end of time 1, or Start2, meaning the start of time 2. These two times are the same, but the start time shows the aircraft after the rotation. For the rotation, it makes the most sense for the leader to drop to the back of the formation, as it requires backing off the thrust instead of increasing thrust (and fuel burn) trying to catch the front of the formation if the last ship were to rotate up to lead. Therefore, Lead becomes #3, #3 becomes #2, and #2 becomes Lead. Table 2-2 assumes the #1 wingman saves 15% in fuel while the #2 wingman saves 17.5%.

Table 2-2. Effect of Rotating Formation Positions

<u>TIME</u>	<u>LEAD</u>	<u>#2 WING</u>	<u>#3 WING</u>
Start1	10.00 (#1)	10.00 (#2)	10.00 (#3)
End1	9.00 (#1)	9.150 (#2)	9.175 (#3)
Start2	9.150 (#2)	9.175 (#3)	9.000 (#1)

End2	8.150 (#2)	8.325 (#3)	8.175 (#1)
Start3	8.325 (#3)	8.175 (#1)	8.150 (#2)
End3	7.325 (#3)	7.325 (#1)	7.325 (#2)
Start4	7.325 (#1)	7.325 (#2)	7.325 (#3)
End4	6.325 (#1)	6.475 (#2)	6.500 (#3)
Start5	6.475 (#2)	6.500 (#3)	6.325 (#1)
End5	5.475 (#2)	5.650 (#3)	5.500 (#1)
Start6	5.650 (#3)	5.500 (#1)	5.475 (#2)
End6	4.650 (#3)	4.650 (#1)	4.650 (#2)
Start7	4.650 (#1)	4.650 (#2)	4.650 (#3)
End7	3.650 (#1)	3.800 (#2)	3.825 (#3)
Start8	3.800 (#2)	3.825 (#3)	3.650 (#1)
End8	2.800 (#2)	2.975 (#3)	2.825 (#1)
Start9	2.975 (#3)	2.825 (#1)	2.800 (#2)
End9	1.975 (#3)	1.975 (#1)	1.975 (#2)
Start10	1.975 (#1)	1.975 (#2)	1.975 (#3)
End10	0.975 (#1)	1.125 (#2)	1.150 (#3)
Start11	1.125 (#2)	1.150 (#3)	0.975 (#1)
End11	0.125 (#2)	0.300 (#3)	0.150 (#1)
Start12	0.300 (#3)	0.150 (#1)	0.125 (#2)
End12.15	0.148 (#3)	0.021 (#1)	0.000 (#2)

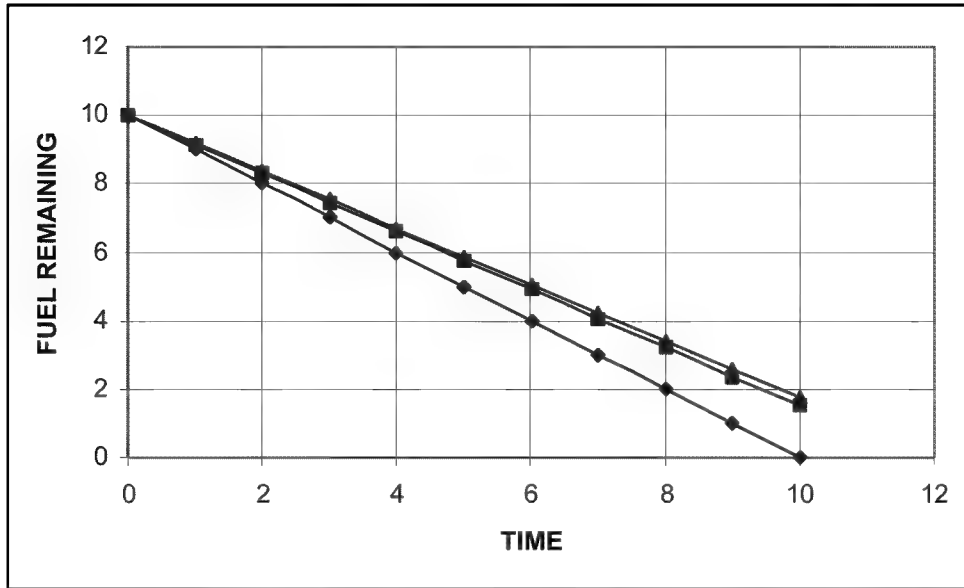


Figure 2-11. Fuel Savings without Rotation

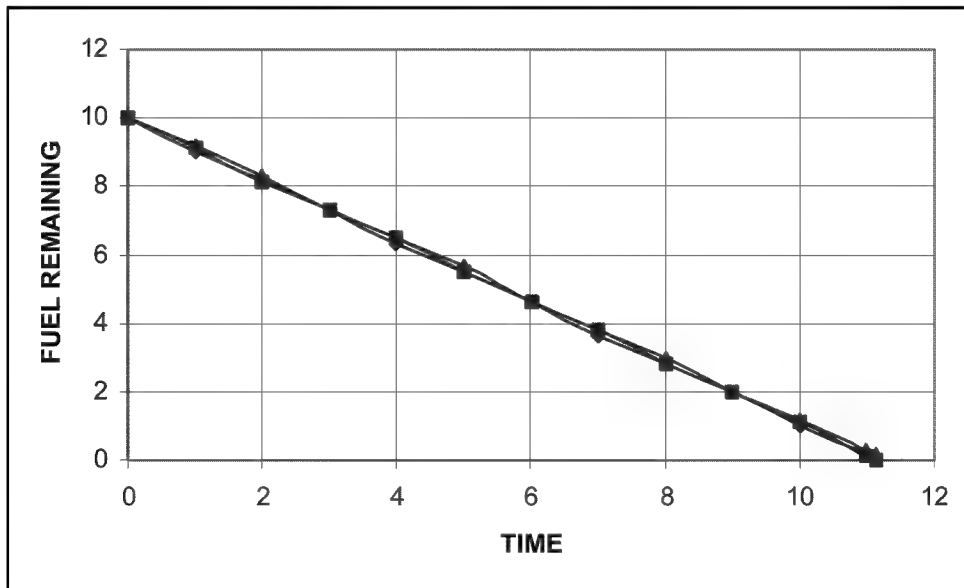


Figure 2-12. Fuel Savings with Rotation

From the table and figures above, we can see that the formation's cruise range has increased a significant 11.5%! Again, this is a FREE reduction in fuel. Although this analysis was accomplished on T-38s, it could easily be applied to large aircraft as well using HASC95 as a predictive tool. An interesting follow-on study to this thesis would be to incorporate large aircraft geometry into the code and look at the predictions. Another interesting follow-on would be to look at dissimilar aircraft such as a formation with a tanker lead and a fighter formation of wingmen. It could also increase a fighter's range while providing cover to a bomber acting as the lead aircraft. This is discussed again in Chapter 5.

III. Flight Test Setup

Overview

The analytical portion of this thesis dealt with drag savings because the HASC95 code produced drag numbers. The flight test portion of the research used fuel savings, since that was directly measured by the instrumentation system on the aircraft. The fuel savings could then be converted to drag savings using an engine model, although since it is essentially a one-to-one conversion, they can be considered to be the same thing.

The flight test had two phases. The first phase was to determine the formation position of a wingman that provided the best fuel savings. This phase was flown with a two-ship formation of Northrop T-38 *Talon* aircraft. The wingman explored four discrete points in the vortex behind the leader and data were post-processed to determine the optimal position. The second phase determined the effects of adding an additional wingman. This phase was flown with a three-ship of T-38s. The formation was flown with the optimal formation position as determined by the two-ship flight tests. The fuel savings of each wingman was compared to determine if the second wingman derived any additional fuel savings benefits over the first wingman. All fuel savings comparisons were made by comparing the fuel flow in the vortex to the required fuel flow for the same aircraft flying outside the vortex in free stream air. The test team also gathered qualitative workload data from flying in the formation positions. The workload assessment was not an objective of the test team, although it offered additional insight into the operational feasibility of flying the vortex position.

The test team consisted of four pilots (two C-5, one F-16, one B-1), a weapons system officer (B-1), and a flight test engineer. The team was put together from the USAF Test Pilot School (TPS), Class 01A. The author of this thesis was the Program Manager for the project. The project was known as TALON GAGGLE. Much of this information is also presented in the test team's final report (13).

It is worthwhile to review the numbering scheme for the wingmen. The aircraft in the formation are referred to as lead, #1 wingman, and #2 wingman. For example, the #1 wingman is the second aircraft in the formation, flying in the lead's vortex.

The flight test evaluated four different formation positions. Two of the positions were theorized to be optimal in Hummel (6) and Blake (3), another was the position found in the previous chapter (the test team called it the Wagner optimal point), and a fourth that bounded the investigation. For this flight test, the aircraft were kept in-plane, or co-altitude, with a constant longitudinal (downstream) spacing of $2\frac{1}{2}$ wingspans, which equated to an 11.5 feet nose-tail separation for the T-38. This downstream spacing gave the wingman essentially all of the assumed benefit and provided good visual cues to the wingman for maintaining position. The four different positions were defined as the 'vortex' positions. The vortex positions are described in Table 3-1 and illustrated in Figure 3-1. The test aircraft consisted of T-38As and a T-38C.

Table 3-1: Lateral Positions

Test Point	Wingspan Separation (percent)	Wing Overlap (feet)	Description
A	75	6.3	Hummel optimal point
B	86	3.6	Wagner optimal point
C	100	0	Blake and Multhopp optimal point
D	114	-3.6	Outer bound

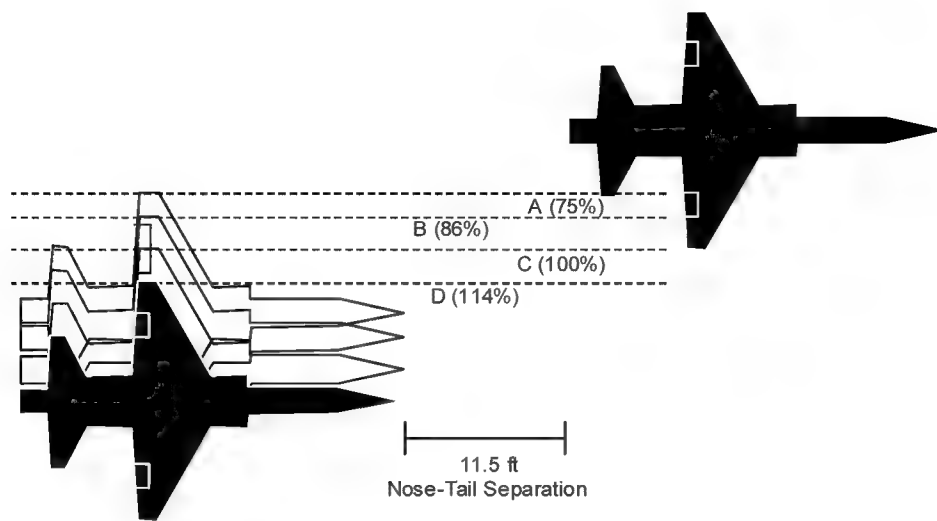


Figure 3-1: Lateral Separation Definitions

The T-38 was used for this project because of the ready availability of four instrumented aircraft at USAF TPS. Three T-38A's and one T-38C were fully instrumented, which eliminated the need for modifications. The T-38 also had another advantage, in that all the test team pilots had previous experience in formation flying in the T-38, although not in the vortex positions. This allowed for a quick build-up approach to flying in the vortex positions. To maintain the proper vortex positions, the T-38's were fitted with special tape markings on the fuselage, wing, and the stabilator. These tape markings provided the necessary visual references to identify and maintain the proper vortex positions. Although the tape allowed the pilot to get close to the position, the pilot was never quite sure if it was exact due to the absence of a relative position sensor.

All testing was conducted at the Air Force Flight Test Test Center (AFFTC), Edwards Air Force Base, California in October 2001. The test team flew seventeen T-38

sorties (21.9 hours) including two-ship, three-ship, and calibration formation flights as well as chase and photo support flights. Three ground tests verified instrumentation and determined aircraft formation references.

Test Procedures

None of the pilots had previous flying experience in the vortex position, therefore the test team decided to follow a build-up approach. The first two calibration flights consisted of a two-ship of T-38's plus a chase ship, also a T-38. The chase crew verified that the wingman flew the proper vortex positions, and coached the wingman if required. The chase ship provided an opportunity to spot check the tape markings on the airplanes for the different vortex positions, while the wingman had a chance to practice flying in the four vortex positions. The test team then proceeded with two, two-ship data flights to evaluate which vortex position rendered the best fuel savings. Next the test team executed two, three-ship flights, in which the wingmen flew in the previously determined optimal vortex position. During the three-ship flights, the wingmen swapped positions multiple times in order to get the primary data aircraft into each position. This was important because the resolution of the C-model data was much higher than the A-model's data, making it the primary data aircraft.

Since this was a new flight test procedure, the test team developed a special flight test technique (FTT) to gather data. The procedure for the FTT started with the wingman, or wingmen, in the route position. This position was defined as a 15-50 feet lateral spacing, with the wingmen slightly aft of lead. The lead aircraft stabilized on the test conditions, nominally 300 ± 2 KIAS and $10,000 \pm 100$ feet pressure altitude. The

wingman then moved into the vortex after clearance from the leader. The formation then flew straight and level, unaccelerated flight at the test condition previously stated. Once the wingman was stable in the vortex, the throttles were not moved in order to collect a stable cruise point of approximately 20 seconds. At the conclusion of each data run the wingman recorded the airspeed, V_{vortex} , and called for the formation to take spacing. The lead then gently moved away from the wingman, effectively taking the wingman out of the vortex. The wingman would then slow down out of the vortex while maintaining altitude, heading, and power setting. The wingman recorded the new stabilized airspeed, V_{cruise} , when stable at the new cruise point (this was the Airspeed Method). Finally, the wingman readjusted the throttles for a cruise point (30 second duration target) at the same airspeed flown in the vortex, V_{vortex} , to collect fuel flow data (this was the Fuel Flow Method).

The in-the-vortex portion of the data run consisted of at least a 20 second stable point before the lead moved away from the wingman. While data were recorded during the entire run, only the 20 second stable points designated by the wingman were used for data reduction. Recorded UHF radio calls and cockpit interphone were used as the primary means of correlating data. In addition, handheld data and timing information collected by the flight test engineer were used to reference the data on the data acquisition system (DAS) tape. Due to inadequate resolution of the onboard fuel counters, handheld data were found to be unsuitable for data analysis and DAS-recorded data were used exclusively for data reduction.

Three-ship formation test flights were flown using the optimal location, position B, as was determined in the two-ship formation test flights. The same FTT was used to

collect data during the three-ship flights. Specific procedures were developed to safely orchestrate the formation changes, position swaps, and data collection. At the conclusion of each data run, the wingmen independently noted their airspeeds, V_{vortex} . Then both wingmen determined V_{cruise} . Finally, the two wingmen independently adjusted their throttles to return to V_{vortex} , thus collecting the out-of-vortex fuel flow data. The primary data aircraft, the T-38C, was mostly flown as the #2 wingman but was occasionally swapped into the #1 wingman position.

IV. Flight Test Results

Overview

The results of the two-ship flight tests show with 80% confidence that the wingman saved fuel in position B (86% lateral spacing). This position yielded fuel savings of $8.8\% \pm 5.0\%$. The other positions did not show a statistically significant fuel savings. The results were inconclusive as to the best of the four positions for the wingman to fly since none of them are statistically distinct. Although not statistically better than the other positions, the test team felt that position B tended to be the best position and therefore chose it to fly the three-ship formation.

The three-ship formation did not yield the expected results. Not only was there no significant difference between the two wingmen, neither wingman showed any statistically significant fuel savings. The test team felt that the three ship formation data was inconclusive due to the difficulty of trying to fly a stable position as the third aircraft in the formation. While the pilots felt that flying as a lone wingman was relatively easy, they all thought that trying to fly as the third aircraft introduced errors by compounding position errors of the #1 wingman. These position errors were most likely in altitude (not quite co-planar) since any small change by the second aircraft was magnified to the third aircraft. The stability of the position also challenged the pilots in the three-ship formation. The #2 wingman had to wait to call a point stable until the #1 wingman was stable in position B. After both wingmen were stable, they had to stay on conditions together for at least 20 seconds, which was hard enough for one airplane to do in the two-

ship formation. The three-ship formation has the potential for excellent results, however accurate station-keeping is needed to achieve them.

Two-Ship Data

The objective of the two-ship flight test was to evaluate the fuel savings for four different vortex positions. The only position that showed statistically significant savings with 80% confidence was position B, the predicted optimal point. The measured fuel flow savings were $8.8\% \pm 5.0\%$ compared to the predicted fuel flow savings of 15% as shown by the HASC95 analysis. The predicted results assume the upwash vector is acting perpendicular to the wing, so if the wingman were not in the exact position, some of the benefit would be lost. Since it was hard to tell if the aircraft were in-plane or even the effects of the vortex sinking as it left the lead aircraft, the actual results were not as large as the computational results. The primary result of the first phase was confirmation that the predicted position produced measurable improvement in fuel flow. The other three positions did not yield statistically significant differences in fuel savings. Although the means of the other three positions showed positive savings, they were not statistically significant when compared to the out-of-vortex cruise points. The data are summarized in Figure 4-1, Figure 4-2, and Table 4-1. Figure 4-1 shows the fuel flow savings measured with both the “fuel flow” and “airspeed” methods, while Figure 4-2 shows the average of the results. The data reduction for these techniques is reported in detail in Appendix D. The results were inconclusive as to which of the positions was the best since the four positions did not yield statistically significant (80% confidence) differences. It is important to note that these data were for one altitude, configuration,

and airspeed. The program did not explore the effects of flying at different altitudes, configurations and airspeeds. All the flight hours were dedicated to increasing the fidelity of the data at the one test condition.

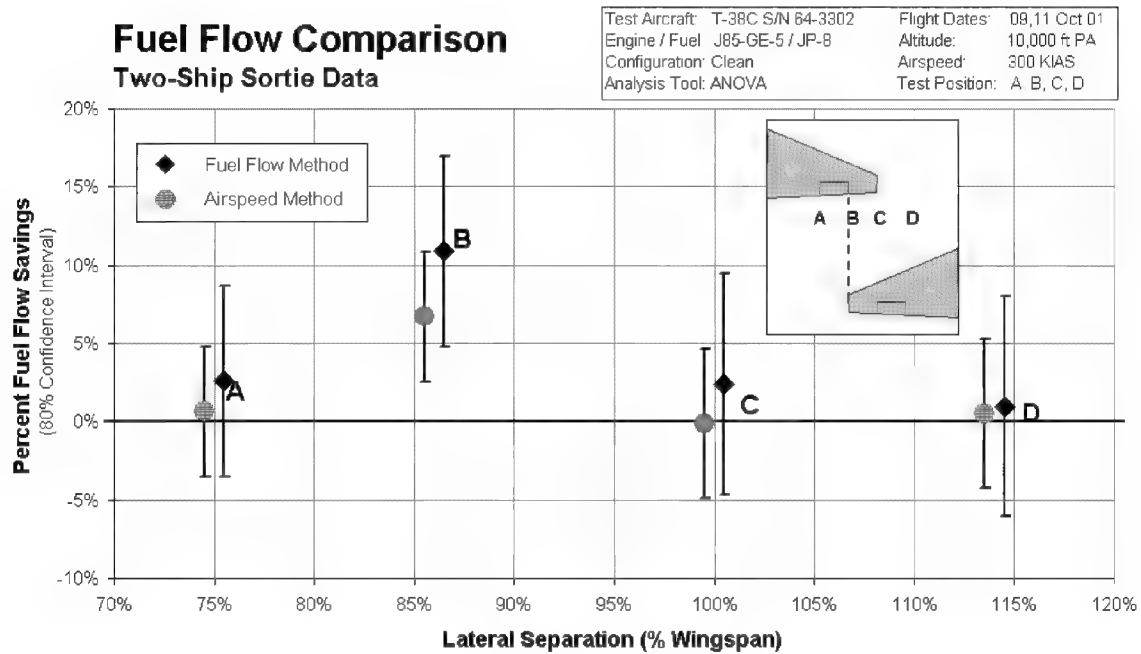


Figure 4-1: Two Method Comparisons Between Lateral Positions

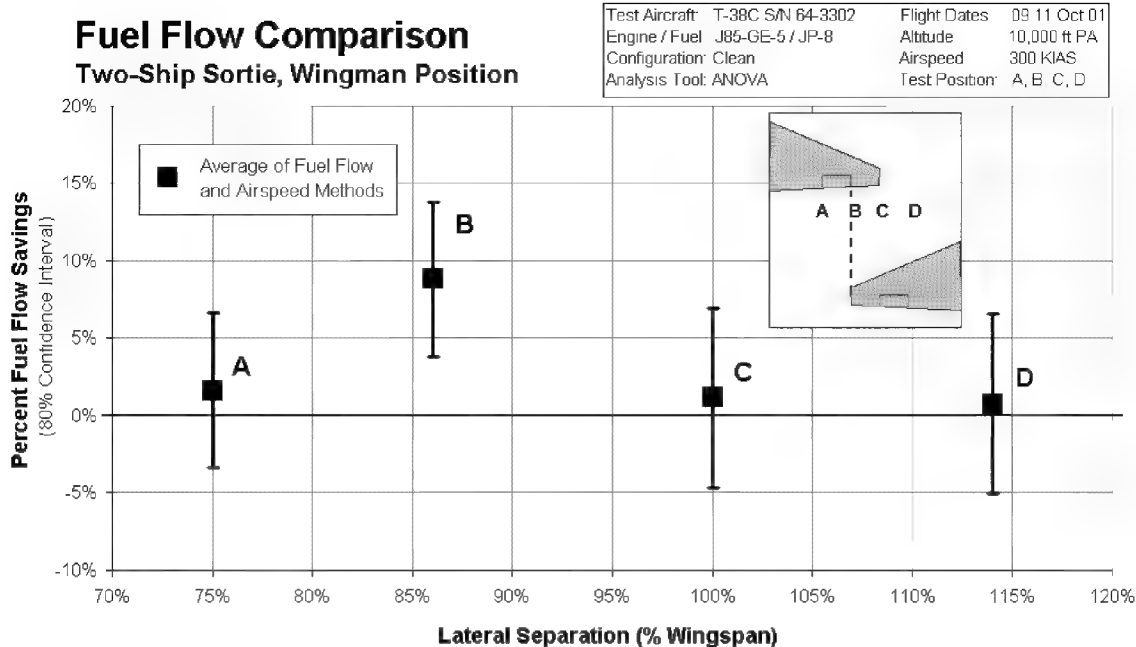


Figure 4-2: Average Fuel Flow Comparison Between Lateral Positions

Table 4-1: Two-Ship Results for Each Lateral Position

LATERAL SPACING	# OF RUNS	FUEL FLOW METHOD	AIRSPEED METHOD	AVERAGE
A	4	2.6 ± 6.1	0.6 ± 4.1	1.6 ± 5.0
B	4	10.9 ± 6.1	6.7 ± 4.1	8.8 ± 5.0
C	3	2.4 ± 7.1	-0.1 ± 4.8	1.1 ± 5.8
D	3	1.0 ± 7.1	0.5 ± 4.8	0.8 ± 5.8

Three-Ship Data

The objective of the three-ship formations was to determine the difference in fuel flow savings between the first and second wingman. Based on the analytical work in the preceding chapters, the test team expected slightly better fuel savings from the #2 wingman in a three-ship formation than the #1 wingman in a two-ship formation. During

test planning, the test team predicted the difference would not be statistically significant due to the small sample size and resolution of the DAS. All three-ship formations were flown in position B since that tended to be the best position from the two-ship sorties.

The actual results were surprising since there was no apparent advantage to flying a three-ship formation. Neither wingman recorded a statistically significant fuel saving. The #2 wingman in the three-ship formation recorded a fuel benefit of $0.5\% \pm 3.7\%$ compared to the #1 wingman who, from the previous section, recorded a benefit of $8.8\% \pm 5.0\%$ in a two-ship formation. The data are summarized in Figure 4-3, Figure 4-4, Figure 4-5, and Table 4-2. Figure 4-3 shows the “fuel flow” method results, while Figure 4-4 shows the “airspeed” method results. Figure 4-5 is the average of the two results. When the data aircraft changed formation position from the #2 wingman position to the #1 wingman position, calculated fuel flow savings suffered significantly. The test team did not anticipate this result and only had the data aircraft fly the #1 wingman position in the formation three times as a spot check when area orientation would not allow for a full three-ship run. Two of the three runs with the data aircraft in the #1 wingman position resulted in the test team accomplishing the “airspeed” method test, hitting an area boundary, then turning around and accomplishing the “fuel flow” method test. This was not as “clean” a data technique as the two-ship data points, but the group only planned on using it as a spot check. The small sample size and questionable data quality made this result inconclusive.

A factor that could have contributed to the three-ship result was the wingmen flying in positions that deviated slightly from the correct formation position. The

backseat pilot of the T-38C, who flew every data sortie, observed small differences between the individual pilots when they flew in position B. If the #1 wingman had a small error in his formation position, it may have influenced the vortex from the lead airplane and thereby the data taken in the #2 wingman position, whether the #2 pilot flew the correct position or not. Pilots who flew in formation positions were generally good at observing small relative changes in their position, but generally not very good in assessing their absolute position. The lack of accurate feedback on the formation position in which the test team flew could have easily degraded the quality of the test data. Small errors in the #1 wingman's position were carried on to the #2 wingman, especially in altitude. This would decrease the fidelity of the three-ship data since the vortex savings are sensitive to being in-plane with the leader. Data quality could be significantly improved if accurate feedback on the actual formation position relative to the planned formation position were available. The test team's recommendation was to improve the station-keeping capability of the wingmen.

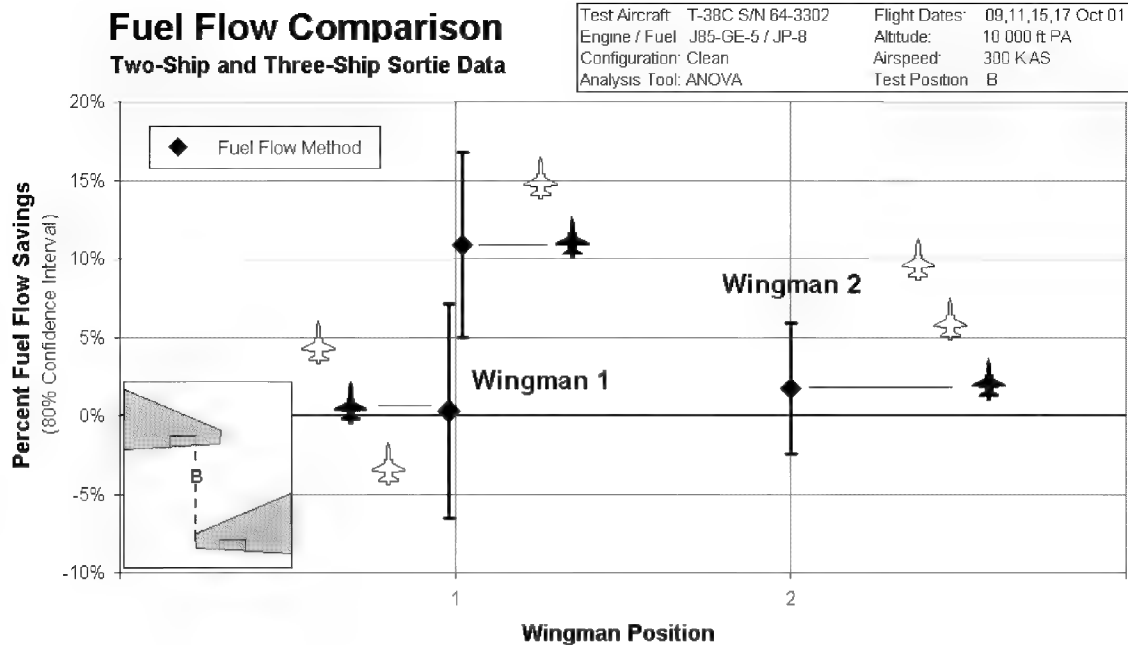


Figure 4-3: Comparison Between Formation Positions – Fuel Flow Method

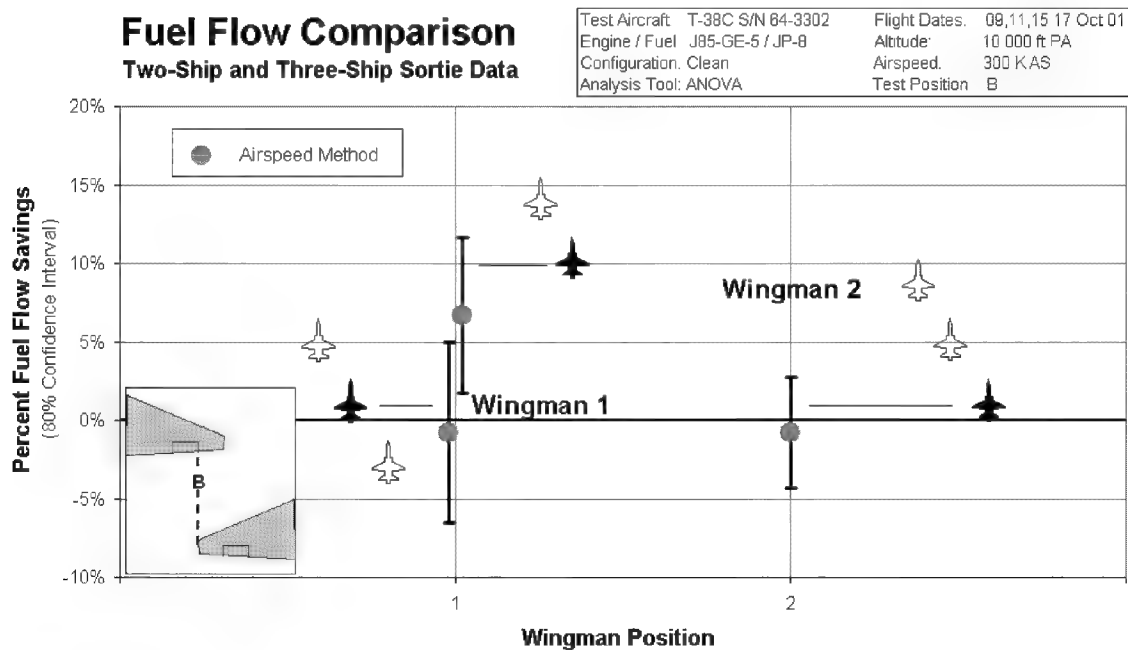


Figure 4-4: Comparison Between Formation Positions – Airspeed Method

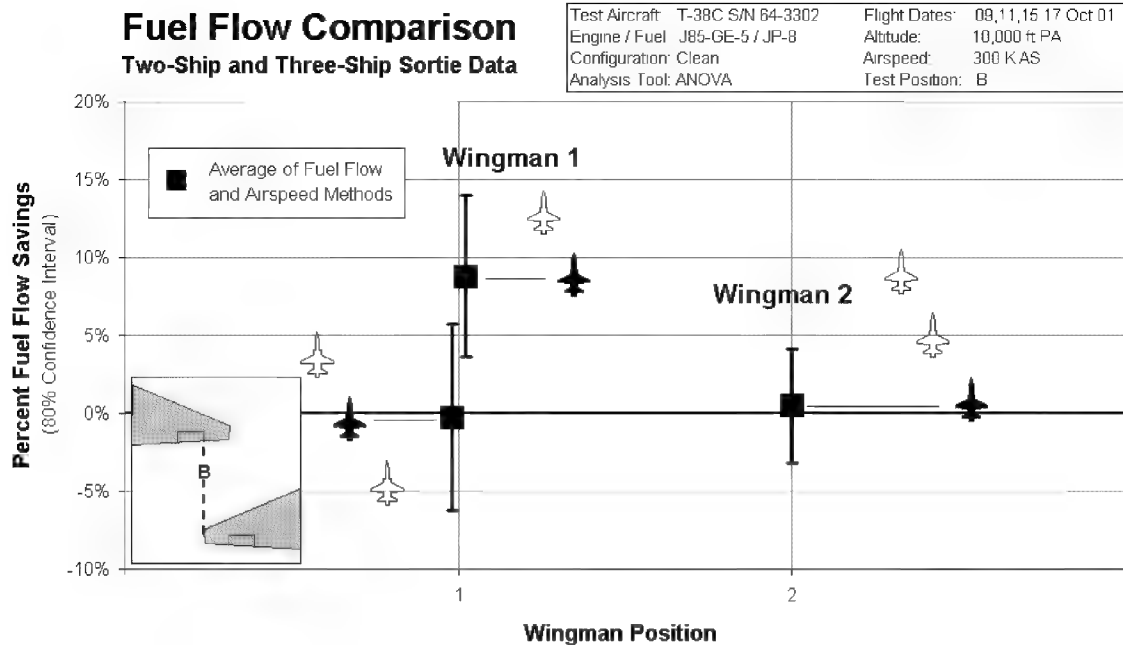


Figure 4-5: Average Fuel Flow Comparison Between Formation Positions

Table 4-2: Three-Ship Results For Varying Wingman Position

WINGMAN POSITION	# OF RUNS	FUEL FLOW METHOD	AIRSPEED METHOD	AVERAGE
1	3	0.3 ± 6.8	-0.8 ± 5.7	-0.3 ± 6.0
2	8	1.8 ± 4.2	-0.8 ± 3.5	0.5 ± 3.7

Pilot Comments

The test team made a qualitative assessment of the workload in the different formation positions. Workload data were gathered via a questionnaire that pilots filled out after each flight. The workload was compared between flying in a vortex position and flying in other operational formation positions. These were formation positions taught at Undergraduate Pilot Training (UPT) and widely used throughout the USAF. These

positions were fingertip, route, and tactical formation positions. The fingertip formation positions were divided in different configurations, cruise (CR) and powered approach (PA), while accomplishing different maneuvers. The PA configuration for the T-38 was defined as landing gear down and flaps at 60%. The maneuvers were straight and level, unaccelerated flight (both CR and PA configurations), lazy-eight type maneuvers up to three-G (CR configuration only), and turns up to 45° angle of bank (PA configuration only). The lowest workload task was assessed flying in tactical formation straight and level, unaccelerated flight. Flying in the fingertip position while accomplishing turns up to 45° angle of bank in the PA configuration, landing gear and flaps extended, was rated as the highest workload task. The workload in vortex position B, after four flights, was assessed as higher than flying in fingertip straight and level, unaccelerated cruise flight (CR). This means that flying normal formation was determined to be easier than vortex formation. However, the workload in position B was assessed as lower than flying in the fingertip position, straight and level, unaccelerated flight in the PA configuration. So although it was harder than the CR configuration, it was easier than PA configured formation. See Figures 4-6 and 4-7.

Question 5: How would you characterize the overall workload in Fingertip position, straight and level, cruise configuration?

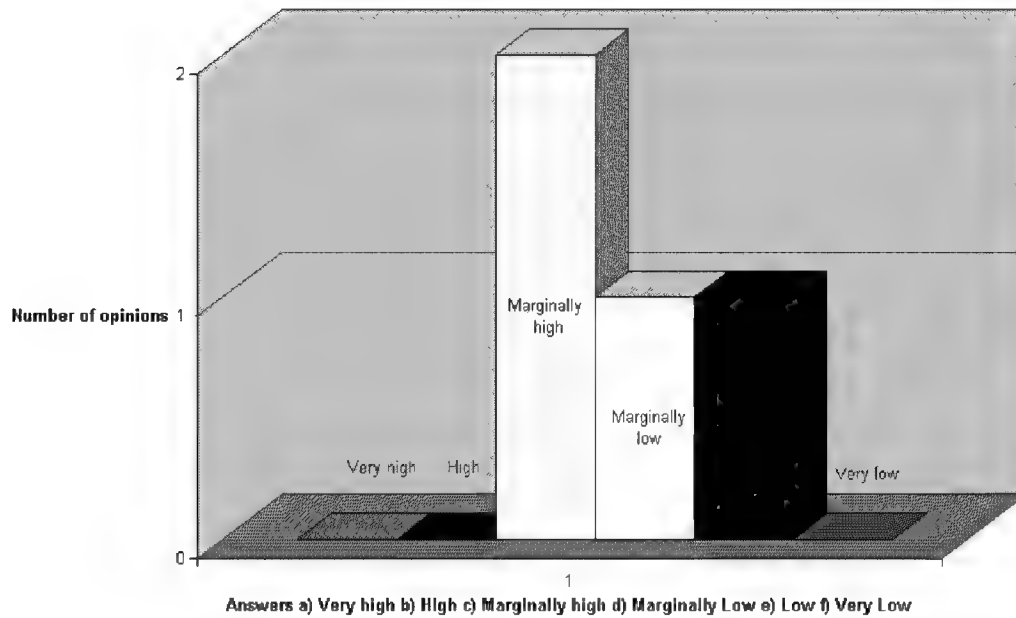


Figure 4-6: Workload in Fingertip Formation - Cruise

Question 6: How would you characterize the overall workload in Fingertip position, straight and level, powered approach configuration?

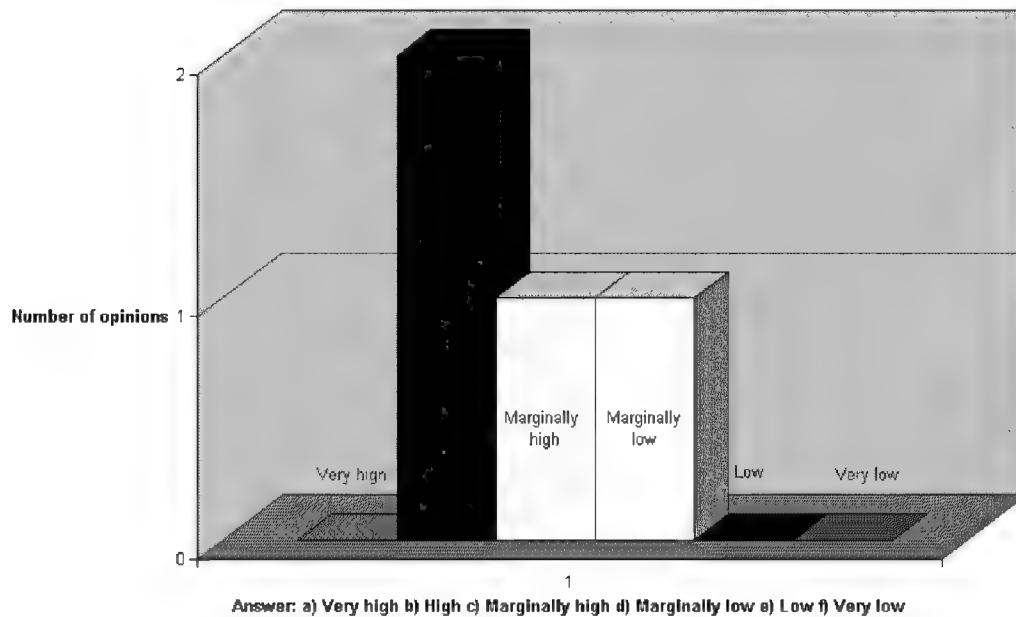


Figure 4-7: Workload in Fingertip Formation – Powered Approach

Positions C and D

The most noticeable effect when entering the vortex was the airplane's tendency to slide forward. This effect was comparable to the air-refueling experience with a large airplane. This was easily corrected for by a very small power reduction. It was easy to maintain the correct position, and the power setting was steady for prolonged periods of time (30 seconds to one minute). Positions C and D were easy to maintain.

Position B

In the 86% wingspan separation position, the roll moment, which seemed to push number two away from lead, was more apparent than the forward pull. Approximately six small clicks of aileron trim into lead significantly facilitated position keeping and almost trimmed the airplane laterally. To maintain position B was easy, once trimmed, and the learning curve was steep. This position felt very much like surfing on a wave. Figure 4-8 shows the results for position B.

Question 11: How would you characterize the overall workload in Vortex position B?
(after 4 flights).

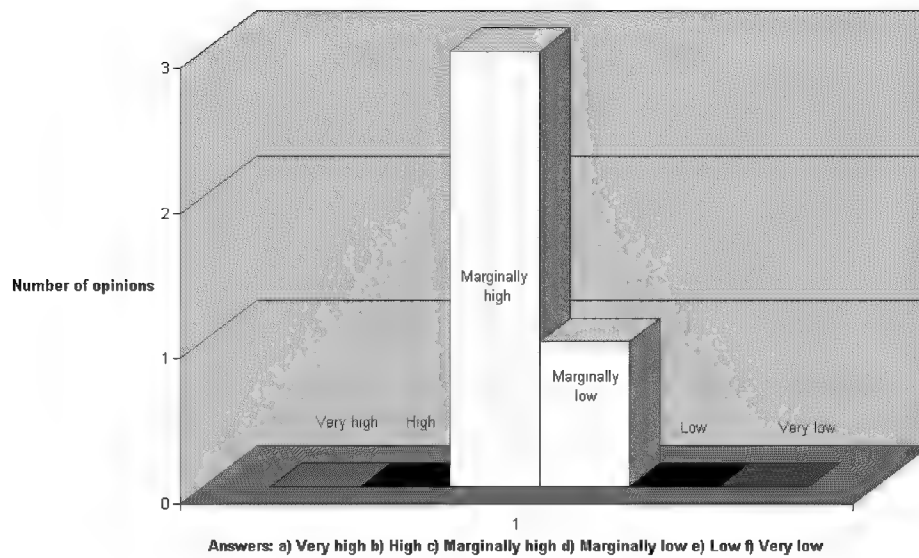


Figure 4-8: Workload in Test Position B

Position A

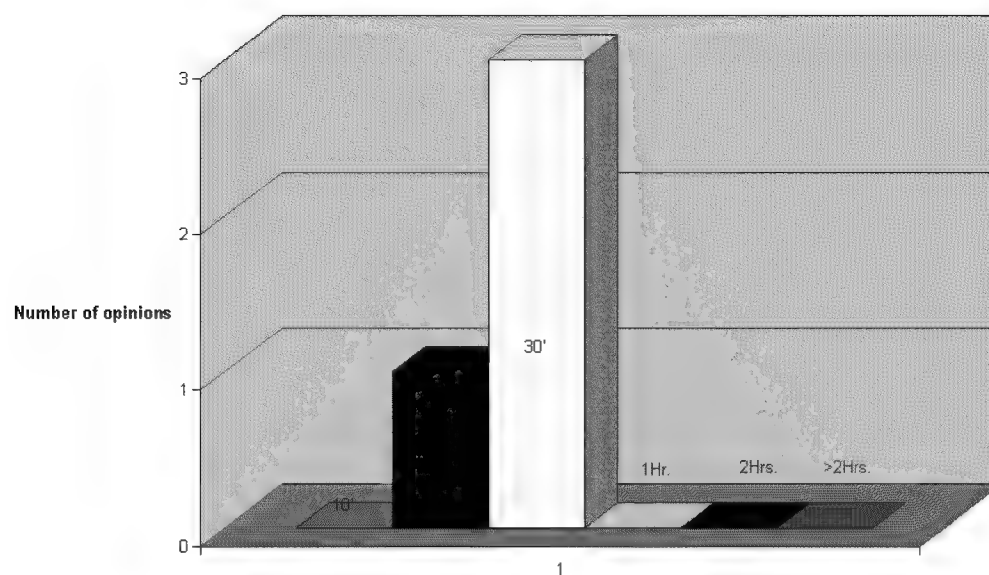
Position A represented the 75% wingspan separation, and was the innermost position that was evaluated. The roll moment was very tricky at this point because it would change from rolling towards lead to rolling away from lead in a very small lateral distance. Aileron trim was not useful to trim out lateral forces since they tended to reverse as the aircraft made small changes laterally. The chase ship was able to observe the aileron deflections as the wingman manually fought to maintain position near the roll reversal point. This position felt unstable, therefore a position inboard from position A should be avoided. When the aircraft ended up inadvertently on a position inboard from A, the pilot found that the airplane was still controllable, and could be moved out easily. The workload in position A was significantly higher than positions B, C, and D. This

resulted in less time in the correct position and less data. Once lead moved away, the pilot had to re-trim the airplane laterally to take a cruise point.

Operational Feasibility of Vortex Position B

The learning curve of tight formation vortex flying was steep. This was illustrated by the fact that only two out of the four pilots thought the vortex position would have an operational potential after the first flight. After four flights all four pilots thought the vortex position could be operationally feasible. The workload while flying in the vortex position was slightly higher than in an expected operational formation because the test team always strived for the perfect data point in which the throttles were not adjusted for at least 20 seconds. To achieve this the pilot had to find the optimal formation geometry, which was a relatively small envelope. It was not hard to fly the position, but it did require constant attention to be precise. An operational mission, flying in the vortex position without a formation hold autopilot, would result in less savings than experienced during this test program since the pilot would not be able to keep such tight tolerances and perform checklists, navigate, etc. Although this would result in slightly less fuel savings, the net result would still be a gain over not flying in tight formation at all. Figure 4-9 shows that the pilots thought that in the absence of an automatic controller, the workload was feasible for a 20-30 minute time period before swapping positions.

Question 29: How do you think the Vortex position could be flown operationally?



Answer: Continuous duration in Vortex position B would be:
a) Feasible for 10 minute stretch to the practice area
b) 20 minutes c) 30 minutes, then swap
d) 1Hr, then swap e) 2Hrs. f) >2 Hrs.

Figure 4-9: Operational Suitability

V. Conclusions and Recommendations

The objective of this thesis is to examine the beneficial induced drag reduction effect achieved by flying aircraft in tight formation. The intent was to also validate the predictive power of the HASC95 vortex code by comparing the results to flight test data. The flight test data validated the vortex lattice method as a predictive tool in predicting drag savings for the two-ship formation. The flight test data showed a saving for the wingman of a two-ship formation of $8.8\% \pm 5.0\%$ with 80% confidence. This compares to computational predictions of a 15% fuel savings. The difference was most likely a result of the aircraft not being perfectly in position so that the upwash vector was perpendicular to the wing. The three-ship formation was analytically shown to slightly improve the results, but the flight test data were inconclusive.

This is a limited investigation in that it explored only one aircraft geometry, one altitude, and one airspeed. It was also limited in sample size by the time it took to take data points without the benefit of automatic station-keeping equipment.

It was clear that flying in a lead aircraft's vortex improved fuel consumption, thus increasing range. As mentioned above, a formation-hold autopilot would greatly enhance the pilot's ability to hold a near-perfect position and enjoy the full benefits of flying in the vortex. With a formation-hold autopilot, a formation of aircraft or UAVs could increase its range significantly for almost no additional cost other than the automatic control system. The author recommends research be continued using formation-hold autopilots to further define the savings at each position and reinvestigate the three-ship formation. Another recommendation of the author is to expand the

envelope of testing to a more realistic cruise altitude. The flight test for this work was done at 10,000 feet due to perceived engine anomalies with vortex ingestion at high altitude with the T-38. This was found not to be a factor at 10,000 feet. The use of F-16-type aircraft with a more robust engine would allow the test envelope to be expanded. A final recommendation would be to look at dissimilar formations such as tanker aircraft flying with fighter-size aircraft on the wing. Multiple smaller aircraft may be able to easily take advantage of a large aircraft vortex to significantly increase range for overseas deployments.

Appendix A: FORTRAN Files

Note: Mr. Bill Blake of AFRL at Wright-Patterson AFB, OH wrote a large portion of this code (prisrf in particular) for a similar project. I was mostly responsible for reworking the subroutines to fit the T-38 geometry and allowing for a third aircraft.

WING FILE (Also called Lead and Twowing in three-ship portion)

This is the file that puts the T-38 geometry into a form to be called by hasc. The X,Y, and Z columns are the forward most point of the panel, with the length being the column labeled CORD1. The last line of each panel is the number of lateral elements (8.5 inches), the number of chordwise elements, the SPC number, an unused number, then the incidence number for aileron deflections (in degrees). The last number is unused.

```
PORT WING
*SR TYP      LNPAN      ISYMFLG      ENETAR      FTAIL
05           20         00           0.0         0.0  0.  0.
*X1          Y1         Z1           CORD1      AINC1
544.85      -17.0       0.0         37.25       0.
546.34       0.0       0.0         35.76       0.
2.          2.         0.          00          00          0.0
*****
546.34       0.0       0.0         35.76       0.
544.85      17.0       0.0         37.25       0.
2.          2.         0.          00          00          0.0
*****
518.9       -85.0       0.0         20.0        0.
466.34       0.0       0.0         80.0        0.
10.         8.         0.45        00          00          0.0
*****
466.34       0.0       0.0         80.0        0.
518.9       85.0       0.0         20.0        0.
10.         8.         0.45        00          00          1.0
*****
426.46      -34.0       0.0         60.9        0.
429.15       0.0       0.0         37.19       0.
4.          4.         0.          00          00          0.0
*****
429.15       0.0       0.0         37.19       0.
426.46      34.0       0.0         60.9        0.
4.          4.         0.          00          00          0.0
*****
390.11      -153.0      0.0         26.93       0.
363.55      -110.5     0.0         56.86       0.
5.          11.        1.0         00          00          0.0
*****
403.80      -110.5     0.0         16.61       0.
399.50      -76.5     0.0         23.60       0.
4.          5.         0.0         00          00          1.0
*****
363.55      -110.5     0.0         40.25       0.
342.30      -76.5     0.0         57.20       0.
4.          8.         1.0         00          00          0.0
```



```

*****
342.3    -76.5      0.0      80.80      0.
315.75   -34.0      0.0     110.71      0.
5.        11.       1.0       00        00        0.0
*****
315.75   -34.0      0.0     110.71      0.
294.5     0.0       0.0     134.65      0.
4.        11.       0.0       00        00        0.0
*****
294.5     0.0       0.0     134.65      0.
315.75    34.0      0.0     110.71      0.
4.        11.       0.0       00        00        0.0
*****
315.75    34.0      0.0     110.71      0.
342.3     76.5      0.0      80.80      0.
5.        11.       1.0       00        00        0.0
*****
399.5     76.5      0.0      23.60      0.
403.8    110.5      0.0      16.61      0.
4.         5.       0.0       00        00        1.0
*****
342.30    76.5      0.0      57.20      0.
363.55   110.5      0.0      40.25      0.
4.         8.       1.0       00        00        0.0
*****
363.55   110.5      0.0      56.86      0.
390.11   153.0      0.0      26.93      0.
5.        11.       1.0       00        00        1.0
*****
264.0     -34.0      0.0      51.75      0.
264.0     -17.0      0.0      41.12      0.
2.         4.       0.0       00        00        0.0
*****
264.0      17.0      0.0      41.12      0.
264.0      34.0      0.0      51.75      0.
2.         4.       0.0       00        00        0.0
*****
142.50    -17.0      0.0     162.62      0.
52.5      0.0       0.0     242.0       0.
2.         9.       0.0       00        00        0.0
*****
52.5      0.0       0.0     242.0       0.
142.50    17.0      0.0     162.62      0.
2.         9.       0.0       00        00        1.0
*****

```

HEADER FILE (Two-Ship)

This file defines such things as the number of surfaces, number of panels, Mach number, span length, reference area, number and values of AOA and Beta to run, etc. The three-ship header file is similar, but with 60 panels and 3 surfaces.

```
AFIT T-38
*
*
*LAX      LAY      HAG      RUN      NPAN      NSURF
00        01        0.        1.        40        02        0
*REY      NMACH     MACH     MACH
1900000.  01        0.54
*NALPHA    ALPHAS
04    0. 1. 2. 3. 4.
*NBETA     BETAS
01        0.0    10.0
*PITCHQ    ROLLQ    YAWQ      VINQ
0.         0.         0.         1.
*SREF      CBAR      XBAR      ZBAR      WSPAN
24480.     92.76     350.0     0.0      306.0
*****
```

MT38 FILE (Two-Ship)

This file reads in the geometry of the aircraft, then runs the sweep by calling the hasc routine at each iteration. It treats the last wingman as the origin and moves lead to the right in 8.5 inch increments.

```
      program move
c
c  this code shifts the coordinates of a
c  HASC95 input file to simulate a formation of
c  aircraft by defining new aircraft positions
c
c  file "header2" is the hasc header input
c  file "wing" is the basic wing geometry for wingman
c  file "lead" is the basic wing geometry for leader
c  file "ftemp" is the aerodynamic result file from hasc
c  file "fout" is the printed aerodynamic result file from hasc
c  file "final" is the normalized force/moment increment file
c  file "hasc.inp" is the generated hasc input file
c
c  +x = other vehicle upstream
c  +y = other vehicle right
c  +z = other vehicle below
```

```

c
c      character*80 f1
c
c      data for sim tables
c
c      dimension xi(1),yi(43),zi(6)
c      data xi/-4.,-3.,-2.,-1.6,-1.4,-1.2,-1.,-.8,-.6,-.4,-.3,-.2,-.1,0.,
c x      .1,.2,.3,.4,.6,.8,1.,1.2,1.4,1.6,2.,3.,4./
c      data yi/1.0/
c      data zi/0.,0.25,0.5,1.0,2.0,50.0/
c
c      data for mesh plots  xi=2
c
c      dimension xi(1),yi(24)
c      dimension yi(24)
c      data xi/2.0/
c      data yi/0.,0.0833,.1667,0.25,0.3333,0.4167,0.5,0.5833,0.6667,
c x      0.75,0.8333,0.9167,1.0,1.0833,1.1667,
c x      1.25,1.333,1.5,1.6667,1.8333,2.,2.3333,2.6667,3./
c      data zi/0.,0.001,0.002,0.005,0.01,0.02,0.04,0.0833,
c x      .1667,0.25,0.3333,0.4167,0.5,0.5833,0.6667,
c x      0.75,0.8333,0.9167,1.0,1.0833,1.1667,
c x      1.25,1.333,1.5,1.6667,1.8333,2.,2.3333,2.6667,3./
c
c      open(90,file='header2',status='old')
c      open(91,file='wing',status='old')
c      open(95,file='lead',status='old')
c      open(92,file='ftemp',status='unknown')
c      open(102,file='fout',status='unknown')
c      open(103,file='final',status='unknown')
c      alpl=0.
c      span=306.
c
c      enter downstream spacing (Set to 2.5 spans)
c
c      write(*,*) 'enter x/b'
c      read(*,*) xi
c      xi=2.5
c
c      loop on relative aircraft x,y,z positions
c      for this thesis, only looped on y from 0 to 1.5 spans
c
c      do 1000 ix=1,1
c      delx=xi*span
c      delx=xi(1)*span
c      do 2000 iz=1,1
c      delz=zi*span
c      delz=0.
c      do 3000 iy=1,55
c      dely=(iy-1)*8.5
c      open(15,file='hasc.inp',status='unknown')
c
c      write header to hasc input file
c
c      do 3100 ii=1,16
c      read(90,900) f1
c      write(15,900) f1
3100      continue

```

```

c
c      rewind header for next case
c
c          rewind(90)
c
c      write trail wing to hasc input file
c
c          do 3200 ii=1,4
c              read(91,900) f1
c              write(15,900) f1
3200      continue
c              do 3250 ii=1,20
c                  read(91,900) f1
c                  write(15,900) f1
c                  read(91,900) f1
c                  write(15,900) f1
c                  read(91,900) f1
c                  write(15,900) f1
c                  read(91,900) f1
c                  write(15,900) f1
3250      continue
c
c      rewind wing geometry file for lead wing processing
c
c          rewind(91)
c
c      write lead wing to hasc input file
c
c          do 3400 ii=1,4
c              read(95,900) f1
c              write(15,900) f1
3400      continue
c              do 3450 ii=1,20
c                  read(95,910) x1,y1,z1,c1,a1
c                  write(15,910) x1-delx,y1+dely,z1-delz,c1,a1+alpl
c                  read(95,910) x1,y1,z1,c1,a1
c                  write(15,910) x1-delx,y1+dely,z1-delz,c1,a1+alpl
c                  read(95,900) f1
c                  write(15,900) f1
c                  read(95,900) f1
c                  write(15,900) f1
3450      continue
c
c      rewind wing geometry file for next case
c
c          rewind(91)
c          rewind(95)
c
c      rewind input file for hasc run
c      rewind aero file so it can be written
c
c          rewind(15)
c          rewind(92)
c
c      run hasc
c
c          call hasc
c

```

```

c      rewind aero file written by hasc so it can be read
c
c          rewind(92)
c          read(92,920)  aoa,cl1,cd1,cl2,cd2,cm2,cy2,cll2,cln2
c
c
c      print output files
c
c          write(103,925)  dely/span,aoa,cl1,cd1,
c          1              cl2,cd2,cm2,cy2,cll2,cln2
c
c          close(15,status='keep')
c
c      3000 continue
c      2000  continue
c      1000 continue
c
c      900 format(a80)
c      910 format(5(f9.3,1x))
c      910 format(f8.3,f9.3,f9.3,f9.3,f9.3)
c      920 format(1x,1f8.3,8f9.4)
c      925 format(1x,10f11.5)
c      935 format(1x,9f10.5)
c          close(90,status='keep')
c          close(91,status='keep')
c          close(92,status='keep')
c          close(95,status='keep')
c          close(102,status='keep')
c          close(103,status='keep')
c          stop
c          end

```

PRISRF FILE (Two-Ship)

This subroutine is responsible for breaking out the hasc data into a usable form for output by providing such information as lift, drag, forces, and moments for each aircraft.

```

      subroutine prisrf

c...purpose:
c  prints, by surface, forces and moments in body axis,
c  wind axis, and stability axis.

c...output:  unit 75 (hasc.out)

c...subroutine called by hasc
c  subroutine calls:  none

c...discussion:  forces and moments are initially in body axis,
c  they are translated to wind and stability axis, and printed
c  out as a summary for each axis.

      parameter (lun=201, nta1=30)

```

```

include 'flowopts.cmn'
include 'set3.cmn'
include 'set5.cmn'
include 'set6.cmn'
include 'set8.cmn'
include 'set9.cmn'
include 'set11.cmn'
include 'set12.cmn'
include 'set13.cmn'
include 'set14.cmn'
include 'set15.cmn'
include 'set17.cmn'
include 'set21.cmn'
include 'set23.cmn'
include 'set24.cmn'
include 'forces.cmn'
include 'print.cmn'
include 'srffrc.cmn'
include 'surtit.cmn'
include 'version.cmn'

character*30 tempsrf

pi = 4.0 * atan(1.0)
dtr = pi / 180.

c...print heading with hasc version and release date

      write(75,104) vtitle
104   format(/,1x,a55)

      write(75,107)
107   format(1x,'** Surface Force and Moments **',/)

c...print out surface data

      write(75,105) jobtitl
105   format(1x,a)

      write(75,120) mach(iq), -yawstb(ib),
& pitchq,-rollq,-yawq,vinf
120   format(' Mach = ',f6.2,' beta = ',f7.2,/,
& 1x,'Pitch rate = ',f7.2,'/sec',/,
& 1x,'Roll rate  = ',f7.2,'/sec',/,
& 1x,'Yaw rate   = ',f7.2,'/sec',/,
& 1x,'Vinf       = ',f10.2)

      write(75,6662) sref,wspan,cbar
6662   format(/,1x,'Sref = ',f9.3,' Wspan = ',f9.3,' Cbar = ',f9.3)
      write(75,6663) xbar, zbar
6663   format(1x,'Xbar = ',f9.3,' Zbar  = ',f9.3)

      write(75,190)
190   format (/,' ***** BODY AXIS SYSTEM *****')

      do 600 isf = 1,nsurf

```

```

        tempsrf = srftitl(isf)

        write(73,7316) isf, mach(iq), -yawstb(ib)
7316    format('ZONE T="Surf ',i2,' M=',f5.2,' Beta=',f6.2,' ", F=POINT')

        write(75,7503) isf,tempsrf
7503    format(/,1x,'Surface ',i2,' ',a30,' Body Axis')

        write(75,310)
310    format(1x,' Alpha      Beta      CNsrf      CAsrf      Cmsrf ',
&          '      CYsrf      Crsrf      Cnsrf')

        do 601 ihh = 1,nalpha
            write(75,320) alfstb(ihh),-yawstb(ib),
&          scztot(isf,ihh),scxtot(isf,ihh),scqtot(isf,ihh)/cbar,
&          scytot(isf,ihh),scptot(isf,ihh)/wspan,
&          scrtot(isf,ihh)/wspan
320    format(1x,2f8.3,6f9.4)
321    format(1x,1f8.3,8f9.4)

c...unit 73 for tecplot
        cltemp=scztot(isf,ihh)*cos(alfstb(ihh)*dtr)
&          -scxtot(isf,ihh)*sin(alfstb(ihh)*dtr)
        cdtemp=scxtot(isf,ihh)*cos(alfstb(ihh)*dtr)
&          +scztot(isf,ihh)*sin(alfstb(ihh)*dtr)
        write(73,7332) alfstb(ihh),-yawstb(ib),
&          scztot(isf,ihh),scxtot(isf,ihh),scqtot(isf,ihh)/cbar,
&          scytot(isf,ihh),scptot(isf,ihh)/wspan,
&          scrtot(isf,ihh)/wspan,cltemp,cdtemp
7332    format(1x,2f6.2,6f9.4,2f11.6)
601    continue

600    continue

        write(75,290)
290    format (/,' ***** WIND AXIS SYSTEM *****')

        do 602 isf = 1,nsurf

            tempsrf = srftitl(isf)

            write(75,7504) isf, tempsrf
7504    format(/,1x,'Surface ',i2,' ',a30,' Wind Axis')

            write(75,410)
410    format(1x,' Alpha      Beta      CLsrf      CDsrf      Cmsrf ',
&          '      CYsrf      Crsrf      Cnsrf')

            do 603 ihh = 1,nalpha
                astb = alfstb(ihh)

c... yawstb multiplied by -1 to give betstb
                sinast = sin(dtr*astb)
                sinbst = sin(dtr*(-yawstb(ib)))
                cosast = cos(dtr*astb)
                cosbst = cos(dtr*(-yawstb(ib)))

```

c...transform panel forces to wind axes

```

      cltotw = -sinast*scxtot(isf,ihh) + cosast*scztot(isf,ihh)
      cdtotw = cosbst*cosast*scxtot(isf,ihh) + sinbst*scytot(isf,ihh)
&      + cosbst*sinast*scztot(isf,ihh)
      cytotw = sinbst*cosast*scxtot(isf,ihh) + cosbst*scytot(isf,ihh)
&      + sinbst*sinast*scztot(isf,ihh)
      cmtotw = -sinbst*cosast*scptot(isf,ihh) + cosbst*scqtot(isf,ihh)
&      - sinbst*sinast*scrtot(isf,ihh)
      crtotw = cosbst*cosast*scptot(isf,ihh) + sinbst*scqtot(isf,ihh)
&      + cosbst*sinast*scrtot(isf,ihh)
      cntotw = -sinast*scptot(isf,ihh) + cosast*scrtot(isf,ihh)

      cmtotw = cmtotw /cbar
      crtotw = crtotw /wspan
      cntotw = cntotw /wspan

      write(75,320) alfstb(ihh), -yawstb(ib), cltotw, cdtotw,
&      cmtotw, cytotw, crtotw, cntotw

603   continue
602   continue

      write(75,490)
490   format (/,' ***** STABILITY AXIS SYSTEM *****')

      do 604 isf = 1,nsurf

         tempsrf = srftitl(isf)

         write(75,7505) isf, tempsrf
7505    format(/,1x,'Surface ',i2,' ',a30,' Stab Axis')
         write(75,510)
510    format(1x,'   Alpha      Beta      CLsrf      CDsrf      Cmsrf ',
&           '   CYsrf      Crsrf      Cnsrf')

         do 605 ihh = 1,nalpha

            astb   = alfstb(ihh)
            sinast = sin(dtr*astb)
            cosast = cos(dtr*astb)

```

c...transfer total forces and moments to stability axis

```

      cltots = -sinast*scxtot(isf,ihh) + cosast*scztot(isf,ihh)
      cdtots = cosast*scxtot(isf,ihh) + sinast*scztot(isf,ihh)
      cytots = scytot(isf,ihh)
      cmtots = scqtot(isf,ihh)
      crtots = cosast*scptot(isf,ihh) + sinast*scrtot(isf,ihh)
      cntots = -sinast*scptot(isf,ihh) + cosast*scrtot(isf,ihh)
      cmtots = cmtots / cbar
      crtots = crtots / wspan
      cntots = cntots / wspan

      write(75,320) alfstb(ihh), -yawstb(ib), cltots,
&      cdtots, cmtots, cytots, crtots, cntots

```



```

        if(isf.eq.2) clf1=cltots
        clf1 = -sinast*scxtot(2,ihh) + cosast*scztot(2,ihh)
        cdf1 =  cosast*scxtot(2,ihh) + sinast*scztot(2,ihh)
        clf2 = -sinast*scxtot(1,ihh) + cosast*scztot(1,ihh)
        cdf2 =  cosast*scxtot(1,ihh) + sinast*scztot(1,ihh)
        cyf2 =  scytot(1,ihh)
        cmtots = scqtot(1,ihh)
        crtots = scptot(1,ihh)
        cntots = scrtot(1,ihh)
        cmf2 =  cmtots / cbar
        crf2 =  crtots / wspan
        cnf2 =  cntots / wspan
        alf2=alfstb(ihh)
605      continue
604      continue
        write(92,321) alf2,clf1,cdf1,clf2,cdf2,cmf2,cyf2,crf2,cnf2

        return
        end

```

MT38a FILE (Three-Ship)

This is the three-ship version.

```

        program move
c
c  this code shifts the coordinates of a
c  HASC95 input file to simulate a formation of
c  aircraft by defining new aircraft positions
c
c  file "header" is the hasc header input
c  file "wing" is the basic wing geometry
c  file "ftemp" is the aerodynamic result file from hasc
c  file "fout" is the printed aerodynamic result file from hasc
c  file "final" is the normalized force/moment increment file
c  file "hasc.inp" is the generated hasc input file
c
c  +x = other vehicle upstream
c  +y = other vehicle right
c  +z = other vehicle below
c
c      character*80 f1
c
c      data for sim tables
c
c      dimension xi(1),yi(43),zi(6)
c      data xi/-4.,-3.,-2.,-1.6,-1.4,-1.2,-1.,-.8,-.6,-.4,-.3,-.2,-.1,0.,
c      x      .1,.2,.3,.4,.6,.8,1.,1.2,1.4,1.6,2.,3.,4./
c      data yi/1.0/
c      data zi/0.,0.25,0.5,1.0,2.0,50.0/
c
c      data for mesh plots  xi=2
c
c      dimension xi(1),yi(24)

```

```

        dimension yi(24)
c      data xi/2.0/
c      data yi/0.,0.0833,.1667,0.25,0.3333,0.4167,0.5,0.5833,0.6667,
c      x      0.75,0.8333,0.9167,1.0,1.0833,1.1667,
c      x      1.25,1.333,1.5,1.6667,1.8333,2.,2.3333,2.6667,3./
c      data zi/0.,0.001,0.002,0.005,0.01,0.02,0.04,0.0833,
c      x      .1667,0.25,0.3333,0.4167,0.5,0.5833,0.6667,
c      x      0.75,0.8333,0.9167,1.0,1.0833,1.1667,
c      x      1.25,1.333,1.5,1.6667,1.8333,2.,2.3333,2.6667,3./
c
        open(90,file='header2',status='old')
        open(91,file='wing',status='old')
        open(92,file='ftemp',status='unknown')
        open(95,file='lead',status='old')
        open(96,file='twowing',status='old')
        open(102,file='fout',status='unknown')
        open(103,file='final',status='unknown')
        alpl=0.
        span=306.
c
c      enter downstream spacing
c
c      write(*,*) 'enter x/b'
c      read(*,*) xi
c      xi=2.5
c
c      loop on relative aircraft x,y,z positions
c
c      do 1000 ix=1,1
c      delx=xi*span
c      delx=xi(1)*span
c      do 2000 iz=1,1
c      delz=zi*span
c      delz=0.
c      do 3000 iy=3,55
c      do 3000 iy=37,37
c      dely=(iy-1)*8.5
c      open(15,file='hasc.inp',status='unknown')
c
c      write header to hasc input file
c
c      do 3100 ii=1,16
c      read(90,900) f1
c      write(15,900) f1
3100      continue
c
c      rewind header for next case
c
c      rewind(90)
c
c      write trail wing #3 to hasc input file
c
c      do 3200 ii=1,4
c      read(91,900) f1
c      write(15,900) f1
3200      continue
c      do 3250 ii=1,20
c      read(91,900) f1

```

```

        write(15,900) f1
        read(91,900) f1
        write(15,900) f1
        read(91,900) f1
        write(15,900) f1
        read(91,900) f1
        write(15,900) f1
3250      continue
c
c      rewind wing geometry file for lead wing processing
c
c          rewind(91)
c
c      write wing #2 to hasc input file
c
c          do 3300 ii=1,4
c          read(96,900) f1
c          write(15,900) f1
3300      continue
c          do 3350 ii=1,20
c          read(96,*) x1,y1,z1,c1,a1
c          write(15,*) x1-delx,y1+dely,z1-delz,c1,a1+alpl
c          read(96,*) x1,y1,z1,c1,a1
c          write(15,*) x1-delx,y1+dely,z1-delz,c1,a1+alpl
c          read(96,900) f1
c          write(15,900) f1
c          read(96,900) f1
c          write(15,900) f1
3350      continue
c
c      rewind wing geometry file for lead wing processing
c
c          rewind(91)
c          rewind(96)
c
c      write lead wing to hasc input file
c
c          do 3500 ii=1,4
c          read(95,900) f1
c          write(15,900) f1
3500      continue
c          do 3550 ii=1,20
c          read(95,*) x1,y1,z1,c1,a1
c      the first line is for equal spacing, the second is for a fixed #2
c          write(15,*) x1-2*delx,y1+2*dely,z1-2*delz,c1,a1+alpl
c          write(15,*) x1-2*delx,y1+dely+263.5,z1-2*delz,c1,a1+alpl
c          read(95,*) x1,y1,z1,c1,a1
c          write(15,*) x1-2*delx,y1+2*dely,z1-2*delz,c1,a1+alpl
c          write(15,*) x1-2*delx,y1+dely+263.5,z1-2*delz,c1,a1+alpl
c          read(95,900) f1
c          write(15,900) f1
c          read(95,900) f1
c          write(15,900) f1
3550      continue
c
c      rewind wing geometry file for next case
c
c          rewind(91)

```

```

                rewind(95)
c
c      rewind input file for hasc run
c      rewind aero file so it can be written
c
                rewind(15)
                rewind(92)
c
c run hasc
c
                call hasc
c
c      rewind aero file written by hasc so it can be read
c
                rewind(92)
                read(92,920) aoa,cl1,cd1,cl2,cd2,
x                cl3,cd3,cm3,cy3,cll3,cln3
c
c compute increments for sim table look-up
c
c print output files
c
                write(103,925) dely/span,aoa,cl1,cd1,cl2,cd2,
1                cl3,cd3,cm3,cy3,cll3,cln3
c
                close(15,status='keep')
c
3000 continue
c 2000 continue
c 1000 continue
c
900 format(a80)
c 910 format(f8.3,f9.3,f9.3,f9.3,f9.3)
920 format(1x,1f8.3,10f10.5)
925 format(1x,12f11.5)
935 format(1x,9f10.5)
                close(90,status='keep')
                close(91,status='keep')
                close(92,status='keep')
                close(95,status='keep')
                close(96,status='keep')
                close(102,status='keep')
                close(103,status='keep')
                stop
                end

```

PRISRF FILE (Three-Ship)

This is the three-ship version.

```

                subroutine prisrf
c...purpose:
c  prints, by surface, forces and moments in body axis,

```

```

c   wind axis, and stability axis.

c...output:  unit 75 (hasc.out)

c...subroutine called by hasc
c   subroutine calls:  none

c...discussion:  forces and moments are initially in body axis,
c   they are translated to wind and stability axis, and printed
c   out as a summary for each axis.

      parameter (lun=201, ntal=30)

      include 'flowopts.cmn'
      include 'set3.cmn'
      include 'set5.cmn'
      include 'set6.cmn'
      include 'set8.cmn'
      include 'set9.cmn'
      include 'set11.cmn'
      include 'set12.cmn'
      include 'set13.cmn'
      include 'set14.cmn'
      include 'set15.cmn'
      include 'set17.cmn'
      include 'set21.cmn'
      include 'set23.cmn'
      include 'set24.cmn'
      include 'forces.cmn'
      include 'print.cmn'
      include 'srffrc.cmn'
      include 'surtit.cmn'
      include 'version.cmn'

      character*30 tempsrf

      pi  = 4.0 * atan(1.0)
      dtr = pi / 180.

c...print heading with hasc version and release date

      write(75,104) vtitle
104   format(/,1x,a55)

      write(75,107)
107   format(1x,'** Surface Force and Moments **',/)

c...print out surface data

      write(75,105) jobtitl
105   format(1x,a)

      write(75,120) mach(iq), -yawstb(ib),
& pitchq,-rollq,-yawq,vinf
120   format(' Mach = ',f6.2,' beta = ',f7.2,/,
& 1x,'Pitch rate = ',f7.2,'/sec',/,
& 1x,'Roll rate  = ',f7.2,'/sec',/,
& 1x,'Yaw rate   = ',f7.2,'/sec',/,

```

```

& 1x,'Vinf          =',f10.2)

write(75,6662) sref,wspan,cbar
6662 format(/,1x,'Sref = ',f9.3,' Wspan = ',f9.3,' Cbar = ',f9.3)
write(75,6663) xbar, zbar
6663 format(1x,'Xbar = ',f9.3,' Zbar = ',f9.3)

write(75,190)
190 format (/,' ***** BODY AXIS SYSTEM *****')

do 600 isf = 1,nsurf

    tempsrf = srftitl(isf)

    write(73,7316) isf, mach(iq), -yawstb(ib)
7316 format('ZONE T="Surf ',i2,' M=',f5.2,' Beta=',f6.2,'" F=POINT')

    write(75,7503) isf,tempsrf
7503 format(/,1x,'Surface ',i2,' ',a30,' Body Axis')

300 write(75,310)
310 format(1x,' Alpha      Beta      CNsrf      CAsrf      Cmsrf ',
&          ' CYsrf      Crsrf      Cnsrf')

    do 601 ihh = 1,nalpha
        write(75,320) alfstb(ihh),-yawstb(ib),
&      scztot(isf,ihh),scxtot(isf,ihh),scqtot(isf,ihh)/cbar,
&      scytot(isf,ihh),scptot(isf,ihh)/wspan,
&      scrtot(isf,ihh)/wspan
320 format(1x,2f8.3,6f9.4)
321 format(1x,1f8.3,10f10.5)

c...unit 73 for tecplot
    cltemp=scztot(isf,ihh)*cos(alfstb(ihh)*dtr)
&      -scxtot(isf,ihh)*sin(alfstb(ihh)*dtr)
    cdtemp=scxtot(isf,ihh)*cos(alfstb(ihh)*dtr)
&      +scztot(isf,ihh)*sin(alfstb(ihh)*dtr)
    write(73,7332) alfstb(ihh),-yawstb(ib),
&      scztot(isf,ihh),scxtot(isf,ihh),scqtot(isf,ihh)/cbar,
&      scytot(isf,ihh),scptot(isf,ihh)/wspan,
&      scrtot(isf,ihh)/wspan,cltemp,cdtemp
7332 format(1x,2f6.2,6f9.4,2f11.6)
601 continue

600 continue

write(75,290)
290 format (/,' ***** WIND AXIS SYSTEM *****')

do 602 isf = 1,nsurf

    tempsrf = srftitl(isf)

    write(75,7504) isf, tempsrf
7504 format(/,1x,'Surface ',i2,' ',a30,' Wind Axis')

```

```

        write(75,410)
410  format(1x,'  Alpha      Beta      CLsrf      CDsrf      Cmsrf ',
&      '      CYsrf      Crsrf      Cnsrf')

        do 603 ihh = 1,nalpha
            astb = alfstb(ihh)

c... yawstb multiplied by -1 to give betstb
            sinast = sin(dtr*astb)
            sinbst = sin(dtr*(-yawstb(ib)))
            cosast = cos(dtr*astb)
            cosbst = cos(dtr*(-yawstb(ib)))

c...transform panel forces to wind axes

            cltotw = -sinast*scxtot(isf,ihh) + cosast*scztot(isf,ihh)
            cdtotw = cosbst*cosast*scxtot(isf,ihh) + sinbst*scytot(isf,ihh)
&            + cosbst*sinast*scztot(isf,ihh)
            cytotw = sinbst*cosast*scxtot(isf,ihh) + cosbst*scytot(isf,ihh)
&            + sinbst*sinast*scztot(isf,ihh)
            cmtotw = -sinbst*cosast*scptot(isf,ihh) + cosbst*scqtot(isf,ihh)
&            -sinbst*sinast*scrtot(isf,ihh)
            crtotw = cosbst*cosast*scptot(isf,ihh) + sinbst*scqtot(isf,ihh)
&            + cosbst*sinast*scrtot(isf,ihh)
            cntotw = -sinast*scptot(isf,ihh) + cosast*scrtot(isf,ihh)

            cmtotw = cmtotw /cbar
            crtotw = crtotw /wspan
            cntotw = cntotw /wspan

            write(75,320) alfstb(ihh), -yawstb(ib), cltotw, cdtotw,
&            cmtotw, cytotw, crtotw, cntotw

603    continue
602    continue

        write(75,490)
490  format (/,' ***** STABILITY AXIS SYSTEM *****')

        do 604 isf = 1,nsurf

            tempsrf = srftitl(isf)

            write(75,7505) isf, tempsrf
7505  format(/,1x,'Surface ',i2,' ',a30,' Stab Axis')
            write(75,510)
510  format(1x,'  Alpha      Beta      CLsrf      CDsrf      Cmsrf ',
&      '      CYsrf      Crsrf      Cnsrf')

            do 605 ihh = 1,nalpha

                astb = alfstb(ihh)
                sinast = sin(dtr*astb)
                cosast = cos(dtr*astb)

c...transfer total forces and moments to stability axis

```

```

        cltots = -sinast*scxtot(isf,ihh) + cosast*scztot(isf,ihh)
        cdtots =  cosast*scxtot(isf,ihh) + sinast*scztot(isf,ihh)
        cytots =  scytot(isf,ihh)
        cmtots =  scqtot(isf,ihh)
        crtots =  cosast*scptot(isf,ihh) + sinast*scrtot(isf,ihh)
        cntots = -sinast*scptot(isf,ihh) + cosast*scrtot(isf,ihh)
        cmtots =  cmtots / cbar
        crtots =  crtots / wspan
        cntots =  cntots / wspan

        write(75,320) alfstb(ihh), -yawstb(ib), cltots,
&      cdtots, cmtots, cytots, crtots, cntots
        if(isf.eq.2) clf1=cltots
        clf1 = -sinast*scxtot(3,ihh) + cosast*scztot(3,ihh)
        cdf1 =  cosast*scxtot(3,ihh) + sinast*scztot(3,ihh)
        clf2 = -sinast*scxtot(2,ihh) + cosast*scztot(2,ihh)
        cdf2 =  cosast*scxtot(2,ihh) + sinast*scztot(2,ihh)
        clf3 = -sinast*scxtot(1,ihh) + cosast*scztot(1,ihh)
        cdf3 =  cosast*scxtot(1,ihh) + sinast*scztot(1,ihh)
        cyf3 =  scytot(1,ihh)
        cmtots =  scqtot(1,ihh)
        crtots =  scptot(1,ihh)
        cntots =  scrtot(1,ihh)
        cmf3 =  cmtots / cbar
        crf3 =  crtots / wspan
        cnf3 =  cntots / wspan
        alf2 = alfstb(ihh)
605      continue
604      continue
        write(92,321) alf2,clf1,cdf1,clf2,cdf2,clf3,cdf3,cmf3,
x          cyf3,crf3,cnf3

        return
        end

```


Appendix B: Data and Matlab Files

This appendix shows the data and the Matlab files used to produce the plots in the thesis.

The first set set of data is from moving the aircraft with equal spacings in the three-ship

case. The second set of data shows the data from fixing the #1 wingman and only

moving #2 wingman on both the inboard and outboard side of the #1 wingman.

This is the Two-Ship data with my final 38 model # Data is: Redshift, abs_m, CL1, CL2, CL3, CL4, CL5, CL6, CL7, CL8, CL9, CL10, CL11, CL12, CL13, CL14, CL15, CL16, CL17, CL18, CL19, CL20, CL21, CL22, CL23, CL24, CL25, CL26, CL27, CL28, CL29, CL30, CL31, CL32, CL33, CL34, CL35, CL36, CL37, CL38, CL39, CL40, CL41, CL42, CL43, CL44, CL45, CL46, CL47, CL48, CL49, CL50, CL51, CL52, CL53, CL54, CL55, CL56, CL57, CL58, CL59, CL60, CL61, CL62, CL63, CL64, CL65, CL66, CL67, CL68, CL69, CL70, CL71, CL72, CL73, CL74, CL75, CL76, CL77, CL78, CL79, CL80, CL81, CL82, CL83, CL84, CL85, CL86, CL87, CL88, CL89, CL90, CL91, CL92, CL93, CL94, CL95, CL96, CL97, CL98, CL99, CL100, CL101, CL102, CL103, CL104, CL105, CL106, CL107, CL108, CL109, CL110, CL111, CL112, CL113, CL114, CL115, CL116, CL117, CL118, CL119, CL120, CL121, CL122, CL123, CL124, CL125, CL126, CL127, CL128, CL129, CL130, CL131, CL132, CL133, CL134, CL135, CL136, CL137, CL138, CL139, CL140, CL141, CL142, CL143, CL144, CL145, CL146, CL147, CL148, CL149, CL150, CL151, CL152, CL153, CL154, CL155, CL156, CL157, CL158, CL159, CL160, CL161, CL162, CL163, CL164, CL165, CL166, CL167, CL168, CL169, CL170, CL171, CL172, CL173, CL174, CL175, CL176, CL177, CL178, CL179, CL180, CL181, CL182, CL183, CL184, CL185, CL186, CL187, CL188, CL189, CL190, CL191, CL192, CL193, CL194, CL195, CL196, CL197, CL198, CL199, CL200, CL201, CL202, CL203, CL204, CL205, CL206, CL207, CL208, CL209, CL210, CL211, CL212, CL213, CL214, CL215, CL216, CL217, CL218, CL219, CL220, CL221, CL222, CL223, CL224, CL225, CL226, CL227, CL228, CL229, CL230, CL231, CL232, CL233, CL234, CL235, CL236, CL237, CL238, CL239, CL240, CL241, CL242, CL243, CL244, CL245, CL246, CL247, CL248, CL249, CL250, CL251, CL252, CL253, CL254, CL255, CL256, CL257, CL258, CL259, CL260, CL261, CL262, CL263, CL264, CL265, CL266, CL267, CL268, CL269, CL270, CL271, CL272, CL273, CL274, CL275, CL276, CL277, CL278, CL279, CL280, CL281, CL282, CL283, CL284, CL285, CL286, CL287, CL288, CL289, CL290, CL291, CL292, CL293, CL294, CL295, CL296, CL297, CL298, CL299, CL300, CL301, CL302, CL303, CL304, CL305, CL306, CL307, CL308, CL309, CL310, CL311, CL312, CL313, CL314, CL315, CL316, CL317, CL318, CL319, CL320, CL321, CL322, CL323, CL324, CL325, CL326, CL327, CL328, CL329, CL330, CL331, CL332, CL333, CL334, CL335, CL336, CL337, CL338, CL339, CL340, CL341, CL342, CL343, CL344, CL345, CL346, CL347, CL348, CL349, CL350, CL351, CL352, CL353, CL354, CL355, CL356, CL357, CL358, CL359, CL360, CL361, CL362, CL363, CL364, CL365, CL366, CL367, CL368, CL369, CL370, CL371, CL372, CL373, CL374, CL375, CL376, CL377, CL378, CL379, CL380, CL381, CL382, CL383, CL384, CL385, CL386, CL387, CL388, CL389, CL390, CL391, CL392, CL393, CL394, CL395, CL396, CL397, CL398, CL399, CL400, CL401, CL402, CL403, CL404, CL405, CL406, CL407, CL408, CL409, CL410, CL411, CL412, CL413, CL414, CL415, CL416, CL417, CL418, CL419, CL420, CL421, CL422, CL423, CL424, CL425, CL426, CL427, CL428, CL429, CL430, CL431, CL432, CL433, CL434, CL435, CL436, CL437, CL438, CL439, CL440, CL441, CL442, CL443, CL444, CL445, CL446, CL447, CL448, CL449, CL450, CL451, CL452, CL453, CL454, CL455, CL456, CL457, CL458, CL459, CL460, CL461, CL462, CL463, CL464, CL465, CL466, CL467, CL468, CL469, CL470, CL471, CL472, CL473, CL474, CL475, CL476, CL477, CL478, CL479, CL480, CL481, CL482, CL483, CL484, CL485, CL486, CL487, CL488, CL489, CL490, CL491, CL492, CL493, CL494, CL495, CL496, CL497, CL498, CL499, CL500, CL501, CL502, CL503, CL504, CL505, CL506, CL507, CL508, CL509, CL510, CL511, CL512, CL513, CL514, CL515, CL516, CL517, CL518, CL519, CL520, CL521, CL522, CL523, CL524, CL525, CL526, CL527, CL528, CL529, CL530, CL531, CL532, CL533, CL534, CL535, CL536, CL537, CL538, CL539, CL540, CL541, CL542, CL543, CL544, CL545, CL546, CL547, CL548, CL549, CL550, CL551, CL552, CL553, CL554, CL555, CL556, CL557, CL558, CL559, CL560, CL561, CL562, CL563, CL564, CL565, CL566, CL567, CL568, CL569, CL570, CL571, CL572, CL573, CL574, CL575, CL576, CL577, CL578, CL579, CL580, CL581, CL582, CL583, CL584, CL585, CL586, CL587, CL588, CL589, CL590, CL591, CL592, CL593, CL594, CL595, CL596, CL597, CL598, CL599, CL600, CL601, CL602, CL603, CL604, CL605, CL606, CL607, CL608, CL609, CL610, CL611, CL612, CL613, CL614, CL615, CL616, CL617, CL618, CL619, CL620, CL621, CL622, CL623, CL624, CL625, CL626, CL627, CL628, CL629, CL630, CL631, CL632, CL633, CL634, CL635, CL636, CL637, CL638, CL639, CL640, CL641, CL642, CL643, CL644, CL645, CL646, CL647, CL648, CL649, CL650, CL651, CL652, CL653, CL654, CL655, CL656, CL657, CL658, CL659, CL660, CL661, CL662, CL663, CL664, CL665, CL666, CL667, CL668, CL669, CL670, CL671, CL672, CL673, CL674, CL675, CL676, CL677, CL678, CL679, CL680, CL681, CL682, CL683, CL684, CL685, CL686, CL687, CL688, CL689, CL690, CL691, CL692, CL693, CL694, CL695, CL696, CL697, CL698, CL699, CL700, CL701, CL702, CL703, CL704, CL705, CL706, CL707, CL708, CL709, CL710, CL711, CL712, CL713, CL714, CL715, CL716, CL717, CL718, CL719, CL720, CL721, CL722, CL723, CL724, CL725, CL726, CL727, CL728, CL729, CL730, CL731, CL732, CL733, CL734, CL735, CL736, CL737, CL738, CL739, CL740, CL741, CL742, CL743, CL744, CL745, CL746, CL747, CL748, CL749, CL750, CL751, CL752, CL753, CL754, CL755, CL756, CL757, CL758, CL759, CL760, CL761, CL762, CL763, CL764, CL765, CL766, CL767, CL768, CL769, CL770, CL771, CL772, CL773, CL774, CL775, CL776, CL777, CL778, CL779, CL780, CL781, CL782, CL783, CL784, CL785, CL786, CL787, CL788, CL789, CL790, CL791, CL792, CL793, CL794, CL795, CL796, CL797, CL798, CL799, CL800, CL801, CL802, CL803, CL804, CL805, CL806, CL807, CL808, CL809, CL810, CL811, CL812, CL813, CL814, CL815, CL816, CL817, CL818, CL819, CL820, CL821, CL822, CL823, CL824, CL825, CL826, CL827, CL828, CL829, CL830, CL831

```

CL2 = x(:,5);
CL1 = x(:,3);
KL2 = (CD2*K0*CL2.^2)./(CL1.*CL2);
Ratio = KL2/K0;
plot(spacing,Ratio)
title('Drag Savings for Formation Flight')
xlabel('lateral Spacing (° - Wingtip to Wingtip)')
ylabel('Ratio of Drag Correction Factors')
hold on

# y is the free ship data
# Data is spaced 400, CL1, CL2, CD2, CL3, CD3, Cm3, Cy3, CL3, CL3
y= [0.19444 3.00000 0.23400 0.11686 0.00527 0.00283 0.11079 0.00220 -0.02748 -0.00214 0.01874 0.00135;
0.22222 3.00000 0.23404 0.12593 0.00527 0.00293 0.12500 0.00241 -0.02994 -0.00245 0.02006 0.00145;
0.25000 3.00000 0.23409 0.13678 0.00527 0.00307 0.13923 0.00260 -0.02960 -0.00275 0.02091 0.00155;
0.27778 3.00000 0.23414 0.14758 0.00527 0.00321 0.15322 0.00277 -0.02861 -0.00304 0.02145 0.00164;
0.30556 3.00000 0.23419 0.15833 0.00527 0.00334 0.16693 0.00292 0.02754 -0.00332 0.02170 0.00167;
0.33333 3.00000 0.23424 0.16895 0.00527 0.00346 0.18031 0.00305 -0.02694 -0.00357 0.02166 0.00170;
0.36111 3.00000 0.23428 0.17940 0.00527 0.00357 0.19330 0.00317 -0.02470 -0.00379 0.02133 0.00169;
0.38889 3.00000 0.23432 0.18969 0.00527 0.00365 0.20588 0.00325 -0.02300 -0.00398 0.02075 0.00167;
0.41667 3.00000 0.23437 0.20007 0.00528 0.00406 0.21827 0.00374 -0.02428 -0.00378 0.01995 0.00162;
0.44444 3.00000 0.23441 0.21014 0.00528 0.00446 0.23014 0.00420 -0.02165 -0.00357 0.01890 0.00155;
0.47222 3.00000 0.23447 0.22024 0.00528 0.00479 0.24182 0.00458 -0.01924 -0.00335 0.01759 0.00149;
0.50000 3.00000 0.23453 0.22985 0.00528 0.00509 0.25278 0.00491 -0.00469 -0.00310 0.01608 0.00140;
0.52778 3.00000 0.23457 0.23888 0.00528 0.00534 0.26294 0.00517 0.00066 -0.00282 0.01440 0.00131;
0.55556 3.00000 0.23461 0.24722 0.00528 0.00553 0.27215 0.00536 0.00132 -0.00248 0.01259 0.00119;
0.58333 3.00000 0.23462 0.25461 0.00528 0.00565 0.28009 0.00546 -0.00434 -0.00209 0.01072 0.00106;
0.61111 3.00000 0.23464 0.26153 0.00528 0.00560 0.28729 0.00560 0.00000 -0.00159 0.00875 0.00091;
0.63889 3.00000 0.23466 0.26752 0.00528 0.00502 0.29323 0.00458 -0.01422 -0.00074 0.00674 0.00071;
0.66667 3.00000 0.23467 0.27307 0.00528 0.00480 0.29850 0.00428 -0.01859 -0.00011 0.00472 0.00050;
0.69444 3.00000 0.23468 0.27799 0.00528 0.00465 0.30291 0.00407 -0.02238 0.00035 0.00273 0.00028;
0.72222 3.00000 0.23469 0.28220 0.00528 0.00452 0.30638 0.00391 0.02578 0.00073 0.00083 0.00006;
0.75000 3.00000 0.23470 0.28561 0.00528 0.00441 0.30884 0.00378 -0.02883 0.00105 -0.00094 -0.00015;
0.77778 3.00000 0.23470 0.28805 0.00528 0.00431 0.31008 0.00368 -0.03141 0.00131 -0.00248 -0.00035;
0.80556 3.00000 0.23469 0.28867 0.00528 0.00424 0.30908 0.00364 -0.03305 0.00146 -0.00341 -0.00048;
0.83333 3.00000 0.23469 0.28960 0.00528 0.00417 0.30862 0.00359 -0.03491 0.00161 -0.00456 -0.00065;
0.86111 3.00000 0.23469 0.29013 0.00528 0.00410 0.30780 0.00355 -0.03660 0.00174 -0.00566 -0.00081;
0.88889 3.00000 0.23468 0.29009 0.00528 0.00405 0.30643 0.00351 -0.03799 0.00183 -0.00663 -0.00095;
0.91667 3.00000 0.23467 0.28939 0.00528 0.00401 0.30440 0.00351 -0.03904 0.00188 -0.00740 -0.00107;
0.94444 3.00000 0.23465 0.28790 0.00528 0.00399 0.30158 0.00354 -0.03963 0.00188 -0.00791 -0.00116;
0.97222 3.00000 0.23464 0.28538 0.00528 0.00402 0.29771 0.00361 -0.03964 0.00182 -0.00804 -0.00119;
1.00000 3.00000 0.23461 0.28126 0.00528 0.00412 0.29214 0.00378 -0.03874 0.00164 -0.00754 -0.00112;
1.02778 3.00000 0.23457 0.27227 0.00527 0.00458 0.28125 0.00436 -0.03527 0.00105 -0.00514 -0.00067;
1.05556 3.00000 0.23455 0.26754 0.00527 0.00474 0.27538 0.00457 -0.03370 0.00082 -0.00410 -0.00051;
1.08333 3.00000 0.23453 0.26409 0.00527 0.00483 0.27107 0.00469 -0.03267 0.00068 -0.00342 -0.00041;
1.11111 3.00000 0.23451 0.26136 0.00527 0.00490 0.26764 0.00478 -0.03191 0.00057 -0.00292 -0.00035;
1.13889 3.00000 0.23450 0.25910 0.00527 0.00495 0.26480 0.00485 -0.03132 0.00049 -0.00254 -0.00030;
1.16667 3.00000 0.23448 0.25718 0.00527 0.00499 0.26238 0.00499 -0.03083 0.00043 -0.00224 -0.00026;
1.19444 3.00000 0.23447 0.25553 0.00527 0.00502 0.26029 0.00494 -0.03043 0.00038 -0.00223 -0.00023;
1.22222 3.00000 0.23446 0.25407 0.00527 0.00504 0.25846 0.00497 -0.03009 0.00034 -0.00219 -0.00020;
1.25000 3.00000 0.23445 0.25279 0.00527 0.00507 0.25684 0.00500 -0.02980 0.00030 -0.00178 -0.00020;
1.27778 3.00000 0.23444 0.25164 0.00527 0.00508 0.25540 0.00503 -0.02955 0.00027 -0.00145 -0.00016;
1.30556 3.00000 0.23443 0.25060 0.00527 0.00510 0.25410 0.00505 -0.02933 0.00025 -0.00132 -0.00014;
1.33333 3.00000 0.23442 0.24967 0.00527 0.00511 0.25292 0.00506 -0.02913 0.00023 -0.00121 -0.00013;
1.36111 3.00000 0.23441 0.24882 0.00527 0.00512 0.25185 0.00508 -0.02896 0.00021 -0.00111 -0.00012;
1.38889 3.00000 0.23440 0.24804 0.00527 0.00514 0.25087 0.00509 -0.02885 0.00019 -0.00102 -0.00011;
1.41667 3.00000 0.23439 0.24733 0.00527 0.00514 0.24998 0.00511 -0.02865 0.00017 -0.00094 -0.00010;
1.44444 3.00000 0.23438 0.24667 0.00527 0.00515 0.24916 0.00512 -0.02853 0.00016 -0.00087 -0.00009;
1.47222 3.00000 0.23438 0.24607 0.00527 0.00516 0.24841 0.00513 -0.02841 -0.00015 -0.00081 -0.00009;
1.50000 3.00000 0.23437 0.24550 0.00527 0.00517 0.24770 0.00514 -0.02830 0.00014 -0.00075 -0.00008];

CD3 = y(:,8);

```

```

CL3 = Y(:,7);
CL23 = CL2(8:55);
CL13 = CL1(8:55);
K13 = (CD3 K0*CL3.^2-K12(8:55).*CL23.*CL3)./(CL13.*CL3);

% Data from running different aileron deflections
trimspace=[.1944 .2111 .2381 .3056 .3472 .4121 .4495 .4745 .5 .5214 .5408 .5611 .5798 .5980 ...
.6160 .6340 .6503 .6682 .6852 .6929 .7026 .7108 .7191 .7292 .7378 .7467 .7574 .7680 .7778 ...
.7932 .8079 .8207 .8333 .8459 .8611 .875 .8889 .9074 .9306 .9722 1.0026 1.0093 1.0159 ...
1.0238 1.034 1.0494 1.0741 1.1042 1.1482 1.2083 1.3333 1.5];
trimdrag=[1.2597 1.2772 1.2180 .9921 .8117 .5589 .4772 .3956 .3028 .2409 .1769 .1103 .0430 ...
-.0213 -.1014 -.2136 -.2868 -.3501 -.3982 -.4109 -.4431 -.4571 -.4703 -.4999 -.5133 ...
-.5253 -.5388 -.5510 -.5615 -.5637 -.5675 -.5763 -.5714 -.5808 -.5899 -.5826 -.5746 ...
-.5656 -.5654 -.5284 -.4828 -.4605 -.4409 -.4101 -.3773 -.3519 -.3132 -.2711 -.2412 ...
-.2044 -.1557 -.1050];

% Plot the 2-ship with and w/o trim
plot(trimspace,trimdrag,'k.')
legend('2-Ship - K12/K0','2-Ship with Trimmed Aileron')

% Plot the 3 ship, no trim case
figure
plot(spacing(8:55),K13/K0,'k+',spacing(8:55),(K13+K12(8:55))/K0,'r.',trimspace,trimdrag,'m'))
legend('2-Ship - K12/K0','3 Ship - K13/K0','3-Ship - (K12 + K13)/K0','2 Ship with Trimmed Aileron')

```



```

0.80556 3.00000 0.23469 0.00528 0.29012 0.00423 0.31048 0.00355 -0.03287 0.00152 -0.00324 -0.00049;
0.83333 3.00000 0.23469 0.00528 0.29012 0.00423 0.31206 0.00344 0.03554 0.00176 -0.00072;
0.86111 3.00000 0.23469 0.00528 0.29012 0.00423 0.31261 0.00335 -0.03778 0.00195 -0.00092;
0.88889 3.00000 0.23468 0.00528 0.29011 0.00423 0.31130 0.00331 -0.03917 0.00204 -0.00064;
0.91667 3.00000 0.23468 0.00528 0.29009 0.00423 0.30938 0.00329 -0.04022 0.00209 -0.00108;
0.94444 3.00000 0.23468 0.00528 0.29008 0.00423 0.30668 0.00331 -0.04082 0.00210 -0.00120;
0.97222 3.00000 0.23468 0.00528 0.29006 0.00423 0.30294 0.00338 -0.04084 0.00203 -0.00130;
1.00000 3.00000 0.23467 0.00528 0.29004 0.00423 0.29748 0.00356 -0.03991 0.00184 -0.00127;
1.02778 3.00000 0.23466 0.00528 0.29000 0.00423 0.28662 0.00420 -0.03629 0.00130 -0.00077;
1.05556 3.00000 0.23466 0.00528 0.28997 0.00423 0.28071 0.00443 -0.03465 0.00095 -0.00059;
1.08333 3.00000 0.23466 0.00528 0.28995 0.00423 0.27634 0.00457 -0.03357 0.00079 -0.00048;
1.11111 3.00000 0.23465 0.00528 0.28994 0.00423 0.27283 0.00467 -0.03276 0.00067 -0.00041;
1.13889 3.00000 0.23465 0.00528 0.28992 0.00423 0.26989 0.00475 -0.03212 0.00059 -0.00035;
1.16667 3.00000 0.23465 0.00528 0.28991 0.00423 0.26738 0.00481 -0.03160 0.00052 -0.00031;
1.19444 3.00000 0.23465 0.00528 0.28990 0.00423 0.26519 0.00485 -0.03117 0.00046 -0.00027;
1.22222 3.00000 0.23465 0.00528 0.28988 0.00423 0.26325 0.00489 -0.03080 0.00041 -0.00024;
1.25000 3.00000 0.23464 0.00528 0.28987 0.00423 0.26153 0.00493 -0.03049 0.00037 -0.00022;
1.27778 3.00000 0.23464 0.00528 0.28986 0.00423 0.25998 0.00496 -0.03021 0.00034 -0.00020;
1.30556 3.00000 0.23464 0.00528 0.28985 0.00423 0.25857 0.00498 -0.02996 0.00031 -0.00018;
1.33333 3.00000 0.23464 0.00528 0.28984 0.00423 0.25730 0.00500 -0.02975 0.00028 -0.00016;
1.36111 3.00000 0.23464 0.00528 0.28984 0.00423 0.25613 0.00502 -0.02955 0.00026 -0.00015;
1.38889 3.00000 0.23464 0.00528 0.28983 0.00423 0.25506 0.00504 -0.02938 0.00024 -0.00014;
1.41667 3.00000 0.23463 0.00528 0.28982 0.00423 0.25407 0.00505 -0.02922 0.00022 -0.00013;
1.44444 3.00000 0.23463 0.00528 0.28981 0.00423 0.25315 0.00507 -0.02907 0.00021 -0.00012;
1.47222 3.00000 0.23463 0.00528 0.28980 0.00423 0.25230 0.00508 -0.02894 -0.00019 -0.00011;
1.50000 3.00000 0.23463 0.00528 0.28979 0.00423 0.25152 0.00509 -0.02882 -0.00018 -0.00010;

```

```

spacinga = trim_3in(:,1);
spacingb = trim_3out(:,1);
c1a = trim_3in(:,3);
c1b = trim_3out(:,3);
CD2a = trim_3in(:,6);
CD2b = trim_3out(:,6);
CL2a = trim_3in(:,5);
CL2b = trim_3out(:,5);
CD3a = trim_3in(:,8);
CD3b = trim_3out(:,8);
CL3a = trim_3in(:,7);
CL3b = trim_3out(:,7);

K0 = .09646;
% K12 comes from the previous file
% Flip the K12 matrix to give the symmetrical result on the left side of #2
% K12 cores from the previous Matlab file, so it needs to be run first
flipper = flipud(K12);
K23a = flipper(23:50);
K23b = K12(3:55);
K13a = (CD3a-K0*CL3a.^2-K23a.*CL2a.*CL3a)./(CL1a.*CL3a);
K13b = (CD3b-K0*CL3b.^2-K23b.*CL2b.*CL3b)./(CL1b.*CL3b);

plot(spacinga,K13a/K0,'k','s',spacinga,(K13a+K23a)/K0,'r','s',spacinga,K23a/K0,'b')
hold on
plot(spacingb,K13b/K0,'k','s',spacingb,(K13b+K23b)/K0,'r','s',spacingb,K23b/K0,'b')
legend('3-Ship - K13/K0','3-Ship - (K23 + K13)/K0','3-Ship - K23/K0')
hold off

```

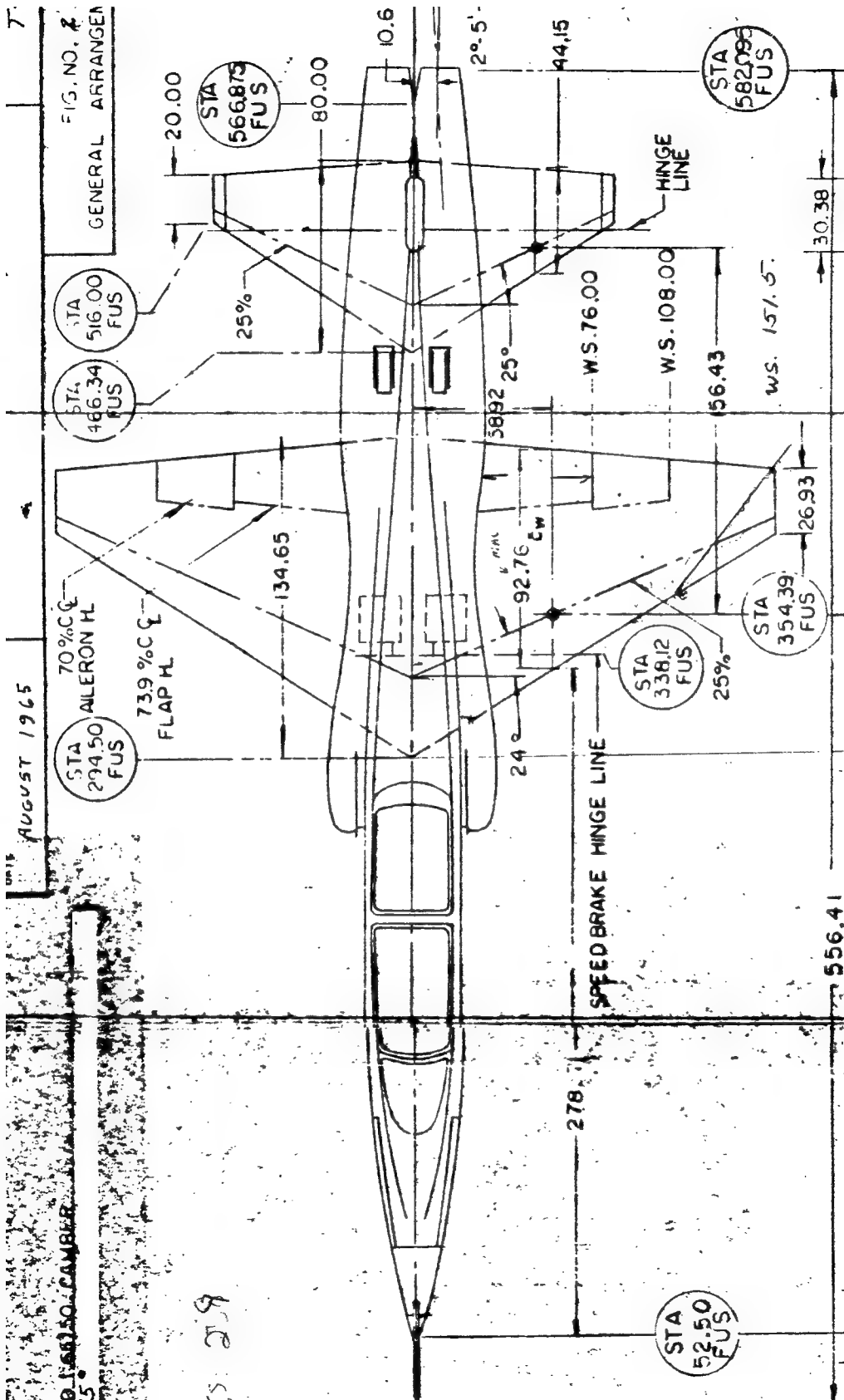
```

figure
plot(spacinga,trim_3in(:,1),spacingb,trim_3out(:,1))

```

Appendix C: Actual T-38 Dimensional Data

The next page is a schematic showing the actual T-38 dimensions that the model was built from. The picture is compliments of the T-38 SPO at Kelly AFB. The dimensions can be compared to the wing file from Appendix A to see where dimensions vary. The actual aircraft and the model are very close, however this schematic is shown for completeness.



Appendix D: Data Reduction Process

This appendix is taken directly from the test team's final report, Reference 13.

The cruise point for each run was qualitatively evaluated to verify approximately stabilized fuel flow, airspeed, and pressure altitude. This was necessary because the fuel flow was the baseline for comparison to the fuel flow in the vortex. The duration of most cruise points was approximately 25 seconds. For comparison, the T-38C Propulsion Modernization Program used a minimum of 30 seconds of stabilized data for their cruise test points because they had the ability to correct their data for non-zero test day excess thrust. They determined their test day excess thrust using the inertial velocities from the T-38C production embedded GPS/INS (EGI).

In this particular test program, the stabilized cruise airspeed was compared to vortex data available from that data run. If the airspeed of the data taken in the vortex was not within two knots of the stabilized cruise airspeed, the data were assumed to be invalid. The data from only one of 26 runs were determined to be invalid. The test team used a similar method to account for any excess thrust as a function of altitude and airspeed deviations. The correction method to account for imperfect stabilized cruise and vortex runs will be described later in this section.

The test team recorded a stable vortex point, a stable reduced-airspeed point, and a stable cruise point on each run. The stable reduced-airspeed point was recorded by not moving the throttle after a stable vortex point until the airspeed stopped decreasing after the lead aircraft moved away. There was fuel to accomplish approximately six runs per

test sortie. There were 14 runs recorded on the two two-ship data sorties and 11 runs recorded on the two three-ship data sorties for a total of 25 runs. The objective of the two-ship data sorties was to evaluate the fuel savings at four lateral positions in the vortex. Then the lateral position at which the highest average fuel flow savings was achieved was selected to be flown in the three-ship data sorties. The highest average fuel flow savings was achieved in position B. The number of runs for the two-ship and three-ship formations is shown in Table D-1 and Table D-2 respectively.

There were three types of corrections applied to the fuel flow measurements before determining the percent fuel flow savings on each run. The first correction accounted for the different gross weights and ambient air temperatures at which the test aircraft was flown on different runs over different flight test sorties. The next correction accounted for the difference in fuel flow between runs as a function of how far away from 300 KCAS the test run was flown. Finally, the last correction accounted for excess thrust that was experienced during each of the vortex and cruise runs. The following paragraphs describe how each of these corrections were calculated.

Gross Weight and Ambient Air Temperature Correction

Both fuel flow differences and airspeed differences between in and out of the vortex were measures of performance used to evaluate the fuel flow savings. The airspeed measurement differences were converted to fuel flow differences to obtain an overall percent fuel flow savings per run to compare to the overall fuel flow savings achieved on each run using fuel flow measurements. The ambient air temperature and the aircraft gross weight for each sample were used to correct the data from each run to

standard day atmospheric conditions at 10,000 feet pressure altitude and a gross weight of 11,000 pounds.

The cruise section in the T-38A performance manual, T.O. 1T-38A-1, Part 4 (13) was used to determine a gross weight and ambient air temperature standardization formula. This correction factor formula was imbedded in the data processing spreadsheet. The test team used Figure FA4-1, Sheet 1 to determine a cruise basic reference number at 500 pound gross weight intervals for 0.55 Mach number, the Mach number associated with 300 KIAS at 10,000 feet. The test team then used this basic reference number in Sheet 3 to determine the nautical air miles per pound of fuel at each gross weight interval. Finally, the test team used this nautical air miles per pound of fuel at each gross weight interval in Sheet 4 to determine the fuel flow in pounds per hour per engine for different ambient air temperatures in 5° C intervals. At 10,000 feet, the standard day ambient air temperature is -5° C. The runs were flown over an average ambient air temperature range between 5° C and 9° C and an average aircraft gross weight range between 9,830 pounds and 11,650 pounds.

The data standardization factor from the flight manual was very small (i.e. 15 pounds-per-hour-per-engine for every 10° C temperature deviation from standard day and 20 pounds-per-hour-per-engine for every 500 pounds deviation from 11,000 pounds of aircraft gross weight). Since the nominal fuel flow at 10,000 feet and 300 KCAS was 1000 pounds-per-hour per engine, these corrections were 1.5 percent and 2 percent of the total fuel flow per-engine respectively. The charts showed a roughly linear relationship between changes in fuel flow as a result of changes in ambient temperature and aircraft gross weight. The linear approximation for the fuel flow correction per engine from

standard day at 10,000 feet is plotted in Figure D-1. Two weight and temperature fuel flow correction lines are plotted in Figure D-1. The top line is a correction factor for 5° C and the bottom line is simply a weight correction for -5° C, the standard day ambient air temperature. The following formulas show how to derive the final weight and temperature correction to standard day and mid-band weight.

W is the aircraft gross weight in pounds.

T is the ambient air temperature in degrees Celcius.

δFF_{WT} is the weight and temperature correction factor in gallons-per-minute (gpm) to standard day ambient temperature at mid-band gross weight of 11,000 pounds at 10,000 feet.

$$\delta FF_{WT}(W, T) = mW + b(W, T)$$

$$m_2 = \frac{b(0, T_2) - b(0, T_1)}{T_2 - T_1}$$

$$m_2 = \frac{-440 - (-425)}{-5 - (-5)} = 1.5$$

$$b(W, T) = b(0, T_1) - m_2 T_1$$

$$b(W, T) = -425 - 1.5(5) = -432.5$$

$$\delta FF_{WT}(W, T) = 0.04W + 1.5T - 432.5$$

$$\delta FF_{WT} = 0.04W + 1.5T - 432.5$$

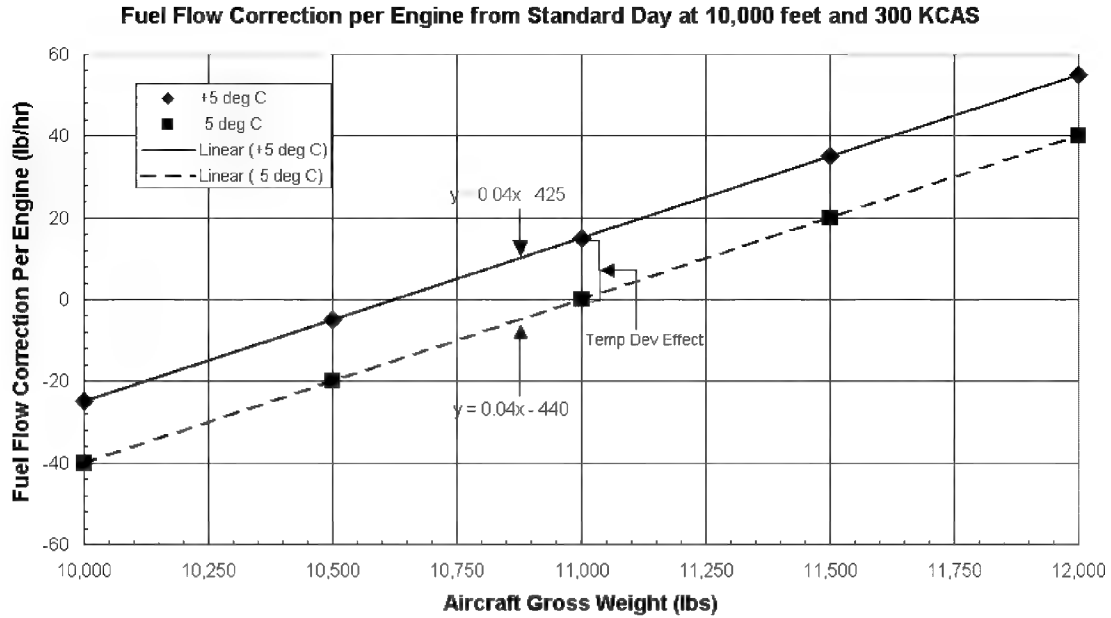


Figure D-1: Fuel Flow Model Correction for Gross Weight and Ambient Air Temperature

The test team used the following conversion to convert the fuel flow correction factor formula obtained from the performance manual in lbs/hr/eng to gpm for both engines, assuming JP-8 fuel:

$$\delta FF_{WT} [gpm] = \delta FF_{WT} \left[\frac{lb/hr}{eng} \right] \left[\frac{2eng}{60 \text{ min/hr}} \right] \left[\frac{gal}{6.8lb} \right]$$

Fuel Flow Correction to 300 KCAS

The calibrated airspeed, V_C (knots), at each sample during the run was used to calculate a standardized fuel flow, FF_V (lb/hr). The following graph and accompanying formula, obtained from the T-38C Propulsion Modernization Program, illustrates this conversion.

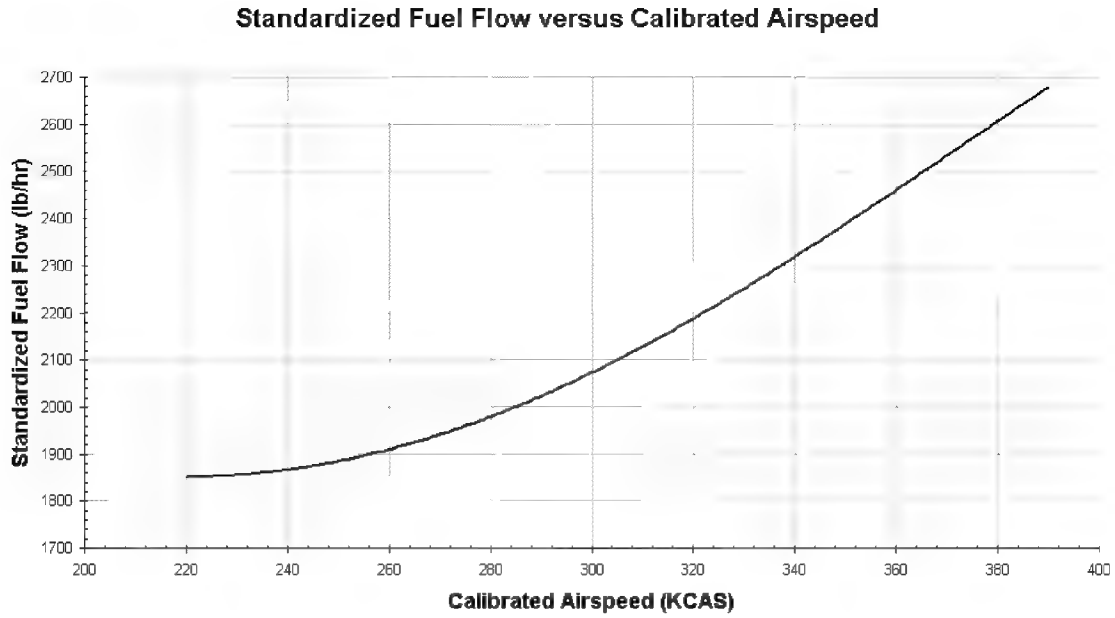


Figure D-2: Standardized Fuel Flow versus Calibrated Airspeed

$$FF_V = -2.7081 \times 10^{-7} V_C^4 + 2.4386 \times 10^{-4} V_C^3 - 4.7184 \times 10^{-2} V_C^2 - 3.0401 V_C + 2.841403 \times 10^3$$

The factor to correct the fuel flow, δFF_V (gpm), back to 2073 lbs/hr, the standardized fuel flow at 300 KCAS and 10,000 feet was calculated as follows:

$$\delta FF_V [\text{gpm}] = [2073 - FF_V] \left[\frac{\text{lb}}{\text{hr}} \right] \left[\frac{\text{hr}}{60 \text{ min}} \right] \left[\frac{\text{gal}}{6.8 \text{ lb}} \right]$$

This correction was only applied to the fuel flow measurement data since this correction factor would have cancelled itself out if it was applied to the fuel flow calculated from airspeed measurement differences in and out of the vortex.

Excess Thrust Correction

To account for small variations in altitude, H (ft), and true airspeed, V_T (ft/sec), during each vortex and cruise run, the following procedure was applied to determine an excess thrust correction, δFF_{Fex} (gpm). First, the specific excess power, P_S (ft/sec), was

calculated per run for both the vortex run and the cruise run using the following formula with g (32.2 ft/sec²):

$$P_S = \frac{dH}{dt} + \frac{V_T}{g} \frac{dV_T}{dt}$$

The excess thrust, F_{ex} (lbs), for both the vortex run and the cruise run, was calculated by using the average gross weight, W_{avg} (lbs), and the average V_T (ft/sec) for the vortex run and the cruise run respectively in the following formula:

$$F_{ex} = \frac{P_S W_{avg}}{V_{T_{avg}}}$$

Then, this excess thrust was converted to fuel flow, δFF_{Fex} (gpm), using the following formula for thrust specific fuel consumption, $TSFC$ (per-hr):

$$TSFC = -3.8027 \times 10^{-9} V_C^4 + 4.9149 \times 10^{-6} V_C^3 - 2.3722 \times 10^{-3} V_C^2 + 5.0550 \times 10^{-1} V_C - 38.0230$$

$$\delta FF_{F_{ex}} [gpm] = -F_{ex} TSFC \left[\frac{lb}{hr} \right] \left[\frac{hr}{60 \text{ min}} \right] \left[\frac{gal}{6.8 lb} \right]$$

Fuel Flow Savings using the Fuel Flow Method

The percent savings in fuel flow rates for each run at a specific lateral spacing were calculated using the average corrected fuel flow per run, $\overline{FF_{run}}$, for both the vortex run and the cruise run. The actual fuel flow measurement at each sample, $FF_{reading_i}$, was corrected over N samples per run in the following formula to calculate, $\overline{FF_{run}}$:

$$\overline{FF_{run}} = \frac{\sum_{i=1}^N (FF_{reading_i} + \delta FF_{WT_i} + \delta FF_{V_i})}{N} + \delta FF_{F_{ex}}$$

Since the goal was to calculate the percent fuel flow savings of flying in lead's vortex versus flying at cruise, the following formula was used to calculate the percent fuel flow savings per run at a specific lateral spacing treatment.

$$\%FF_{savings} = \left[\frac{\overline{FF_{cruise}} - \overline{FF_{vortex}}}{\overline{FF_{cruise}}} \right] \times 100$$

Fuel Flow Savings using the Airspeed Method

The average corrected fuel flow per run had to be calculated by first converting the calibrated airspeed into standardized fuel flow, FF_V (lb/hr), at each sample in the vortex and outside the vortex after the lead aircraft moved away. Once again, the fuel flow correction back to 300 KCAS, δFF_V (gpm), was not applied here since this correction factor would have cancelled itself out if it was applied to the fuel flow calculated from airspeed measurement differences in and out of the vortex. Therefore, the calculated average fuel flow from the airspeed measurements during the vortex run was corrected only for gross weight, temperature, and excess thrust variations using the following formula:

$$\overline{FF_{vortex}} = \frac{\sum_{i=1}^N (FF_{V_i} + \delta FF_{WT_i})}{N} + \delta FF_{F_{ex}}$$

The data were simply collected for the cruise run in the airspeed measurement method by using the following procedure. Once the lead aircraft moved away from the test aircraft, without adjusting the throttle, the aircraft decelerated. As soon as the aircraft stopped decelerating, the new airspeed was read and this was used to calculate the average corrected cruise fuel flow, $\overline{FF_{cruise}}$. The average airspeed was taken ± 1 second

of the determined new slower airspeed. Therefore, it was assumed that there were no excess thrust effects. The \overline{FF}_{cruise} was calculated using the following formula:

$$\overline{FF}_{cruise} = \frac{\sum_{i=1}^N (FF_{V_i} + \delta FF_{WT_i})}{N}$$

In this case, in order to calculate the percent fuel flow savings, since there was no actual power reduction between in the vortex and out of the vortex, a power reduction corresponding to a fuel flow savings must be calculated based upon the decrease in airspeed once the aircraft left the vortex. Logically, the greater the airspeed loss, the greater the calculated power reduction and hence fuel flow savings, because in order to compare fuel flow at the new “cruise” power setting, the pilot would have to reduce power. The graph in Figure D-2 shows that as calibrated airspeed increases, the standardized fuel flow also increases. Therefore, the larger the airspeed difference, the larger the percent fuel flow difference, $\%FF_{difference}$.

$$\%FF_{difference} = \left[\frac{\overline{FF}_{vortex} - \overline{FF}_{cruise}}{\overline{FF}_{cruise}} \right] \times 100$$

Remember, however, the larger the required power reduction, the larger the percent fuel flow savings. Therefore,

$$\%FF_{savings} = -\%FF_{difference}$$

$$\%FF_{savings} = \left[\frac{\overline{FF}_{cruise} - \overline{FF}_{vortex}}{\overline{FF}_{cruise}} \right] \times 100$$

The $\%FF_{savings}$ formula was the same for both the fuel flow method and the airspeed method, even though the derivation was different.

Both the percent fuel flow savings from the fuel flow method and the airspeed method are shown along with the data used to apply all the described corrections in Table D-1. These were the results for the two-ship runs flown in the 75% lateral spacing treatment. All of the data summary tables for all of the different lateral spacing treatments flown in either the two-ship or three-ship formations are included at the end of this appendix.

Table D-1: Data Summary Table – Test Position A

A	2-Ship	Measured Parameter	Run Number			
			1	2	3	4
M.O.P.	Time (sec)	Vortex Run	22	25	36	41
		Cruise Run	67	30	12	32
Data Used for Corrections	Average	Ambient Air Temperature (degrees C)	5.1	5.7	6.3	7.3
		Pressure Altitude (feet)*	10,227	10,752	10,653	10,119
		Gross Weight (pounds)	10,915	10,750	10,599	10,272
		Vortex Airspeed (KCAS)	307.0	309.3	308.2	307.9
		Reduced Airspeed (KCAS)	292.2	302.2	303.1	304.5
		Cruise Airspeed (KCAS)	307.0	308.8	310.1	308.7
Fuel Flow Method	Average	Corrected Vortex Fuel Flow (gal/min)	4.40	4.96	4.97	4.84
		Corrected Cruise Fuel Flow (gal/min)	5.01	5.06	4.56	5.11
		Fuel Flow Savings (percent)	12.17%	1.92%	-8.80%	5.14%
Airspeed Method	Average	Corrected Vortex Fuel Flow (gal/min)	4.67	5.28	5.27	5.05
		Corrected Reduced A/S Fuel Flow (gal/min)	5.05	5.14	5.12	5.09
		Fuel Flow Savings (percent)	7.43%	-2.61%	-2.88%	0.61%

* An average of all the in and out of vortex pressure altitude data per run.

Analysis of Variance

In order to evaluate the fuel flow savings at four lateral positions in the vortex, the analysis of variance (ANOVA) method was used. The ANOVA method was used to analyze the variation of the response and assign portions of this variation to effects caused by different treatments. In this test, the response observation was either $\%FF_{savings}$ obtained from the fuel flow method or the airspeed method found by flying in

the vortex. The treatments for this test were the four lateral spacings. If these treatments had big enough effects on the response, the ANOVA method would statistically show their significance. The single classification ANOVA function in Microsoft® Excel was used because the data were only classified a single way, that is by treatment. The statistical model for the completely randomized design is as follows:

$$Y_{ij} = \mu + \tau_i + \varepsilon_{ij}, \quad i = 1, 2, \dots, k \quad j = 1, 2, \dots, n_i$$

Y_{ij} is the j th response observation from treatment i

k is the number of treatments

n_i is the number of runs per treatment

μ is the overall mean

τ_i is the nonrandom effect of treatment

ε_{ij} is the random error terms that are independent and randomly distributed

The following table lists the percent fuel flow savings calculated from the two-ship sortie data by treatment and by run per treatment. In this case, the ANOVA method assumes the random samples have been drawn from four normal populations with means μ_1, μ_2, μ_3 , and μ_4 with equal variances, $\sigma_1=\sigma_2=\sigma_3=\sigma_4$. A complete set of tables is shown at the end of this appendix.

Table D-2: Two Ship Sortie Analysis of Variance Table

% Fuel Flow Savings (Fuel Flow Method)				
Treatment (Lateral Position)	Run			
	1	2	3	4
75%	12.17%	1.92%	-8.80%	5.14%
86%	23.88%	19.92%	3.76%	-3.98%
100%	1.92%	5.62%	-0.36%	
114%	3.26%	-2.87%	2.60%	

Anova: Single Factor

SUMMARY

	Groups	Count	Sum	Average	Variance
Row 1		4	0.104373	0.026093	0.007613294
Row 2		4	0.435838	0.108959	0.017413254
Row 3		3	0.071799	0.023933	0.00090816
Row 4		3	0.029878	0.009959	0.001132373

ANOVA

Source of Variation	SS	df	MS	F	P-value	F crit
Between Groups	0.022798	3	0.007599	0.959989962	0.448833	1.861398
Within Groups	0.079161	10	0.007916			
Total	0.101959	13				

In order to detect a difference in a set of more than two treatment population means, the following null hypothesis was established:

$$H_0 : \mu_1 = \mu_2 = \mu_3 = \dots = \mu_k$$

The null hypothesis can hold only if all the treatment effects were zero.

$$H_0 : \tau_1 = \tau_2 = \tau_3 = \dots = \tau_k = 0$$

The alternate hypothesis was that at least one of the equalities in the null hypothesis did not hold,

$$H_a : \mu_i \neq \mu_l \text{ for some } i \text{ and } l \text{ if and only if } H_a : \tau_i \neq 0 \text{ for some } i, i = 1, 2, \dots, k \text{ is true}$$

In order to reject the null hypothesis, the variance between groups must be significantly greater than the variance within groups. In other words, if ε_{ij} became too large, it tended to cloud the treatment effect. The test team found that the data collected on each run had very small variances. However, because each treatment was flown with four different pilots and with no differential GPS to validate the pilot's opinion on whether or not the proper position in the vortex was maintained, variances within each treatment hindered the test team from making a decisive decision with respect to treatment effects. The following equations are used by Microsoft® Excel to calculate the ANOVA table values.

\bar{y} is the grand mean of all the runs

\bar{y}_i is the treatment mean

SS is the sum of square errors

MST is the mean sum of square of treatment errors (Between Groups)

MSE is the mean sum of square errors (Within Groups)

$$\sum_{i=1}^k \sum_{j=1}^{n_i} (y_{ij} - \bar{y})^2 = \sum_{i=1}^k n_i (\bar{y}_i - \bar{y})^2 + \sum_{i=1}^k \sum_{j=1}^{n_i} (y_{ij} - \bar{y}_i)^2$$

$$SS_{Total} = SS_{BetweenGroups} + SS_{WithinGroups}$$

Notice that the contribution of the grand mean was factored out because it was of no practical interest. Microsoft® Excel made all the calculations. The null hypothesis was rejected if,

$$F = \frac{MST}{MSE} > F_{\alpha_{crit}}$$

$\alpha = 0.20$ level of risk

$v_1 = (k - 1)$; F-statistic numerator degrees of freedom

$v_2 = (n_1 + n_2 + \dots + n_k - k)$; F-statistic denominator degrees of freedom

$$S = \sqrt{MSE} = \sqrt{\frac{SS_{WithinGroups}}{n_1 + n_2 + \dots + n_k - k}}$$

A confidence interval was established for each treatment using the following formula. This formula was used to create the error bars found in all of the fuel flow comparison plots.

$$C.I._i = \bar{y}_i \pm \frac{t_{v, \alpha/2} S}{\sqrt{n_i}} \quad , \quad v = (n_1 + n_2 + \dots + n_k - k) \text{ degrees of freedom}$$

An example calculation is shown below for the percent fuel flow savings for the 86 percent lateral spacing position in the vortex.

$$\%FF_{savings_{86\% spacing}} = 10.90\% \pm \frac{(1.372)(\sqrt{0.007916})(100)}{\sqrt{4}} = 10.90\% \pm 6.10\% = [4.80\%, 17.00\%]$$

Table D-3: Data Summary Table – Test Position A, Two-Ship Sortie

A	2-Ship	Measured Parameter	Run Number			
			1	2	3	4
M.O.P.	Time (sec)	Vortex Run	22	25	36	41
		Cruise Run	67	30	12	32
Data Used for Corrections	Average	Ambient Air Temperature (degrees C)	5.1	5.7	6.3	7.3
		Pressure Altitude (feet)*	10,227	10,752	10,653	10,119
		Gross Weight (pounds)	10,915	10,750	10,599	10,272
		Vortex Airspeed (KCAS)	307.0	309.3	308.2	307.9
		Reduced Airspeed (KCAS)	292.2	302.2	303.1	304.5
		Cruise Airspeed (KCAS)	307.0	308.8	310.1	308.7
Fuel Flow Method	Average	Corrected Vortex Fuel Flow (gal/min)	4.40	4.96	4.97	4.84
		Corrected Cruise Fuel Flow (gal/min)	5.01	5.06	4.56	5.11
		Fuel Flow Savings (percent)	12.17%	1.92%	-8.80%	5.14%
Airspeed Method	Average	Corrected Vortex Fuel Flow (gal/min)	4.67	5.28	5.27	5.05
		Corrected Reduced A/S Fuel Flow (gal/min)	5.05	5.14	5.12	5.09
		Fuel Flow Savings (percent)	7.43%	-2.61%	-2.88%	0.61%

* An average of all the in and out of vortex pressure altitude data per run.

Table D-4: Data Summary Table – Test Position B, Two-Ship Sortie

B	2-Ship	Measured Parameter	Run Number			
			1	2	3	4
M.O.P.	Time (sec)	Vortex Run	12	27	29	60
		Cruise Run	24	12	7	24
Data Used for Corrections	Average	Ambient Air Temperature (degrees C)	5.3	5.5	6.4	5.8
		Pressure Altitude (feet)*	10,236	10,189	10,525	10,807
		Gross Weight (pounds)	11,562	11,358	10,993	9,836
		Vortex Airspeed (KCAS)	308.9	306.9	310.2	306.6
		Reduced Airspeed (KCAS)	309.0	300.3	305.9	303.1
		Cruise Airspeed (KCAS)	309.6	307.3	310.2	306.0
Fuel Flow Method	Average	Corrected Vortex Fuel Flow (gal/min)	3.98	4.56	5.01	4.73
		Corrected Cruise Fuel Flow (gal/min)	5.23	5.69	5.20	4.55
		Fuel Flow Savings (percent)	23.88%	19.92%	3.76%	-3.98%
Airspeed Method	Average	Corrected Vortex Fuel Flow (gal/min)	4.36	4.75	5.27	5.01
		Corrected Reduced A/S Fuel Flow (gal/min)	5.39	5.23	5.24	4.97
		Fuel Flow Savings (percent)	18.98%	9.26%	-0.59%	-0.86%

* An average of all the in and out of vortex pressure altitude data per run.

Table D-5: Data Summary Table – Test Position C, Two-Ship Sortie

C	2-Ship	Measured Parameter	Run Number		
			1	2	3
M.O.P.	Time (sec)	Vortex Run	19	11	31
		Cruise Run	20	23	112
Data Used for Corrections	Average	Ambient Air Temperature (degrees C)	5.6	5.8	6.9
		Pressure Altitude (feet)*	10,182	10,151	10,408
		Gross Weight (pounds)	10,572	9,914	11,646
		Vortex Airspeed (KCAS)	308.2	306.5	306.5
		Reduced Airspeed (KCAS)	307.4	303.5	305.0
		Cruise Airspeed (KCAS)	308.8	306.9	306.6
Fuel Flow Method	Average	Corrected Vortex Fuel Flow (gal/min)	4.92	4.68	5.35
		Corrected Cruise Fuel Flow (gal/min)	5.02	4.96	5.33
		Fuel Flow Savings (percent)	1.92%	5.62%	-0.36%
Airspeed Method	Average	Corrected Vortex Fuel Flow (gal/min)	5.18	4.84	5.51
		Corrected Reduced A/S Fuel Flow (gal/min)	5.18	4.99	5.33
		Fuel Flow Savings (percent)	0.00%	3.02%	-3.37%

* An average of all the in and out of vortex pressure altitude data per run.

Table D-6: Data Summary Table – Test Position D, Two-Ship Sortie

D	2-Ship	Measured Parameter	Run Number		
			1	2	3
M.O.P.	Time (sec)	Vortex Run	10	11	31
		Cruise Run	38	23	112
Data Used for Corrections	Average	Ambient Air Temperature (degrees C)	5.2	5.8	6.9
		Pressure Altitude (feet)*	10,185	10,151	10,408
		Gross Weight (pounds)	10,147	9,914	11,646
		Vortex Airspeed (KCAS)	309.0	306.5	306.5
		Reduced Airspeed (KCAS)	305.9	303.5	305.0
		Cruise Airspeed (KCAS)	309.3	306.9	306.6
Fuel Flow Method	Average	Corrected Vortex Fuel Flow (gal/min)	4.68	4.68	5.35
		Corrected Cruise Fuel Flow (gal/min)	4.84	4.96	5.33
		Fuel Flow Savings (percent)	3.26%	5.62%	-0.36%
Airspeed Method	Average	Corrected Vortex Fuel Flow (gal/min)	4.96	4.84	5.51
		Corrected Reduced A/S Fuel Flow (gal/min)	5.07	4.99	5.33
		Fuel Flow Savings (percent)	2.31%	3.02%	-3.37%

* An average of all the in and out of vortex pressure altitude data per run.

Table D-7: Data Summary Table – Test Position B, Three-Ship Sortie, First Wingman

B	3-Ship	Wingman 1 Measured Parameter	Run Number		
			1	2	3
M.O.P.	Time (sec)	Vortex Run	19	23	24
		Cruise Run	27	22	25
Data Used for Corrections	Average	Ambient Air Temperature (degrees C)	9.0	9.2	9.0
		Pressure Altitude (feet)*	10,221	10,190	10,240
		Gross Weight (pounds)	10,753	11,064	10,071
		Vortex Airspeed (KCAS)	301.8	307.4	307.6
		Reduced Airspeed (KCAS)	300.4	304.0	303.5
		Cruise Airspeed (KCAS)	303.1	305.8	307.8
Fuel Flow Method	Average	Corrected Vortex Fuel Flow (gal/min)	5.25	5.23	4.85
		Corrected Cruise Fuel Flow (gal/min)	4.96	5.21	5.22
		Fuel Flow Savings (percent)	-5.76%	-0.41%	7.06%
Airspeed Method	Average	Corrected Vortex Fuel Flow (gal/min)	5.26	5.35	4.96
		Corrected Reduced A/S Fuel Flow (gal/min)	5.14	5.25	5.05
		Fuel Flow Savings (percent)	-2.28%	-1.81%	1.66%

* An average of all the in and out of vortex pressure altitude data per run.

Table D-8: Data Summary Table – Test Position B, Three-Ship Sortie, Second Wingman

B	3-Ship	Wingman 2 Measured Parameter	Run Number							
			1	2	3	4	5	6	7	8
M.O.P.	Time (sec)	Vortex Run	16	28	24	21	28	25	23	24
		Cruise Run	20	15	25	27	30	22	25	19
Data Used for Corrections	Average	Ambient Air Temperature (degrees C)	9.2	8.9	9.2	8.6	8.4	9.3	9.2	8.7
		Pressure Altitude (feet)*	10,118	10,183	9,971	10,279	10,339	10,178	10,195	10,282
		Gross Weight (pounds)	11,651	11,361	11,074	10,336	10,070	11,770	11,359	10,414
		Vortex Airspeed (KCAS)	308.3	309.8	305.5	309.2	309.5	309.2	306.4	305.5
		Reduced Airspeed (KCAS)	301.5	308.4	292.9	302.7	306.3	303.7	301.2	303.1
		Cruise Airspeed (KCAS)	308.0	311.7	305.0	308.9	310.6	310.8	305.9	307.0
Fuel Flow Method	Average	Corrected Vortex Fuel Flow (gal/min)	5.30	5.26	5.31	5.00	4.80	4.41	5.30	5.28
		Corrected Cruise Fuel Flow (gal/min)	5.64	5.03	5.25	4.95	4.87	5.20	5.48	5.02
		Fuel Flow Savings (percent)	5.97%	-4.50%	-1.07%	-1.09%	1.49%	15.10%	3.36%	-5.27%
Airspeed Method	Average	Corrected Vortex Fuel Flow (gal/min)	5.59	5.31	5.58	5.28	5.05	4.55	5.37	5.32
		Corrected Reduced A/S Fuel Flow (gal/min)	5.34	5.36	5.13	5.09	5.08	5.38	5.27	5.11
		Fuel Flow Savings (percent)	-4.67%	1.02%	-8.84%	-3.82%	0.59%	15.41%	-1.93%	-4.10%

* An average of all the in and out of vortex pressure altitude data per run.

Table D-9: Two-Ship Sortie ANOVA (Fuel Flow)

% Fuel Flow Savings (Fuel Flow Method)				
Treatment (Lateral Position)	Run			
	1	2	3	4
75%	12.17%	1.92%	-8.80%	5.14%
86%	23.88%	19.92%	3.76%	-3.98%
100%	1.92%	5.62%	-0.36%	
114%	3.26%	-2.87%	2.60%	

Anova: Single Factor

SUMMARY

<i>Groups</i>	<i>Count</i>	<i>Sum</i>	<i>Average</i>	<i>Variance</i>
Row 1	4	0.104373	0.026093	0.007613294
Row 2	4	0.435838	0.108959	0.017413254
Row 3	3	0.071799	0.023933	0.00090816
Row 4	3	0.029878	0.009959	0.001132373

ANOVA

<i>Source of Variation</i>	<i>SS</i>	<i>df</i>	<i>MS</i>	<i>F</i>	<i>P-value</i>	<i>F crit</i>
Between Groups	0.022798	3	0.007599	0.959989962	0.448833	1.861398
Within Groups	0.079161	10	0.007916			
Total	0.101959	13				

Table D-10: Two-Ship Sortie ANOVA (Airspeed)

% Fuel Flow Savings (Airspeed Method)				
Treatment (Lateral Position)	Run			
	1	2	3	4
75%	7.43%	-2.61%	-2.88%	0.61%
86%	18.98%	9.26%	-0.59%	-0.86%
100%	0.00%	3.02%	-3.37%	
114%	2.31%	-1.59%	0.87%	

Anova: Single Factor

SUMMARY

<i>Groups</i>	<i>Count</i>	<i>Sum</i>	<i>Average</i>	<i>Variance</i>
Row 1	4	0.025611	0.006403	0.002302086
Row 2	4	0.268041	0.06701	0.008921174
Row 3	3	-0.00354	-0.00118	0.001021935
Row 4	3	0.01584	0.00528	0.000390282

ANOVA

<i>Source of Variation</i>	<i>SS</i>	<i>df</i>	<i>MS</i>	<i>F</i>	<i>P-value</i>	<i>F crit</i>
Between Groups	0.011527	3	0.003842	1.052854701	0.411533	1.861398
Within Groups	0.036494	10	0.003649			
Total	0.048021	13				

Table D-11: Two-Ship Sortie ANOVA (Average)

% Fuel Flow Savings (Averaging Fuel Flow / Airspeed Methods)				
Treatment	Run			
(Lateral Position)	1	2	3	4
75%	9.80%	-0.34%	-5.84%	2.88%
86%	21.43%	14.59%	1.59%	-2.42%
100%	0.96%	4.32%	-1.86%	
114%	2.79%	-2.23%	1.73%	

Anova: Single Factor

SUMMARY

<i>Groups</i>	<i>Count</i>	<i>Sum</i>	<i>Average</i>	<i>Variance</i>
Row 1	4	0.064992	0.016248	0.004266028
Row 2	4	0.351939	0.087985	0.012367121
Row 3	3	0.034131	0.011377	0.000957348
Row 4	3	0.022859	0.00762	0.000700529

ANOVA

<i>Source of Variation</i>	<i>SS</i>	<i>df</i>	<i>MS</i>	<i>F</i>	<i>P-value</i>	<i>F crit</i>
Between Groups	0.016541	3	0.005514	1.036097623	0.41801	1.861398
Within Groups	0.053215	10	0.005322			
Total	0.069756	13				

Table D-12: Three-Ship Sortie ANOVA (Fuel Flow)

Treatment (Lateral Position B)	% Fuel Flow Savings (Fuel Flow Method)							
	Run							
	1	2	3	4	5	6	7	8
2-Ship	23.88%	19.92%	3.76%	-3.98%				
Pos 2, 3-Ship	-5.76%	-0.41%	7.06%					
Pos 3, 3-Ship	5.97%	-4.50%	-1.07%	-1.09%	1.49%	15.10%	3.36%	-5.27%

Anova: Single Factor

SUMMARY

<i>Groups</i>	<i>Count</i>	<i>Sum</i>	<i>Average</i>	<i>Variance</i>
Row 1	4	0.435838	0.108959	0.017413
Row 2	3	0.008861	0.002954	0.004143
Row 3	8	0.139821	0.017478	0.00433

ANOVA

<i>Source of Variation</i>	<i>SS</i>	<i>df</i>	<i>MS</i>	<i>F</i>	<i>P-value</i>	<i>F crit</i>
Between Groups	0.027181	2	0.013591	1.795364	0.207917	1.845962
Within Groups	0.090837	12	0.00757			
Total	0.118018	14				

Table D-13: Three-Ship Sortie ANOVA (Airspeed)

Treatment (Lateral Position B)	% Fuel Flow Savings (Airspeed Method)							
	Run							
	1	2	3	4	5	6	7	8
2-Ship	18.98%	9.26%	-0.59%	-0.86%				
Pos 2, 3-Ship	-2.28%	-1.81%	1.66%					
Pos 3, 3-Ship	-4.67%	1.02%	-8.84%	-3.82%	0.59%	15.41%	-1.93%	-4.10%

Anova: Single Factor

SUMMARY

<i>Groups</i>	<i>Count</i>	<i>Sum</i>	<i>Average</i>	<i>Variance</i>
Row 1	4	0.268041	0.06701	0.008921
Row 2	3	-0.0243	-0.0081	0.000464
Row 3	8	-0.06334	-0.00792	0.005271

ANOVA

<i>Source of Variation</i>	<i>SS</i>	<i>df</i>	<i>MS</i>	<i>F</i>	<i>P-value</i>	<i>F crit</i>
Between Groups	0.01649	2	0.008245	1.531886	0.255555	1.845962
Within Groups	0.064589	12	0.005382			
Total	0.081079	14				

Table D-14: Three-Ship Sortie ANOVA (Average)

Treatment (Lateral Position B)	% Fuel Flow Savings (Averaging Fuel Flow / Airspeed Methods)							
	Run							
	1	2	3	4	5	6	7	8
2-Ship	21.43%	14.59%	1.59%	-2.42%				
Pos 2, 3-Ship	-4.02%	-1.11%	4.36%					
Pos 3, 3-Ship	0.65%	-1.74%	-4.96%	-2.46%	1.04%	15.26%	0.72%	-4.69%

Anova: Single Factor

SUMMARY

<i>Groups</i>	<i>Count</i>	<i>Sum</i>	<i>Average</i>	<i>Variance</i>
Row 1	4	0.351939	0.087985	0.012367
Row 2	3	-0.00772	-0.00257	0.00181
Row 3	8	0.038239	0.00478	0.004121

ANOVA

<i>Source of Variation</i>	<i>SS</i>	<i>df</i>	<i>MS</i>	<i>F</i>	<i>P-value</i>	<i>F crit</i>
Between Groups	0.021416	2	0.010708	1.847001	0.199841	1.845962
Within Groups	0.069571	12	0.005798			
Total	0.090988	14				

Bibliography

1. Ackerman, N.G., *F-5 Basic Aerodynamic Data, Volume II, Cruise Configurations*, Northrop Report, NOR-64-2, 1964.
2. Albright, Alan E., Charles J. Dixon, and Martin C. Hegedus, *Modification and Validation of Conceptual Design Aerodynamic Prediction Method HASC95 with VTXCHN*, Prepared for Mike Logan at NASA Langley Research Center, CDAP-10, 30 November 1995.
3. Blake, W., and Dieter Multhopp, "Design, Performance and Modeling Considerations for Close Formation Flight," *AIAA Journal of Guidance, Control, and Dynamics*, AIAA-98-4343, August 1998.
4. *Flight Manual, USAF Series T-38C Aircraft*, Technical Order (T.O.) 1T-38C-1, 1 April 2001.
5. Hummel, D., "Aerodynamic Aspects of Formation Flight in Birds," *Journal of Theoretical Biology*, Volume 104, pp. 321-347, 1983.
6. Hummel, D., "The Use of Aircraft Wakes to Achieve Power Reductions in Formation Flight," *Proceedings of the AGARD FDP Symposium on "The Characterization and Modification of Wakes from Lifting Vehicles in Fluid,"* Trondheim, Norway, May 1996.
7. Link Engineering Reports Group, *Undergraduate Pilot Training – Instrument Flight Simulator, Training Equipment Computer Program Documentation, Volume IV, Aerodynamics*, Singer-Link Division, Binghamton NY, Feb 1978.
8. Lissaman, P.B.S., and C.A. Schollenberger, "Formation Flight of Birds," *Science*, Volume 168, pp. 1003-1005, 1970.
9. McCormick, Barnes W., *Aerodynamics, Aeronautics, and Flight Mechanics*. John Wiley & Sons, 1979.
10. Pachter, M., A. Proud, and J.J. D'Azzo, "Tight Formation Flight Control," *AIAA Journal of Guidance, Control, and Dynamics*, Vol 24, No. 2, March-April 2001, pp. 246-254.
11. Prandtl, L., *Induced Drag of Multiplanes*, NACA TN 182, March 1924.

12. Shaw, Robert, *Fighter Combat: Tactics and Maneuvering*. Naval Institute Press, 1987 (Fifth Printing).
13. Wagner, et al., *A Limited Investigation of Fuel Savings Derived from Formation Flight*, Technical Information Memorandum, Air Force Flight Test Center, Edwards Air Force Base CA, December 2001.

Vita

Major Eugene H. Wagner, Jr. was born in Joliet, Illinois. He graduated from Freeport High School in Freeport, Illinois in May 1985. He entered undergraduate studies at the University of Illinois in Urbana-Champaign, Illinois where he graduated with a Bachelor of Science degree in Aeronautical and Astronautical Engineering in May 1990. He was commissioned through the Detachment 190 AFROTC at the University of Illinois.

His first assignment was at Sheppard AFB, Texas as a student in Undergraduate Pilot Training in February 1991. After graduating from Undergraduate Pilot Training in April 1992, he assigned to the 11th Aeromedical Airlift Squadron at Scott AFB, Illinois where he served as an instructor and evaluator pilot in the C-9A aircraft. During this assignment, he earned a Masters in Business Administration from Southern Illinois University in Edwardsville, Illinois. In 1996, he was assigned to the 9th Airlift Squadron at Dover AFB, Delaware where he served as an instructor pilot and Special Operations Low-Level (SOLL II) pilot in the C-5 aircraft. In August 1999, he was selected to enter the USAF Test Pilot School / Air Force Institute of Technology Program. He graduated from the USAF Test Pilot School at Edwards AFB, California in December 2001. Upon graduation from AFIT, he will be assigned to the 418th Flight Test Squadron at Edwards AFB, California.

REPORT DOCUMENTATION PAGE				Form Approved OMB No. 074-0188	
<p>The public reporting burden for this collection of information is estimated to average 1 hour per response, including the time for reviewing instructions, searching existing data sources, gathering and maintaining the data needed, and completing and reviewing the collection of information. Send comments regarding this burden estimate or any other aspect of the collection of information, including suggestions for reducing this burden to Department of Defense, Washington Headquarters Services, Directorate for Information Operations and Reports (0704-0188), 1215 Jefferson Davis Highway, Suite 1204, Arlington, VA 22202-4302. Respondents should be aware that notwithstanding any other provision of law, no person shall be subject to a penalty for failing to comply with a collection of information if it does not display a currently valid OMB control number.</p> <p>PLEASE DO NOT RETURN YOUR FORM TO THE ABOVE ADDRESS.</p>					
1. REPORT DATE (DD-MM-YYYY) 26-03-2002		2. REPORT TYPE Master's Thesis		3. DATES COVERED (From – To) Sep 1999 – Mar 2002	
4. TITLE AND SUBTITLE AN ANALYTICAL STUDY OF T-38 DRAG REDUCTION IN TIGHT FORMATION FLIGHT				5a. CONTRACT NUMBER	
				5b. GRANT NUMBER	
				5c. PROGRAM ELEMENT NUMBER	
6. AUTHOR(S) Eugene H. Wagner, Jr., Major, USAF				5d. PROJECT NUMBER	
				5e. TASK NUMBER	
				5f. WORK UNIT NUMBER	
7. PERFORMING ORGANIZATION NAMES(S) AND ADDRESS(S) Air Force Institute of Technology Graduate School of Engineering and Management (AFIT/EN) 2950 P Street, Building 640 WPAFB OH 45433-7765				8. PERFORMING ORGANIZATION REPORT NUMBER AFIT/GAE/ENY/02-2	
9. SPONSORING/MONITORING AGENCY NAME(S) AND ADDRESS(ES) USAF Test Pilot School 220 S. Wolfe Ave Edwards AFB CA 93524				10. SPONSOR/MONITOR'S ACRONYM(S)	
				11. SPONSOR/MONITOR'S REPORT NUMBER(S)	
12. DISTRIBUTION/AVAILABILITY STATEMENT APPROVED FOR PUBLIC RELEASE; DISTRIBUTION UNLIMITED.					
13. SUPPLEMENTARY NOTES					
14. ABSTRACT <p>This thesis explores the benefits of flying in a tight formation, mimicking the natural behavior of migratory birds such as geese. The first phase of the research was to determine an optimal position for the wingman of a tight formation flight of T-38 <i>Talon</i> aircraft using the HASC95 vortex lattice code. A second wingman was then added to determine the benefit derived by increasing formation size. The second wingman was predicted to derive an even greater induced drag benefit than the first wingman for T-38s operating at Mach 0.54 at a 10,000-foot altitude. The predicted values were 17.5% savings for the second wingman versus 15% for the first wingman.</p> <p>The flight test phase flew two and three-ship formations to validate the computational work. The results of the two-ship flight tests showed with 80% confidence that the wingman saved fuel in the predicted optimal position (86% wingspan lateral spacing). This position yielded actual fuel savings of $8.8\% \pm 5.0\%$ versus the predicted 15%. The other lateral positions did not show a statistically significant fuel savings. The flight test team felt that the three-ship formation data was inconclusive due to the difficulty of trying to fly a stable position as the third aircraft in the formation without station-keeping ability.</p>					
15. SUBJECT TERMS Vortex, Vortices, Vortex Wake Effects, Drag, Drag Reduction, Formation Flight, T-38 Aircraft, Fuel Consumption, Fuel Savings					
16. SECURITY CLASSIFICATION OF:			17. LIMITATION OF ABSTRACT	18. NUMBER OF PAGES	19a. NAME OF RESPONSIBLE PERSON
a. REPORT	b. ABSTRACT	c. THIS PAGE			David R. Jacques, Lt Col, USAF (ENY)
U	U	U	UU	121	19b. TELEPHONE NUMBER (Include area code) (937) 255-3636, ext 4723; e-mail: David.Jacques@afit.edu